Longitudinal vehicle control for smooth autonomous highway driving

Ruissen, T.K.

Award date:
2019

Master's Thesis Report

Project phase

Longitudinal vehicle control for smooth autonomous highway driving

Department:	Mechanical Engineering
Research group:	Dynamics and Control

Student:	T.K. Ruissen
Identity number:	0814716
Supervisor:	Prof. dr. ir. P.W.A. Zegelaar
Mentor:	Prof. dr. H. Nijmeijer
Report number:	DC 2019.036
Place, date:	Eindhoven, March 13, 2019

Abstract

The goal of this project is to investigate and develop longitudinal control for smooth highway driving. A predictive controller is created, which determines the actions that are required to guide the Host vehicle safely through traffic, while minimizing the Host's resulting accelerations. The inputs are relative positions and velocities, which are based on measurement data, coming from RADAR-, LIDAR- or Camera systems. The required longitudinal- and lateral accelerations of the Host are calculated, based on the inputs. The focus is on the longitudinal direction, where a trapezoid acceleration profile is used. The controlled variables are the duration of the longitudinal acceleration and the maximum acceleration (positive or negative). Laterally, the controlled variables are the duration and the start time, using a fifth-order polynomial. The start time of the lateral movement is determined via the Time To Collision and the comfortableness criteria.
Different scenario's are investigated, where the number of other road users is varied, as well as the relative positions- and velocities. Special cases are elaborated in detail (one other road user, driving in front of the Host, and two- and more road users, driving on the adjacent lane). Dependent on the inter-vehicle distance and relative velocity, the controller chooses the best strategy.
Considering the case where several vehicles are driving on the left lane, the Host searches for possible gaps to merge into. After that, for each gap the belonging accelerations and start times are determined. The optimal gap to merge into is the gap for which the resulting acceleration profile of the Host is minimized, while satisfying the constraints (minimal- and maximal moment to start merging, and safe inter-vehicle distances).
This project is offering some new insights and methods in predicting optimal paths for autonomous highway driving and is trying to provide a sound base for future investigation in autonomous driving.

Keywords: autonomous driving, optimal driving path calculation, longitudinal vehicle control, model-based predictive controller

Preface

This Master's Thesis was carried out at the department of Mechanical Engineering, in the research group of Dynamics and Control, at the Eindhoven University of Technology, Eindhoven, the Netherlands.
First, I would like to thank my supervisor, prof. dr. ir. P.W.A. Zegelaar for giving me the opportunity to do this project in his research group, and for all the support and feedback during the project. It was a pleasure for me to work together on this project and have weekly discussions about the topic. In addition, I would like to thank prof. dr. H. Nijmeijer for his guidance during the project. Finally, thanks to my parents, family and friends for mentally supporting me throughout the project.

Eindhoven, March 13, 2019
T.K. Ruissen

Contents

List of Symbols

Symbol	Description	Units
a_{cmd}	commanded longitudinal acceleration	$[m/s^2]$
a_H	longitudinal Host acceleration	$[m/s^2]$
$a_{H,y}$	lateral Host acceleration	$[m/s^2]$
a_{i-1}	predecessor's longitudinal acceleration	$[m/s^2]$
a_i	longitudinal acceleration vehicle i	$[m/s^2]$
a_r	resulting acceleration	$[m/s^2]$
$a_{r,s}$	scaled resulting acceleration	$[m/s^2]$
a_x	longitudinal acceleration	$[m/s^2]$
$a_{x,max}$	maximum longitudinal acceleration	$[m/s^2]$
a_y	lateral acceleration	$[m/s^2]$
$a_{y,max}$	maximum lateral acceleration	$[m/s^2]$
A	system matrix	[-]
A_{lim}	acceleration limit	$[m/s^2]$
b	desired longitudinal acceleration	$[m/s^2]$
B	input matrix	[-]
c_h	constant	[-]
C	output matrix	[-]
d	required lateral distance	$[m]$
d_0	minimum headway distance	$[m]$
d_{des}	desired inter-vehicle distance	$[m]$
$d_{des,i,i-1}(t)$	Desired distance to predecessor	$[m]$
D_{min}	minimal longitudinal inter-vehicle distance	$[m]$
D(s)	delay	$[s]$
DX	inter-vehicle distanc	$[m]$
$DX_{P\rightarrow H}$	inter-vehicle distance between Pre. and Host	$[m]$
$DX_{req,s}$	required inter-vehicle distance for safety	$[m]$
e_v	velocity error	$[m/s]$
e_x	position error	$[m]$
F_a	aerodynamic force	$[N]$

Symbol	Description	Units
F_g	gravitational force	$[m/s^2]$
F_p	propelling force	$[N]$
F_{rr}	rolling resistance	$[N]$
F_z	vertical force	$[N]$
g	gravitational constant	$[m/s^2]$
G(s)	System transfer function	[-]
h	headway time	$[s]$
h_0	constant headway time	$[s]$
H(s)	Spacing policy transfer function	[-]
J_x	Jacobian evaluated at x	[-]
k	slope	[deg.]
k_d	differential gain	$[s]$
k_p	proportional gain	[-]
k_i	integral gain	$[1/s]$
K(s)	controller	[-]
$K_{p,ss}$	set speed controller gain	[-]
L	length of a vehicle	$[m]$
k_a	gain, one or zero	[-]
k_s	gain, design constant	[-]
k_v	gain, design constant	[-]
$k_{v,gain}$	velocity-dependent gain	[-]
L	length lateral movement	$[m]$
L_b	available moving area	$[m]$
L_r	required inter-vehicle distance for safety	$[m]$
L_v	length of a vehicle	$[m]$
$L_{i,0}$	initial driving lane vehicle i	[-]
$L_{H,0}$	initial Host driving lane	[-]
m	vehicle mass	$[kg]$
M_v	mass of a vehicle	$[kg]$
N	probability density function	[-]
p	input signal	[-]
q	output linear DSP function	[-]
s^*	desired minimum gap	$[m]$
s_0	standstill distance	$[m]$
S_i	stopping distance vehicle i	$[m]$
S_H	stopping distance Host	$[m]$
t	time	$[s]$
T_{des}	desired headway time	$[s]$

Symbol	Description	Units
$T_{y,max}$	maximum overtaking time	$[s]$
T_r	reaction time other traffic	$[s]$
$T_{r,h}$	reaction time Host	$[s]$
$T_{x,s}$	start time longitudinal acceleration phase	$[s]$
$T_{x,e}$	end time longitudinal acceleration phase	$[s]$
T_x	duration time longitudinal acceleration phase	$[s]$
$T_{x,j}$	duration non-zero jerk phase	$[s]$
T_y	duration lateral movement	$[s]$
$T_{y,e}$	end time Lateral acceleration phase	$[s]$
TY_{min}	time-multiplication factor	$[s]$
$T_{y,s}$	start lateral acceleration phase	$[s]$
$T_{y,0}$	duration Lateral acceleration phase	$[s]$
u(t)	input	[-]
$u_{tb}(t)$	controller output	$[m/s]$
$U(t)$	controller output	$[m/s]$
$U_{acc}(t)$	ACC controller output	$[m/s]$
v	velocity	$[m/s]$
$\dot{v}$	acceleration	$[m/s^2]$
v_{i-1}	predecessor's speed	$[m/s]$
v_0	velocity previous step	$[m/s]$
V_{max}	maximum speed	$[m/s]$
V_{min}	minimum speed	$[m/s]$
v_{set}	set speed	$[m/s]$
V_H	longitudinal Host velocity	$[m/s]$
$V_{H,0}$	initial longitudinal Host velocity	$[m/s]$
$V_{H,y}$	lateral Host velocity	$[m/s]$
$V_{H,T}$	target Host velocity	$[m/s]$
V_i	longitudinal velocity vehicle i	$[m/s]$
$V_{i,0}$	initial longitudinal velocity vehicle i	$[m/s]$
V_1	noise on the observation signal	$[m/s]$
W_l	width highway lane	$[m]$
W_v	width of a vehicle	$[m]$
W_1	noise on the states	$[m]$
x	longitudinal position	$[m]$
$\dot{x}$	longitudinal velocity	$[m/s]$
$\ddot{x}$	longitudinal acceleration	$[m/s^2]$
X_1	state vector	[-]
$X_{i,0}$	initial longitudinal position vehicle i	$[m]$

Symbol	Description	Units
X_H	Host's longitudinal position	$[m]$
$X_{H,0}$	initial Host longitudinal position	$[m]$
X_P	Predecessor's longitudinal position	$[m]$
y(t)	impulse response, output	$[m/s]$
$Y_{H,0}$	initial Host lateral position	$[m]$
$Y_{i,0}$	initial lateral position vehicle i	$[m]$
Y_{min}	minimal lateral travel distance Host	$[m]$
Y_s	lateral safety distance	$[m]$
Z_1	observation vector	[-]
α	steepness of a curve	[-]
β	interception of lane 2 on the x-axis	$[m]$
δ	acceleration exponent	[-]
ΔT	time step	$[s]$
μ	mean	[-]
σ	standard deviation	[-]
Σ	variance	[-]
θ	communication delay	$[s]$
τ	vehicle time constant	[s]

List of Abbreviations

ABS	Anti-lock Braking System
ACC	Adaptive Cruise Control
AD	Autonomous Driving
ADAS	Advanced Driver Assist Systems
ALC	Automated Lane Change
AWD	All Wheel Driven
CACC	Cooperative Adaptive Cruise Control
CAN	Controller Area Network
CC	Cruise Control
CG	Centre of Gravity
dCACC	degraded Cooperative Adaptive Cruise Control
DSP	Digital Signal Processing
FWD	Front Wheel Driven
IIDM	Intelligent Driver Model
LC	Lane Centering
LCA	Lance Change Assistant
LDW	Lane Departure Warning
LFT	Longitudinal Following Time
LIDAR	LIght Detection And Ranging
LRR	Long Radar Range
RADAR	RAdar Detection And Ranging
RHT	Right-Hand Traffic
RMS	Root Mean Square
RWD	Rear Wheel Driven
SAE	Society for Automotive Engineers
SSC	Set Speed Controller
TTC	Time To Collision
TTP	Time to Predecessor
WAVE	Wireless Access in Vehicular Environments

Chapter 1

Introduction

Over the past few years, much attention is paid to autonomous driving, implemented on cars. On the one hand, car manufactures are trying to be innovative and propose new ideas and systems that customers will most likely buy. Many car manufacturers are currently working on systems that provide (semi-) autonomous driving. Initially, the system will offer autonomous driving on highways, but the ultimate goal is to make vehicles drive autonomously in all circumstances (including busy city centres and congested road situations).
On the other hand, car manufactures are trying to reduce the amount of people that is killed due to driver's errors. In 2016, 629 people were killed in traffic in the Netherlands, ten percent more than in 2014 [1]. 88% of all accidents in traffic are caused by humans, while the other 11% is caused by the environment, indicating why car manufacturers are focussing on implementing systems to assist drivers [2].
Proposed solutions are systems that can be classified either as Advanced Driver Assist Systems (ADAS) or Autonomous Driving (AD). $ADAS$ assist drivers in the driving process (requiring the drivers to monitor the environment), while in AD the driver becomes actually a passenger (vehicle is able to drive autonomously, either in certain conditions or always. The driver could be required as a back-up).

1.1 Advanced Driver Assist Systems

$ADAS$ support the drivers in the driving process, either by warnings to the driver or partial vehicle control. Examples of these systems are: Adaptive Cruise Control (ACC), Anti-lock Braking System (ABS) and Lane Change Assistant (LCA).
Some manufacturers, like Tesla, are already offering so-called 'autopilot' systems, which includes ACC, Lane Centering (LC) and Auto Lane Change (ALC) [3]:

- ACC is 'an optional cruise control system for road vehicles that automatically adjusts the vehicle speed to maintain a safe distance from vehicles ahead' [4].
- LC is an steering mechanism that keeps the vehicle centered in the lane, by small steering corrections [5]. In addition, the autopilot system is equipped with *Lane Departure Warning* (LDW), which warns the driver if the vehicle unintentionally leaves its lane. Lane Keeping Assist provides steering corrections to ensure that the vehicle will stay in the lane [6].
- ALC is a system that performs a lane change. Currently, the driver initiates the system by tipping the turn indicator, in the future this system will start automatically, without driver's input.

In this context, the term 'autopilot' indicates that the system is partly autonomous: the driver is responsible and should monitor the environment (driver supervision is required).

1.2 Autonomous Driving Systems

There is a major difference between *ADAS* and *AD*. *ADAS* support the driver in the driving process, while an *AD* system can operate automatically, not requiring the driver to monitor the situation.

SAE Levels

The Society for Automotive Engineers (*SAE*, [7]) defined six levels of automation. In Figure 1.1 the different *SAE* Levels are shown.

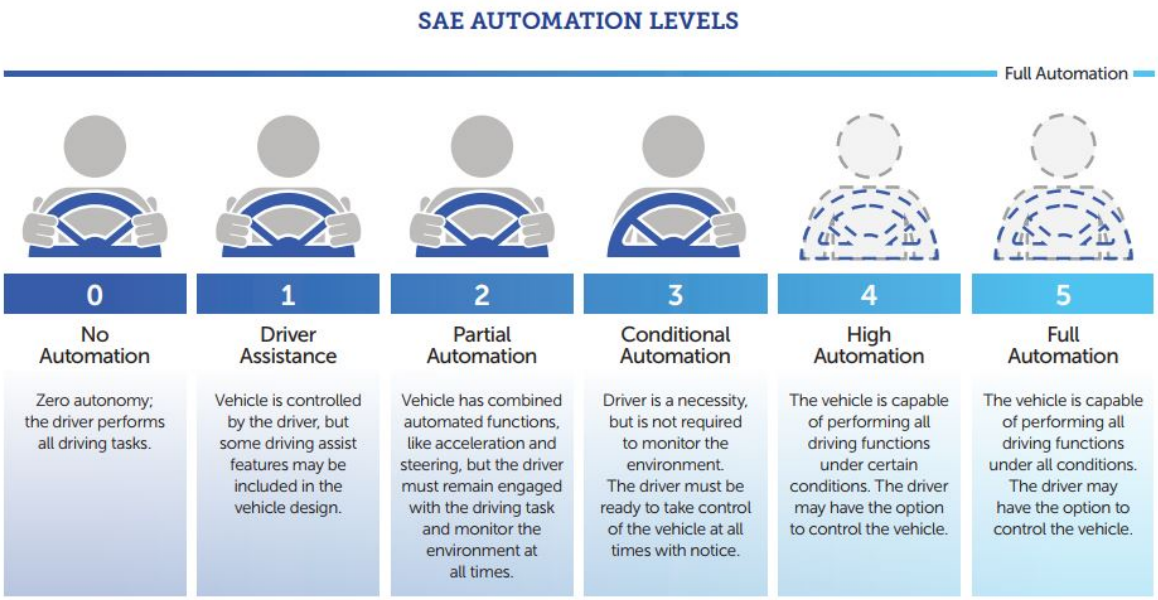

Figure 1.1: *SAE Levels [8]*

The different *SAE* levels are defined as:

- **Level 0:** There is no supporting system, the driver is performing all driving tasks. Driver is fully responsible.
- **Level 1:** Several systems sometimes assist the human driver with either steering (like LCA) or braking/accelerating (like *ACC* and *ABS*). The systems support the driver either in lateral or in longitudinal direction. The driver is fully responsible.
- **Level 2:** Under some circumstances, the vehicle is able to drive partially autonomously (the systems support the driver both in lateral and longitudinal direction), but the driver must always pay full attention and perform the rest of the driving task [9]. Again, the driver is fully responsible. The current Tesla Autopilot system is classified in this level.
- **Level 3:** The vehicle is able to drive autonomously under certain circumstances, the driver is only required as a back-up.
- **Level 4:** The vehicle is monitoring the environment and drives autonomous, in certain circumstances. If the vehicle is driving autonomously, the driver does not have to pay attention to the circumstances, however the driver has the option to control the vehicle in other situations.
- **Level 5:** The vehicle is driving fully autonomous, in all situations.

Assist Systems are classified in Level 1 and 2, while Levels 3,4 and 5 describe (semi-)autonomous systems where the driver does not have to pay attention to the environment, (and is only required as a back-up in Level 3).
Currently, some manufactures (like Tesla, with the autopilot system) offer Level 2 automation [3]. The Tesla autopilot system has the ability to to change lanes automatically, when the driver confirms that a lane change is possible and safe.

Future
A next step is obtaining Level 3 of automation. The step between Level 2 and 3 is a major step, since the driver is only a backup in this system. Conditions for driving with Level 3 might include driving on highways with low density traffic, up to certain limited speeds. Considering the new Audi A8, in 2017 Audi was claiming that it would be equipped with software able to perform Level 3 autonomy [10]. Last year it appeared, however, that due to legalisation, and infrastructural- and consumer issues, the system could not be implemented yet. Although there is substantial technical progress, currently drivers are still responsible for keeping an eye on the situation and intervene if necessary. Also, there is an ongoing discussion about the fact who is responsible in case of an accident [11], preventing governments to legalize autonomous driving currently.

1.3 Problem definition and research question

Problem definition
Current *ADAS* systems use a combination of both longitudinal- and lateral control to assist the driver and control the vehicle, up to a certain level. However, direct combination of both *ALC* and *ACC* could lead to undesired effects, since both systems need to be combined strongly to obtain smooth and safe driving behaviour. Current systems use actual measurement data to decide if for example a lateral motion is possible.
This indicates, however, that a vehicle is slowed down by the *ACC* systems when approaching a predecessor, and only after reaching the predecessor's speed and a safe inter-vehicle distance, the lane change system determines if a lane change is possible. This leads to unnecessary decelerations and accelerations, resulting in uncomfortable highway driving. The 'optimal path predicting challenge' is tackled in this project.
Potential fields are used to select the optimal driving path, while avoiding obstacles. However, potential fields are only offering a 'limited' horizon, since the potential function after an obstacle is not visible at the controlled vehicle's location (elaborated in Section 2.4). A solution is to use a model-based predictive controller, which minimizes an object function while satisfying constraints (to obtain safety).

Research question
The goal of this project is to focus at smooth autonomous highway driving. Since many research is done on lane-changing nowadays, in this project the focus is on preparing a lane-change. This will include *longitudinal control* and *selecting a best gap* to merge into. A controller will be built to obtain smooth driving behaviour for the Host. To visualize the results, simulations are performed in *Matlab*.

The research question is:
In what way can combined longitudinal- and lateral control be used to obtain safe and smooth highway driving?

In this context, smooth highway driving means: predicting an optimal path such that unnecessary accelerations are avoided. Special attention is paid to the selection of the 'best gap'. When approaching a predecessor, in advance the controlled vehicle has to search for a gap in the adjacent lane to merge into. This means that the focus is on longitudinal control or preparing a lane change.

Control design

The controller consists of two main parts: Prediction and Action.

Prediction: In the Prediction part, for all other road users all future states are predicted. In the controller these states are used to determine the optimal path. This includes the optimal switching moments, duration of lateral acceleration and in particular the duration and the maximum value of the longitudinal acceleration.

Action: In the Action part, the optimal path is executed. In addition, in this part the resulting behaviour of the other road users is modelled. The results of the simulations are presented to show the applied methods.

1.4 Structure of the report

In Chapter 2 a literature study is performed on existing autonomous systems, like ACC and longitudinal- and lateral control. It also elaborates on measuring systems like $RADAR$, $LIDAR$ and Camera. In addition, the uncertainties of the measurements are investigated and solutions are suggested to minimize the possible shortcomings.
Chapter 3 describes the derivation of an overtaking manoeuvre. First a list of assumptions is given. Next, it defines some definitions that are used in the simulations. After that, criteria are given, including minimum inter-vehicle distances and acceleration limits. In detail the determination of the comfortableness of an overtaking manoeuvre is explained. Finally, it explains the modelling of a longitudinal- and lateral motion.
Chapter 4 elaborates on three different scenario's. For each scenario, the applied methods of determining the optimal path parameters are given. Simulations are performed to presents the driving behaviour of the Host and other road users due to the implemented driving strategies.
In Chapter 5 the two decision-making algorithms that are used are explained into detail: path optimization and comfort optimization. In the path optimization, a controller performs calculations to suggest an optimal path, satisfying constraints considering safety and comfort. The comfort algorithm varies the acceleration limits for different Comfort levels in case the situation requires higher accelerations.
Finally, in Chapter 6 a conclusion is given about the obtained results. Also, recommendations are given for future work.

Chapter 2

Literature research

This Chapter elaborates on the relevant literature that is present. Different research fields contribute to the global research of autonomous driving. The relevant systems are handled in this chapter.

2.1 Adaptive Cruise Control

ACC controls the speed of a vehicle, without any communication with other vehicles. In addition to Cruise Control (*CC*, which controls the speed of a vehicle, so that the set speed, indicated by the driver, is maintained) *ACC* is used to obtain a safe inter-vehicle distance to the predecessor, while following the predecessor's velocity profile.
In [12] the authors present a good overview about the physical layout, different functions and some disadvantages of this system. The components that are required for *ACC*, are: an *ACC* Module (To process radar information), an Engine Control Module (to control vehicle's speed), a Brake Control Module (for applying brakes when requested), an Instrument Cluster (to Process Cruise Switches), a CAN (Controller Area Network: a wire bus to transmit and receive data) and Cruise Switches (buttons to allow driver to command *ACC* operation).
The four main advantages of using *ACC* are [12]:

- 1. Comfort: relieves the driver from carefully decelerating and accelerating
- 2. Increasing safety: in case a driver is distracted, the system could avoid collisions with the predecessor
- 3: Traffic efficiency increases, since vehicles will smoothly follow each other (decreasing the change of traffic jams)

In [13], the *ACC* methods are elaborated into more detail. In Fig. 2.1 the block diagram of an vehicle, equipped with *ACC*, is given.

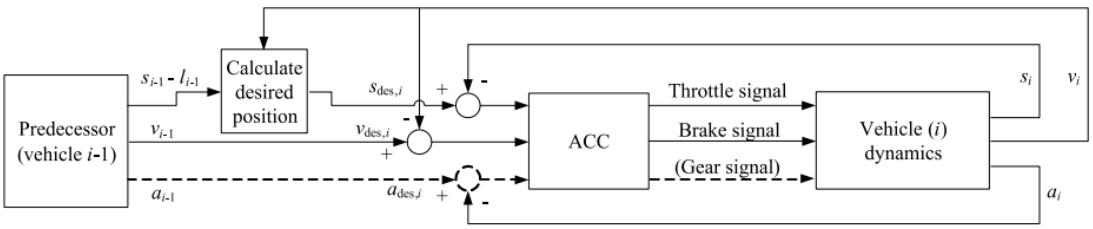

Figure 2.1: *Block scheme of ACC [13]*

The outputs of the *ACC* system are: throttle signals, brake signals and in case the vehicle is equipped with an automatic gearbox, also gear signals are transferred to the vehicle. The inputs to the *ACC*

system are the errors (in position, velocity and acceleration). The desired inter-vehicle distance to the predecessor is given as [13]:

$$d_{des,i,i-1}(t) = d_0 + (h_0 - c_h(v_{i-1}(t) - v_i(t))) \cdot v_i(t) \tag{2.1}$$

where d_0 is a minimum headway distance, h_0 is a constant headway time, v_i is the ACC vehicle's speed, v_{i-1} is the speed of the predecessor and c_h is a constant.
After determining the target, the controller is designed. The output of the PID controller is given [13]:

$$u_{tb}(t) = k_s \cdot (s_{des,i}(t) - s_i(t)) + k_v \cdot (v_{i-1}(t) - v_i(t)) + k_a \cdot (a_{i-1}(t) - a_i(t)) \tag{2.2}$$

where k_s and k_v are positive design constants and k_a is one or zero (in case acceleration is not taken into account). $s_{des,i}$ and s_i are the desired and actual positions, respectively. a_i and a_{i-1} are the accelerations of the controlled vehicle and the predecessor, respectively.

2.2 Cooperative Adaptive Cruise Control

An extension to ACC is Cooperative Adaptive Cruise Control ($CACC$), where a vehicle uses transferred information provided by the preceding vehicle about its acceleration. In addition to ACC (where $RADAR$ and $LIDAR$ measurements are used to estimate preceding vehicle's velocity profile), in $CACC$ the acceleration of the predecessor is used as feed-forward in the control loop. The information about the predecessor's acceleration is transferred via Wireless Access in Vehicular Environments (WAVE), a vehicular communication system.
ACC systems may exhibit string unstable traffic flows in case inter-vehicle distances are small: oscillations in traffic flows are amplified in up-stream direction (if the string's the front vehicle starts decelerating, each vehicle in the string will decelerate more than the predecessor). The main advantage of $CACC$ is that in fact the reaction- or response time is shortened, ultimately improving string stability.

String Stability

In $CACC$, the minimal inter-vehicle distance (or time gap in this context) is determined by investigating the String Stability, which is described as the 'attenuation of the effect of disturbances, e.g., velocity variations, over the vehicle string' [14]. It shows the velocity profiles of a string of vehicles to the input (change in velocity) of the string's front vehicle.
In this case, a string of six equal vehicles is investigated. The first vehicle (host vehicle) suddenly starts braking. It appears that string stability is influenced by the ability to communicate ($CACC$ vs ACC) and that the response time determines the stability of the string.
Stability is investigated based on the transfer function, described with Γ. Based on the block scheme of a $CACC$ system [14], Γ in Laplace Domain is given as:

$$\Gamma_{CACC}(s) = \frac{1}{H(s)} \frac{D(s) + G(s)K(s)}{1 + G(s)K(s)} \tag{2.3}$$

where $H(s)$ (the spacing policy transfer function), $G(s)$ (the system transfer function), $K(s)$ (the controller) and $D(s)$ (a delay) are given as:

$$H(s) = hs + 1 \tag{2.4}$$

$$G(s) = \frac{1}{s^2(\tau + s)} \tag{2.5}$$

$$K(s) = k_p + k_d s \tag{2.6}$$

$$D(s) = e^{-\theta s} \tag{2.7}$$

Here, θ is the communication delay ($\theta = 0.02s$ [14]). h is the headway time, k_p and k_d are the control parameters that have to be tuned, and τ is a vehicle time constant ($\tau = 0.1s$, according to [14]). In

case the control system requires a rational transfer function considering the delay θ, a Padé approximation for dead time is applied.
Considering strict stability, two conditions are involved: the Complementary Sensitivity $\Gamma(s)$ is required to have Bounded energy ($\mathcal{H}_\infty$ norm) and an impulse response $y(t)$ is required to have Bounded amplitude ($\mathcal{L}_1$ norm) so that [14]:

a. Strict $\mathcal{L}_2$ string stability if and only if $||\Gamma(s)||_{\mathcal{H}_\infty} \leq 1$

b. Strict $\mathcal{L}_\infty$ string stability if and only if $||y(t)||_{\mathcal{L}_1} \leq u(t)$

dCACC
An extension to $CACC$ is the so-called 'degraded $CACC$' ($dCACC$). In this case, there is no wireless connection, but the estimated acceleration of the vehicle in front is used as feed-forward. In [14] the authors give a clear overview about the method to implement $dCACC$. A Kalman Filter is used to estimate the states of the predecessor. The plant is given as:

$$\dot{x}(t) = Ax(t) + Bu(t) \tag{2.8}$$
$$y(t) = Cx(t) + v(t) \tag{2.9}$$

where A is the system matrix, B is the input matrix and C is the output matrix. $x(t)$ is the state, $u(t)$ is the input and $y(t)$ is the output of the system.
In Fig. 2.2, 2.3 and 2.4 the results are shown, using a step in velocity of $1m/s$. In Fig. 2.2, the string velocity behaviour for the five vehicles is plotted, in case ACC is used. It shows the influence of having no communication: the overshoot is about $1m/s$, while the settling time is 28 seconds.

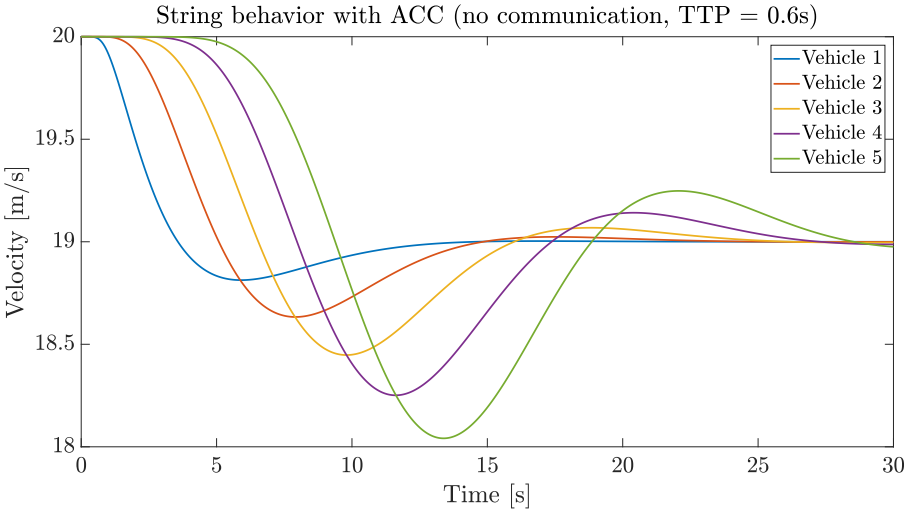

Figure 2.2: *Step response of ACC over time*

In Fig. 2.3, using $CACC$ with a delay $\theta = 0.06$s and a Time to Predecessor (TTP) of 0.6s, the stability of the string of vehicles is shown. After six seconds the oscillation is damped out, resulting in a stable velocity profile.

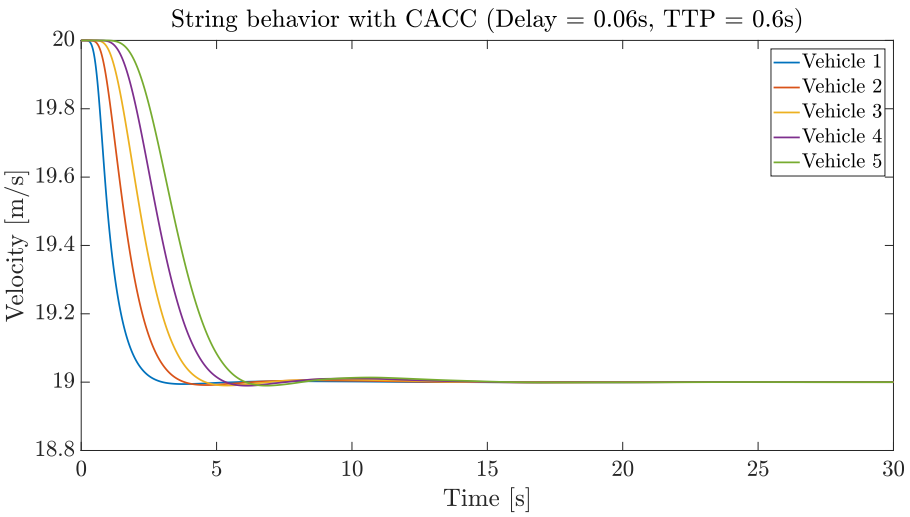

Figure 2.3: *Step response of CACC over time*

Fig. 2.4 shows the results using *dACC*, here the amplitude of the oscillation is lower with respect to *ACC*. The settling time compared to ACC is lower (settling time is 20 seconds).

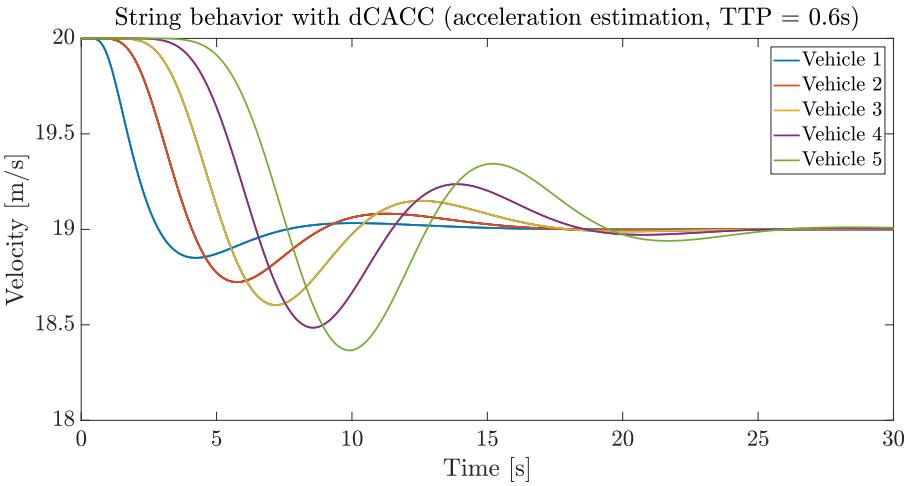

Figure 2.4: *Step response of dCACC over time*

The values for L_2 and L_∞ define the minimal time gap that is required.
In Fig. 2.5 the error in the minimum velocity (compared to the predecessor) is plotted for each time gap h (L_∞ norm). For $h > 1.12s$ each individual vehicle is perfectly following the vehicle in front (no overshoot in the velocity).

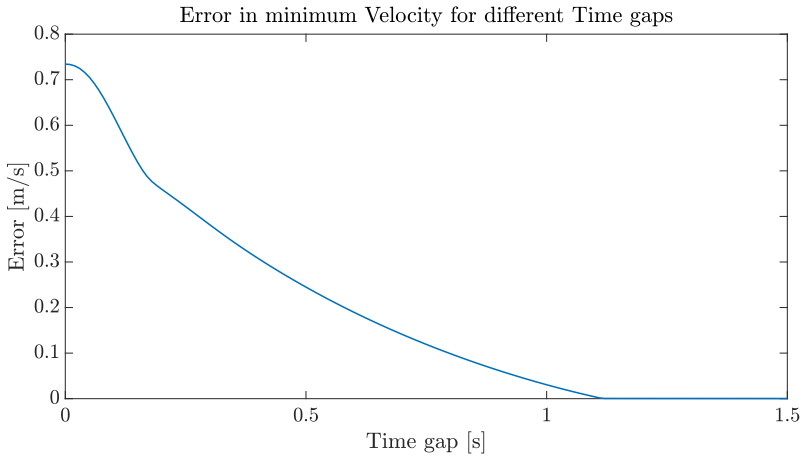

Figure 2.5: *Error in minimum velocity for different Time Gaps, using dCACC*

Relevance
The main disadvantage of $CACC$ are the implementation costs: to make these systems work, all road users have to be equipped with the transferring software. This implementation also takes much time, especially because it is re work both in existing- and new vehicles. Moreover, the risks are high (possibilities to hack the communication, failure of the systems). Because of the disadvantages mentioned above, in this project it is assumed that there is no communication available between the vehicles.

2.3 Autonomous Driving Control

Autonomous driving control is separated in Lateral Control and Longitudinal Control.

2.3.1 Lateral Control

Lateral Control controls the lateral position of the Host vehicle. The goal is to obtain a smooth lane-switching behaviour. Considering automated lateral lane changing, three levels can be distinguished:

1. Driver indicates he wants to take over, the systems investigates if a lane change manoeuvre is safe. The lane change is performed in case safety with respect to the other traffic is obtained.
2. Vehicle gives a signal to the driver that overtaking is possible, the driver has to accept this. After that, the Host vehicle will perform the lane change.
3. Vehicle will automatically perform a lane change, no driver input needed.

In [15], the authors give a clear overview of the Automated Lane Change (ALC) system, and a controller is presented for autonomous lane change manoeuvres. Currently, the system is usually activated when the turning indicator is tipped by the driver (SAE level 1 and 2, see Fig. 1.1).

Merging
In [16], Cao et al. investigate a merging problem. Here, a gap selection- and path generation method is proposed when one vehicle switches to a lane with multiple vehicles. A model predictive control method is used.
The road centrelines are described first. Lane 1 is the main lane, the y-coordinate y_1 (in meter) of this lane is given as:

$$y_1 = 0 \tag{2.10}$$

Considering lane 2 (the merging lane, with an angle k with respect to the main lane), the y-coordinate y_2 is given as:

$$y_2 = k(x - \beta) \tag{2.11}$$

where k is the angle of lane 2 and β is the location of the interception of lane 2 on the x-axis (the x-axis is the longitudinal direction of lane 1).
The curve which the merging vehicle will have to follow is required to be smooth, and the y-coordinates y_3 are given as:

$$y_3 = \frac{k}{2}\Big((x - \beta) - ((x - \beta)^2 - \frac{\alpha}{k})^{\frac{1}{2}}\Big) \tag{2.12}$$

where α is the design parameter that describes the steepness of the curve. After assigning the vehicles dynamics, the merging problem is formulated:

$$min\Big(J = \int_t^{t+T} L(x(\tau), a(\tau))d\tau\Big) \tag{2.13}$$

subject to

$$a1_{x,min} \leq a1_x \leq a1_{x,max} \tag{2.14}$$
$$an_{x,min} \leq an_x \leq an_{x,max} \tag{2.15}$$

where $a1...an$ represent the bounded accelerations of all vehicles. Here, vehicle 1 merges into the main lane. The penalty function L is described as [16]:

$$L = L_r + L_b + L_v + L_a \tag{2.16}$$

where L_r is applied in order to ensure that the relative distances between the vehicles is big enough (to obtain safety), L_b is a available moving area for the merging vehicle. L_v is introduced so that the other vehicles will try to run at the desired, initial velocities. L_a describes the accelerations: in regular merging, the accelerations should be minimized.
The procedure to solve this problem, is described as follows [16]:

1. Set $\tau = t$ and measure states.
2. Solve the optimization problem, so minimize J.
3. Update acceleration.
4. Set $t = t + h$ and go back to step 2.

A Kalman filter is used to estimate the (relative) accelerations between a host vehicle and leading vehicle. The state vector $X_1(k)$ and observation vector $Z_1(k)$ are given as [17]:

$$X_1(k) = A_1X_1(k - 1) + B_1a_{rel}(k - 1) + W_1(k - 1) \tag{2.17}$$
$$Z_1(k) = H_1X_1(k) + V_1(k) \tag{2.18}$$

Here, A_1 and B_1 are the system matrices, W_1 and V_1 represent the noise on the state and observation, respectively. $a_{rel}(k-1)$ is the estimation of the relative acceleration from the previous solution. Using a convex quadratic Approximation, the problem is solved. The paper 'presents a model predictive based longitudinal controller for autonomous driving, while taking lateral interruptions into account' [17].

2.3.2 Longitudinal Control

To perform a lane-change, the Host is required to have the correct (relative) position and velocity on the highway. In [18] a prediction- and cost function based algorithm for automated vehicles is presented. The overall driving ability is separated into three modules: distance keeper, lane selector and merge planner. In the applied algorithm a set of candidate strategies is generated (e.g. assigning different accelerations to the Host) and the results are compared.

A 'prediction engine' is used to accurately predict the movements of other vehicles. The velocity of the Host vehicle is updated:

$$v_0(t + \Delta T) = v_0(t) + a_{cmd}\Delta T \tag{2.19}$$

where ΔT is the time step, $v_0(t)$ is the velocity on a previous time step and a_{cmd} is the commanded acceleration. For each vehicle in the area, the distance d_i to the Host is determined:

$$d_i(t + \Delta T) = d_i(t) + (v_i(t) - v_0(t))\Delta T \tag{2.20}$$

Limitations on the maximum allowed speed are taken into account.

Cost functions are used to determine which commanded actions are required to satisfy different desired situations. Examples are:

- Progress Cost
- Comfort Cost
- Safety Cost

For each cost function, using the prediction engine the costs are calculated and a minimum is found, which describes the optimal driving strategy.

Distance keeper
The goal of this function is to keep the inter-vehicle distance close to d_{des}, which is described as:

$$d_{des} = D_{min} + k_{v,gain}v \tag{2.21}$$

where D_{min} is the minimal inter-vehicle distance, and the term $k_{v,gain}v$ is a velocity-dependent increasing term.

Lane Selector
The lane selector is used to determine whether a overtaking manoeuvre will result in arrival time improvements. A virtual destination is placed before the host vehicle.

Merge Planner
The rule of the Merge Planner is to execute adjustments and allow the car to merge if safety is satisfied. The costs are progressed based on execution time and final travelling distance.

Longitudinal Vehicle Dynamics Control
In [19], an automated vehicle guidance strategy is presented, focussing on longitudinal control. The longitudinal vehicle motion is described as:

$$m\dot{v} = F_p - F_a - F_g - F_{rr} \tag{2.22}$$

where m is the vehicle mass, $\dot{v}$ is the longitudinal acceleration and F_p is the propelling force, produced by the engine. F_a is the aerodynamic force ($F_a = \frac{1}{2}\rho C_d v^2$ with ρ the density of air and C_d the drag coefficient), F_g is the gravitational force due to road slope θ ($F_g = mgsin(\theta)$) and F_{rr} is the rolling resistance ($F_{rr} = C_r mg$ with C_r the rolling resistance coefficient).

These dynamics are combined with gear ratios and the engine power. A non-linear longitudinal controller is built, based on a Lyapunov approach. This work can be used to accurately simulate vehicle's longitudinal dynamics.

2.4 Potential fields

Proposed solutions for path planning of autonomous vehicles are so-called *potential fields*. These fields are constructed via a superposition of different potential functions. In robotics, this method is often used. In their paper [20], Yi and Wang present a method for path planning in robotics, using potential fields to avoid obstacles and conduct path planning. However, only static environments are considered, while highway driving includes dynamic environments.

The method assigns to each component on the highway (like road edges, road lanes and other road users) a potential function (the height, length and width of each function will depend on the type of obstacle). All functions are added in a global field to construct the potential field. The optimal driving path is determined by following the steepest negative gradient [21].
In [22] a potential field method is used in combination with elastic bands. Based on a hazard map (or potential field) an elastic band is determined, along which the vehicle will move. The elastic band is a set of springs that execute a net force on the controlled vehicle, forcing it to move in a certain optimal direction.

Advantages of using potential fields are:

- Simulations are not limited to number of scenarios that are trained on forehand. For example, when an animal is crossing the highway, based on (radar) information about position and size, a potential function will be assigned to that obstacle.
- No limit on the number of obstacles. Each obstacle in the potential field will locally contribute to the potential field.
- The calculation costs using Potential Fields are relatively low, even in the case when various types and a significant number of obstacles is taken into account. Once the potential field has been generated, the path planning proceeds fast, since it only requires calculation of gradient factors [23].
- Different types of obstacles can be modelled. For example, a distinction between crossable (bumps) and non-crossable obstacles (other road users) is made. [24]

However, potential functions are not able of showing vehicle behaviour for a longer distance. A potential function of a car will disturb the potential field that is noticed at the controlled car, indicating that a gap behind an approaching vehicle from the rear is not noticed. This indicates that the use of Potential fields does not allow for long-term path control.

2.5 Acceleration characteristics of other road users

To model and simulate the Host dynamics, it is required to investigate how other road users are responding in different situations. In case the Host wants to merge in front of a vehicle driving with a different (higher) speed, the reaction of the vehicle behind determines the inter-vehicle distance that should be used as a bound to the controller.

2.5.1 Human Driver Car-following Models

The driving and car-following behaviour of the other vehicles can be modelled using a human driver model [25]. Treiber et al. proposed a human driver model named the Intelligent Driver Model (IIDM). It results in an acceleration, which is a continuous function of the current velocity $v(k)$ (for each vehicle k), the gap length L_{gap} and the velocity difference $v(k-1)-v(k)$ to the leading vehicle:

$$a_x(k) = a_{max}\Big[1 - \Big(\frac{v(k)}{v_{max}}\Big)^{\delta} - \Big(\frac{s^*}{\Delta x}\Big)^2\Big] \tag{2.23}$$

Here, a_{max} is the maximum acceleration, δ is the acceleration exponent, v_{set} is set speed and s^* is 'the desired minimum gap', which is given as:

$$s^* = s_0 + v(k)T_{des} + \frac{v(k)(v(k) - v(k-1))}{2\sqrt{a_{max}b}} \tag{2.24}$$

where s_0 is the standstill distance, T_{des} is the desired headway time and b is the desired acceleration. In Table 2.1 the standard Model parameters for the IIDM model are given (calibrated for the specific situation described in the article).

Table 2.1: *IIDM model parameters*

Parameter	Description	Value
v_{set}	Set speed $[km/h]$	120
T_{des}	Desired headway time $[s]$	1.5
a_{max}	Maximum acceleration $[m/s^2]$	0.73
b	Desired deceleration $[m/s^2]$	1.67
δ	Acceleration exponent [-]	4
s_0	Standstill distance $[m]$	2

In [25] some IIDMs are presented. Fig. 2.7 shows the gap length, velocity and acceleration of a vehicle responding to a merging vehicle, both for ACC (left) and an IIDM (right).

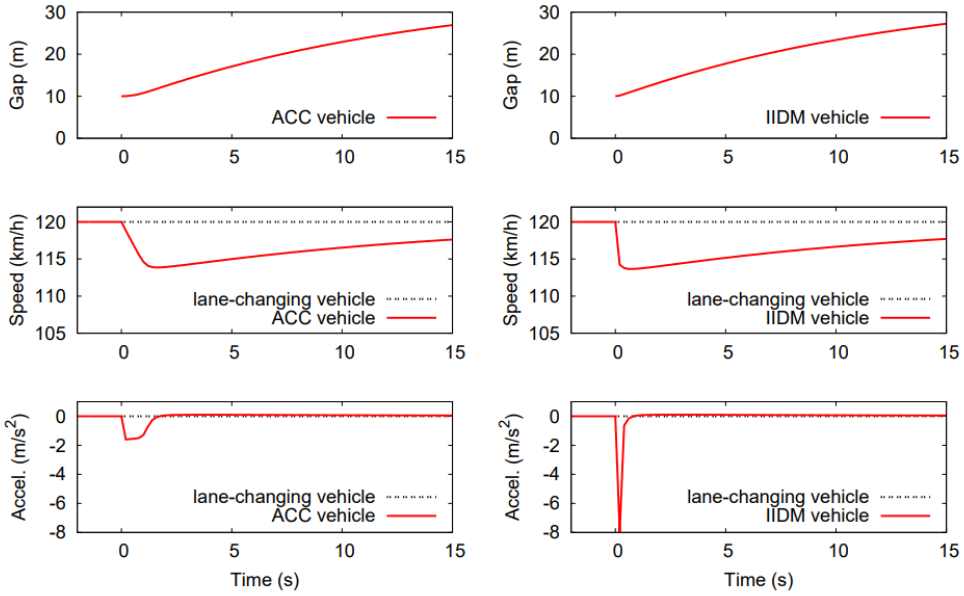

Figure 2.6: *Response of an ACC and an IIDM vehicle, on a merging vehicle driving with 120 km/h [25]*

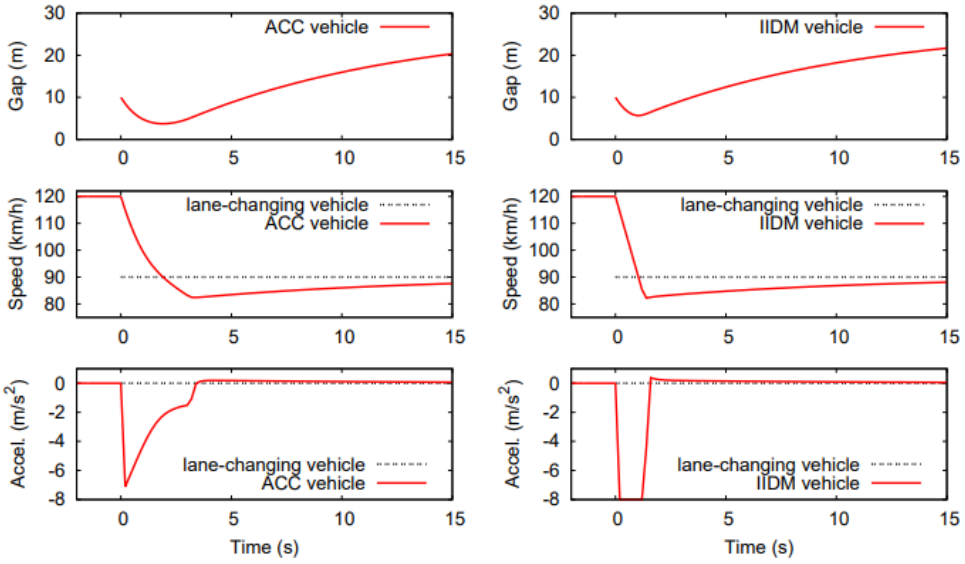

Figure 2.7: *Response of an ACC and an IIDM vehicle, on a merging vehicle driving with 90 km/h [25]*

Dependent on the tuning variables *ACC* and IIDM will give different results. About *ACC*, it is concluded: 'This models a behaviour similar to the human reactions to brake lights, but in a continuous rather than in an off-on way. (...) In summary, the *ACC* model can be considered as a minimal fully operative control model for *ACC* systems. With minor modifications, it has been implemented in real cars and tested on test tracks as well as on public roads and highways.' [25] p. 199.

2.6 Measurement Systems

The inputs for the path-prediction controller are consists of (processed) measurement data (especially relative velocities and distances). In this section, the most important sensors or measurement systems that are used in semi-autonomous vehicle, are investigated: RADAR, LIDAR and Camera. For each system, the relevant advantages and disadvantages are elaborated.

2.6.1 RADAR

RAdio Detection And Ranging (RADAR) uses radio waves that are transmitted and reflected by different surfaces [26]. After reflection the waves are received again and processed by the system. The distance and relative speed to objects, are determined based on the time-of-flight.

Advantages
Advantages of RADAR systems are [26]:

- All-weather solution: weather conditions (like snow, smog) do not influence the functioning of RADAR systems.
- Not sensitive to varying lighting conditions (night/day, driving into a tunnel)
- Long ranges are possible (Long Range Radar (*LRR*) can measure up to 250 m)
- Fast determination of distances (using the time-of-flight) and relative velocities (using the Doppler effect)

In this project, the *LRR* is used, allowing the Host to predict its path over a considerable time span.

Disadvantages
Disadvantages of RADAR systems are [26]:

- RADAR-based systems cannot recognize and classify objects: objects consist of a number of reflecting points. A regular car is equipped with a radar system that does not measure vertically
- In case of short wavelengths, it is difficult to detect small objects
- Interference with other radar systems influences the accuracy of the measurements

2.6.2 LIDAR

The sensing method of LIght Detection And Ranging (or LIDAR) is comparable with RADAR. A LIDAR system uses laser pulses to determine the distance to an object using the time of flight. By numerically differentiating the distance signal, the relative velocity is obtained.

Advantages
Advantages of LIDAR are [27]:

- Not effected varying lighting conditions (night/day, driving into a tunnel)
- Can measure vertically
- Due to smaller wave lengths, smaller objects can be sensed and improved object recognition is obtained

Disadvantages
The disadvantage of a LIDAR systems are:

- Still, LIDAR systems are expensive to produce [28]
- Strongly affected by bad-weather conditions [27].

2.6.3 Camera

A camera is an optical sensor system. Currently, various new cars are equipped with front-looking cameras for traffic sign recognition.

Advantages
The main advantages of cameras are:

- Low cost solution
- The recognition of the environment is accurate (other vehicles, lane markers)
- Cameras are rich in information (they can measure colours, shapes and text)

Disadvantages
The disadvantages of cameras are:

- Strongly affected by changing light conditions
- Strongly affected by bad-weather conditions (rain, smog etc.)
- Increasing computational costs: depending on the resolution of a camera, the processing times will increase in case the required data accuracy increases

Autonomous driving

For automated driving (SAE Levels 3-5, see Fig. 1.1) at least a combination of the two measurement systems is required:

1. A RADAR system to determine the relative positions and differences in velocities (used for path prediction).
2. A camera system for scene recognition: lane markers and objects (cars vs. trucks).
3. Both systems are required to provide a 360 degree scene recognition of the environment.

In this project it is assumed that accurate measurement data from the two measurement systems mentioned above (RADAR and Camera) is available, indicating that for all vehicles in the measurement range the positions and the velocities are known.

2.7 Measurement uncertainties

This Section deals with the influence of uncertainties in the measurements. In each sensor measurement (RADAR, LIDAR and Camera) uncertainties are present influencing the controller inputs and consequently the Host's driving behaviour. The accuracy of measurements determines the control algorithm in an autonomous vehicle.
To use the sensor data in the controller, first the analogue sensor outputs are converted to a digital signal (A/D converter). After that, the digital signal is processed in order to obtain required data that is used by the controller.

Calibration
The sensors, including the A/D converter, are calibrated. In general, the errors in the Digital signal can be classified as Gain errors and Offset errors. These errors are calibrated using the data sheet of an A/D Converter. Offset errors are usually bipolar and often expressed in an A/D Converter data sheet in terms of millivolts' [30].

Signal Processing
After Converting, the digital signal is processed. Three separate steps are distinguished: Preprocessing, analysing, and post-processing. The error in the measurement signals propagates through the Processing system. During processing, three main items are involved: signals, uncertainties and the Digital Processing block. A discrete signal is described as a series of measurements (described by vectors p) over time. The Digital Signal Processing (DSP) block is described as a function $F(p) \rightarrow q$ [31]. q is the output of the Signal Processing system. In general, the uncertainty (or noise) is modelled using a Gaussian distribution [32]. The probability density function N of a Gaussian random variable x is given by:

$$N(x|\mu,\sigma) = \frac{1}{\sigma\sqrt{2\pi}} e^{-\frac{(x-\mu)^2}{2\sigma^2}} \tag{2.25}$$

where μ is the mean and σ is the standard deviation. Using the variance Σ, Eq. 2.25 is written as:

$$N(x|\mu,\Sigma) = \frac{1}{\sqrt{(2\pi)^k|\Sigma|}} e^{-\frac{1}{2}(x-\mu)^T\Sigma^{-1}(x-\mu)} \tag{2.26}$$

where Σ is the variance ($\Sigma = \sigma^2$). The mean μ of noise is zero, indicating that $N(x|\mu,\Sigma)$ becomes $N(0,\Sigma)$. If the input of an input signal p is Normally distributed, the output is Normally distributed, using the Propagation of Uncertainty [33].
The output q of a linear DSP function is given as:

$$q = Ap + b = F(p) \tag{2.27}$$

where p is the input, b is a vector and A is the system matrix. $F(p)$ is the Digital Signal Processing (DSP) function.

The next steps are taken in order to estimate the propagation of the error on the output Σ_{out}. In the first place, the uncertainty in input Σ_{in} is determined (the variance in input signal). Next, the relation between input and output F is investigated ($F = \frac{q}{p}$). After that, the Jacobian J_F of the function F is determined. Finally, the uncertainty in input signal propagates via $\Sigma_{out} = J_F \Sigma_{in} J_F^T$.

2.7.1 Sensor accuracy

The accuracy of each sensor indicates how closely the output (or displayed reading) from a sensor will match the real value. The difference between the real value and the observed value is called the error.

RADAR

Considering a RADAR system, 'the stated value of required accuracy represents the uncertainty of the reported value with respect to the true value and indicates the interval in which the true value lies with a stated probability. The recommended probability level is 95 percent, which corresponds to two standard deviations of the mean for a normal (Gaussian) distribution of the variable ' [34]. The update rate of a RADAR system is around $60 \sim 100$ milliseconds.

LIDAR

The accuracy of LIDAR is higher than the accuracy of RADAR, due to the fact that the wavelengths of LIDAR are smaller (see Section 2.6.2). The Velodyne VLP-16 LIDAR system has a 360 deg. horizontal field of view and a 30 deg. vertical field. The typical accuracy is $\pm$ 3cm [29].
The update rate of a LIDAR system is comparable to RADAR ($60 \sim 100$ milliseconds).

2.7.2 Sensor Fusion

In general, the output analogue data from sensors are noisy, indicating that the measurement of an object is facing an error. To improve the accuracy of the full system, a probabilistic approach is used: sensor fusion. 'Sensor fusion is the combining of sensory data or data derived from sensory data such that the resulting information is in some sense better than would be possible when these sources were used individually' [35]. The advantages of sensor fusion are: [35]

Robustness and reliability: Multiple sensor suites do have an inherent redundancy which enables the system to provide information even in case of partial failure.

Extended spatial and temporal coverage: One sensor can look where others cannot, and one sensor can perform a measurement while others cannot in certain situations.

Increased confidence: A measurement of one sensor is confirmed by measurements of other sensors covering the same domain.

Reduced ambiguity and uncertainty: Joint information reduces the set of ambiguous interpretations of the measured value.

Robustness against interference: By increasing the dimensionality of the measurement space (e. g., measuring the desired quantity with optical sensors and ultrasonic sensors) the system becomes less vulnerable against interference.

Improved resolution: When multiple independent measurements of the same property are fused, the resolution of the resulting value is improved with respect to using a single sensors measurement. Resolution is the number of objects that the output data from a sensor can be broken down into, without any instability in the signal.

Sensor fusion Configuration

Sensor fusion networks are categorized according to the type of sensor configuration. Three types of sensor configuration are: [35]

Complementary: The separate sensors do not depend on each other, but are combined to create a more complete image of the considered domain. It provides information about multiple objects in the investigated domain.

Competitive: Each sensor measures the object, and provides independent data of the measured object. By fusion, accurate and reliable information about the objects is obtained.

Cooperative: A cooperative sensor network uses the information provided by two independent sensors to derive information that would not be available from the single sensors [35]. For example, two two-dimensional cameras can provide information to create a three-dimensional image.

Sensor fusion algorithms

Sensor fusion involves many aspects and methods, including Kalman filtering. The Kalman filter uses 'a mathematical model for filtering signals using measurements with a respectable amount of statistical and systematical errors. The filter uses a discrete-time algorithm to remove noise from sensor signals in order to produce fused data that, for example, estimate the smoothed values of position, velocity, and acceleration at a series of points in a trajectory' [35].
A comparable method is *Image fusion*, where one image is created using several separate images, taken from different camera's. The final image contains more information and is more accurate than the separate images. Using this method, the instant depth of objects is determined, using the disparity [31].

Conclusion

The presented method of fusion of sensor data 'offers a great opportunity to overcome physical limitations of sensing systems. An important point will be the reduction of software complexity, in order to hide the properties of the physical sensors behind a sensor fusion layer' [35]. In Chapter 4 the influence of uncertainties in the measurements is investigated.

Chapter 3

Defining an overtaking manoeuvre

This chapter deals with the modelling of the Host and the other traffic, and describes the longitudinal and lateral motions (which combined result in an overtaking manoeuvre) used in the simulations. First, the assumptions, definitions and criteria are given that are used for modelling and which are taken into account in the simulations. Next, the modelling of the longitudinal and lateral motions is described, and an overtaking manoeuvre is presented.

3.1 Assumptions

In this section, a list of assumptions is defined.

- **Straight highway:** A straight highway is considered, since the focus is on longitudinal control. A curved highway does hardly influence the longitudinal strategies (adding curves to the highway model would mainly influence the lateral control).
- **Flat highway:** It is assumed that the highway is perfectly flat (no slopes).
- **Four-lane highway:** The highway that is considered, has four lanes (two in each direction).
- **Right-Hand Traffic (RHT):** Right-Hand Traffic is assumed, like it is the situation in 68% percent of all countries world-wide [36].
- **Start overtaking manoeuvre:** The overtaking manoeuvre is started when:

  1) The longitudinal velocity increases or,

  2) The lateral motion is started. The Host performs a lateral motion when its lateral position is no longer equal to the initial lateral position.
- **End overtaking manoeuvre:** The overtaking manoeuvre is ended when:

  1) The lateral position is equal to the centre line of the adjacent lane and,

  2) The longitudinal acceleration is equal to zero.
- **One lateral movement in each simulation:** Only one lateral movement is investigated. Since the focus is on longitudinal control for preparing a lane change, merging back to the initial lane after overtaking the predecessor is not investigated.
- **Modelling vehicles:** All vehicles are modelled as point masses, indicating that there are no (internal) dynamics involved. This indicates that roll-over behaviour and rotations around the vertical axis are not investigated.
- **Acceleration, velocity and position other road users:** The acceleration of the other road users is assumed to be zero, initially. This indicates that a 'steady-state' behaviour is obtained, although the other road users will drive with different initial velocities compared to the Host.

- **Behaviour other vehicles:** The behaviour of other vehicles is simulated using *ACC*. *ACC* (with the right tuning parameters) provides comparable results to actual human driving characteristics (see section 2.5).

3.2 Definitions

In this section, definitions that are used throughout the project, are given. Included are: the definitions of 'smooth driving' and TTC and TTP. Also the used simulation parameters are given.

3.2.1 Smooth driving

Mathematically, a function is called 'smooth' (to a certain order k, for a certain domain) when the derivatives (to the k-th order) are continuous. A function is C^k smooth if the derivatives to the k-th order are continuous. To drive the Host 'smoothly', the longitudinal position is taken third order smooth (there is a step in the derivative of the acceleration, called the jerk).
Practically, the goal is to obtain smooth or comfortable driving. This includes minimizing the accelerations. Unnecessary accelerating and braking is avoided, as well as unnecessary lane changing.

3.2.2 Positions, velocities and accelerations

- Initially, the Host vehicle is driving with initial velocity $V_{H,0}$. The initial position is $X_{H,0}$. The initial driving lane is $L_{H,0}$.
- Initially, the other vehicles i are driving with initial velocity $V_{i,0}$. The initial positions are $X_{i,0}$. The initial driving lane is $L_{i,0}$.
- Considering the Host vehicle, V_H is the longitudinal velocity, a_H is the longitudinal acceleration, $V_{H,y}$ is the lateral velocity and $a_{H,y}$ is the lateral acceleration.
- Considering the other vehicles i: V_i are the longitudinal velocities and a_i are the longitudinal accelerations (the other vehicles are assumed not to move laterally).

3.2.3 TTC and TTP

Generally, there are two relevant methods to describe the time to a moving object: the Time To Collision (TTC) and the Time To Predecessor (TTP). In this definition, the considered vehicles are driving in the same direction, on the same highway lane.

TTC
The TTC is defined using the positions and velocities of the Host and a Predecessor. The positions of the Host and the Predecessor are defined as:

$$X_P(t) = X_{P,0} + \int_0^t V_P(t)dt \tag{3.1}$$

$$X_H(t) = X_{H,0} + \int_0^t V_H(t)dt \tag{3.2}$$

where $X_P(t)$ and $X_H(t)$ (and $X_{P,0}$ and $X_{H,0}$) are the (initial) positions of the Predecessor and the Host, respectively. t is the time. $V_P(t)$ and $V_H(t)$ are the velocities of the Predecessor and the Host, respectively. The TTC is based on the actual velocities. The expression for TTC becomes:

$$TTC(t) = \frac{X_H(t) - X_P(t)}{V_P(t) - V_H(t)} \tag{3.3}$$

representing the time before the positions of the Predecessor and Host in Eq. (3.1) and (3.2) are equal. In this project, the TTC to the Predecessor is used to determine how much time is left to perform a lateral movement (this will be elaborated in Chapter 4).

A drawback of using the TTC to follow a vehicle is the fact that the TTC cannot be used when the velocities are equal, since in that case the TTC becomes infinity. This indicates that for vehicle following with a constant inter-vehicle distance, this method is not suitable, indicating the need for a second method.

TTP
The TTP incorporates the positions difference and the actual Host velocity V_H:

$$TTP(t) = \frac{X_P(t) - X_H(t)}{V_H(t)} \tag{3.4}$$

It defines the time the Host needs to travel to actual (or current) Predecessor's location.

3.2.4 Simulation parameters

Table 3.1 shows the main parameters and their values, used in the simulations. It is assumed that all vehicles (including the Host) are identical and have the same parameters. It is clear that all vehicles do have a length and width so that the criteria for collision avoidance are correctly taken into account.

Table 3.1: *Parameters and their values*

Parameter	Description	Value
g	Gravitational constant	9.81 m/s^2
L_v	Length vehicle	4 m
W_v	Width vehicle	2 m
M_v	Mass vehicle	1000 kg
W_l	Width highway lane	4 m
V_{max}	Max. speed	130 km/h
V_{min}	Min. speed	70 km/h
$T_{y,max}$	Max. overtaking time	20 s
T_r	Reaction time other traffic	1.5 s
$T_{r,h}$	Reaction time Host	0.5 s

3.3 Criteria

In this section, criteria are introduced that will be used to limit and evaluate the performance of the controller.

3.3.1 Maximal longitudinal jerk Host vehicle

Considering the typical acceleration profile, as represented in Fig. (3.8), a constant jerk is implemented. It appears that the value of jerk determines the level of comfort of an accelerating manoeuvre. In [37], Hoberock investigated the longitudinal comfort levels in public transportation, like electric buses. As a result, based on the participant's experiences, a jerk level of $0.30g/s \approx 3m/s^3$ is suggested to be the maximal comfortable jerk, beyond that it is 'unlikely that values of jerk would be acceptable for most public transportation' [37].

3.3.2 Minimal longitudinal distance to preceding vehicle

The minimal inter-vehicle distance is an important requirement to design the path for the overtaking manoeuvre. If the Host drives too close behind the Predecessor, a collision might occur if the Predecessor preforms an emergency stop).

Regulations and theory
Considering the minimal inter-vehicle distance DX, in the Netherlands the rule of thumb is that 'a

driver should be able to stop its vehicle within the distance in which the road is free and visible' [38]. In practice, it is advised to follow a vehicle on the highway with a time gap of at least two seconds. When driving at $V = 100km/h = 27.8m/s$, the minimal inter-vehicle distance $DX = 2 \cdot 27.8 = 56m$. A driver is fined when the following time is less than half a second (if $V = 100$ km/h, $DX = 13.9$m.), for the duration of at least half a minute [39]. In the Netherlands, on the highway A13 (a three-lane highway between Rotterdam and The Hague), in 2015 on average 5738 vehicles passed per hour, so that the average time gap is 1.9 seconds [40].

Since the reaction (or respond) time of automated system of the Host is smaller than the reaction time of an average human driver (the Host is equipped with Adaptive Cruise Control, which has a lower reaction time compared to a human driver), the required inter-vehicle distance between the Host and the Predecessor might be smaller (see section 3.3.7).

Calculation
Generally, a safe inter-vehicle distance D_{min} is calculated via:

$$DX_{min} = D_{min} + c \cdot V \tag{3.5}$$

where D_{min} is a minimum inter-vehicle distance when the velocity is zero, and a term $c \cdot V$ with a constant $c > 0$ which leads to an increasing gap for higher velocities. To determine this safe inter-vehicle distance when the vehicles are driving with different velocities, the stopping distances of the Host and the Predecessor are used. The reaction time (or response time, due to measuring, calculating and actuating, see section 3.3.7) of the Host is $T_{r,H}$ seconds. The stopping time t of a vehicle during constant (maximum) acceleration is given as:

$$t = \frac{V}{a_{x,max}} = \frac{V}{\mu g} \tag{3.6}$$

where V is the initial velocity, $a_{x,max}$ is the maximum deceleration, μ is the friction coefficient and g is the gravitational constant. The stopping distance of the Predecessor is:

$$S_P = V_P t \tag{3.7}$$

where V_P describes the Predecessor's velocity and t is the stopping time, see Eq. 3.6. Using the initial position $X_{P,0}$ of the Processor, the stopping distance S_P becomes:

$$S_P = X_{P,0} + \frac{V_P^2}{2\mu g} \tag{3.8}$$

The stopping distance S_H for the Host is given as:

$$S_H = X_{H,0} + \frac{V_P^2}{2\mu g} + T_{r,H} V_H \tag{3.9}$$

where $X_{P,0}$ and $X_{H,0}$ are the initial positions of the Predecessor and Host, respectively. The stopping distance of the Host is extended with a factor $T_{r,H} V_H$, defining the influence of the reaction time of the Host on the stopping distance.
To incorporate variations in available friction, braking force and weight, a minimal inter-vehicle distance is used: $D_{min} = 3m$. In practice, the Host does not have information of the variations, since the parameters of the vehicle in front are not known. When the stopping distances of the two vehicles are equal, D_{min} ensures that the final inter-vehicle distance is 3m. This results in a minimal inter-vehicle distance DX_{min} between the Host and its Predecessor:

$$DX_{min} = S_P - S_H - D_{min} = \frac{V_P^2 - V_H^2}{2\mu g} - T_{r,H} V_H - D_{min} = X_{H,0} - X_{P,0} \tag{3.10}$$

For increasing Velocity V_P, there is a critical velocity $V_{P,crit}$ for which the stopping distances are equal:

$$V_{P,crit} = \sqrt{V_H^2 + 2\mu g T_{r,H} V_H} \tag{3.11}$$

According to the equations, above the critical velocity the safe inter-vehicle distance indicates that the Host might drive in front of the Predecessor, which is not acceptable if initially the Host starts longitudinally behind the Predecessor. To prevent this, above $V_{P,crit}$, the minimal inter-vehicle distance is equal to: $DX_{min} = -D_{min}$.
Fig. 3.1 presents the required minimal inter-vehicle distance $DX_{min,P\rightarrow H}$ over time, using $\mu = 0.9$, $D_{min} = 2m$, $T_{r,H} = 0.5s$ and the Host velocity is $V_H = 80km/h$.

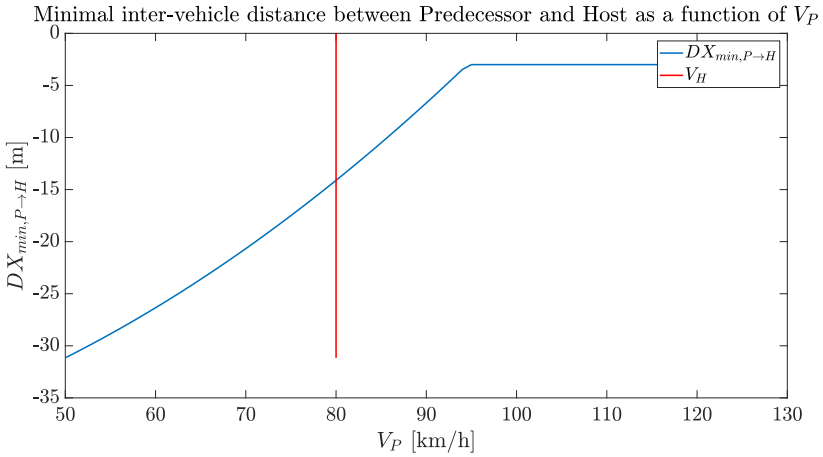

Figure 3.1: *$DX_{min,P\rightarrow H}$ as function of V_P*

Fig. 3.1 shows that for increasing velocity V_P, the inter-vehicle distance decreases. In this case, the critical predecessor velocity $V_{P,crit} = 26.27m/s$ (above $V_{P,crit}$, $DX_{min} = -D_{min}$).

3.3.3 Maximal longitudinal acceleration Host vehicle

The maximal longitudinal acceleration $a_{x,max}$ is physically limited by friction. Moreover, to achieve comfortable highway driving, $a_{x,max}$ is limited even more, which is elaborated in this Section.

Friction

The maximum longitudinal acceleration $a_{x,max}$ is physically limited by friction via:

$$M_v a_{x,max} = \mu F_z = \mu M_v g \tag{3.12}$$

so that the acceleration becomes:

$$a_{x,max} = \mu g \tag{3.13}$$

where M_v is the vehicle mass, μ is the tire-road friction coefficient and F_z is the vertical force.

Tire-road friction coefficient

The tire-road friction coefficient strongly depends on the type of the road and the weather conditions. Table 3.1 presents the the friction coefficients for some road types and for different conditions [41].

Table 3.1: *Tire-road friction coefficient μ for different roads and conditions*

Road type	**Dry**	**Wet**
Asphalt	0.8-0.9	0.5-0.7
Concrete	0.8-0.9	0.8
Ice	0.15	0.05

Assuming dry asphalt, the value for the friction that is used is in this project is $\mu = 0.9$.

Vertical loads
Considering a typical vehicle with length L_v, height h to Centre of Gravity (CG) , distance a from the front wheel to CG , distance b from the rear wheel to CG and mass M_v, the vertical loads on the front axle (F_{z1}) and rear axle (F_{z1}) during longitudinal acceleration a_x are given as:

$$F_{z1} = \frac{M_v g b}{L_v} - \frac{M_v a_x h}{L_v} \tag{3.14}$$

$$F_{z2} = \frac{M_v g a}{L_v} + \frac{M_v a_x h}{L_v} \tag{3.15}$$

Increasing acceleration leads to a higher vertical force on the rear axle and a lower vertical force on the front axle.

Front-, Rear- and All Wheel Driven vehicles
The maximal longitudinal acceleration also depends on the type of car: Front-, Rear- or All Wheel Driven (FWD,RWD,AWD).
For a FWD car, the longitudinal acceleration $a_{x,max}$ is limited by the vertical force on the front axle (F_{z1}, see Eq. 3.14):

$$a_x = a_{x,max} = \frac{F_{z1}}{M_v} = \frac{\mu g b}{L + \mu h} \tag{3.16}$$

In the same way, for a RWD car, using Eq. (3.15):

$$a_x = a_{x,max} = \frac{F_{z2}}{M_v} = \frac{\mu g a}{L - \mu h} \tag{3.17}$$

For AWD, the highest accelerations are possible, since $a_{x,max} = \mu g$. In practice the maximum longitudinal acceleration is limited by the available engine power and the friction forces (air resistance and rolling resistance). When the vehicle is driving at the highway, the there is no difference in FWD- or RWD vehicles (the acceleration is limited by the available engine power).

Comfort

The maximum Host acceleration $a_{x,max}$ is also limited by 'comfort criteria'. To obtain comfortable highway driving, the accelerations are limited by *comfort levels*. In [42], the ride comfort is investigated. The experienced comfortableness of the longitudinal- and lateral accelerations is investigated via measurements. The experiment was performed in China, with five different vehicles and different drivers with ages between 24 and 51 years. The heart rate was used to estimate the rate of comfortableness, while accelerometers and gyroscopes were used to collect the acceleration data. In Table 3.2 different comfort levels are given with their belonging maximum accelerations.

Table 3.2: *Relation Longitudinal Accelerations and Comfortableness [42]*

Long. Acceleration $[\frac{m}{s^2}]$	**Experienced Comfortableness**
$0 < a_x < 1$	Comfortable
$1 < a_x < 1.5$	Relative Comfortable
$a_x > 1.5$	Uncomfortable

The values in Table 3.2 are used to assign comfortable paths for the Host.

3.3.4 Maximum longitudinal deceleration Host vehicle

This section presents the physical- and comfort limits for braking, both for friction and comfort.

Friction

The maximum longitudinal deceleration that can be obtained, depends on the available friction. In theory, assuming the vehicles are equipped with an Anti-lock Braking System (ABS), the maximal deceleration $-a_{x,max}$ is given by:

$$-a_{x,max} = \mu g \tag{3.18}$$

Using $\mu = 0.9$ and $g = 9.81 m/s^2$, $-a_{x,max} = -8.3 m/s^2$. In the Netherlands, the top ten sold cars in 2017 are all equipped with FWD [43]. The FWD car is used in this project, indicating that the absolute deceleration limit is higher than the acceleration limit (braking is done via the four wheels).

Comfort

Based on the same experiment, in Table 3.3 the comfort levels and the belonging decelerations are given.

Table 3.3: *Relation Longitudinal Decelerations and Comfortableness [42]*

Long. Deceleration $[\frac{m}{s^2}]$	**Experienced Comfortableness**
$0 > a_x > -1.3$	Comfortable
$-1.3 > a_x > -2.5$	Relative Comfortable
$a_x < -2.5$	Uncomfortable

The values from Tables 3.2 and 3.3 are used in the controller. The friction limits are the 'strict' limits, while the driving behaviour is optimized for maximum comfort (minimal acceleration).

3.3.5 Maximum lateral acceleration Host vehicle

The lateral acceleration is limited by friction and comfort.

Friction

Laterally, the maximum acceleration $a_{y,max}$ is limited by the amount of lateral force that can be generated. While cornering, the slip angle α increases. For increasing α, the lateral tire force is limited by the grip of a tire (which is equal to μF_z). The maximum lateral acceleration is (omitting aerodynamic forces):

$$a_{y,max} = \frac{|F_{y,max|}}{M_v} = \frac{|M_v \mu g|}{M_v} = \mu \cdot g = 0.9 \cdot 9.81 = 8.83 m/s^2 \tag{3.19}$$

where M_v is the mass of the vehicle, μ is the friction coefficient and g is the gravitational constant (see Tab. 3.1)

Comfort

The Lateral acceleration is also limited by comfortableness, see [42]. In Table 3.4 the levels of comfort and the accelerations are given.

Table 3.4: *Relation Lateral Accelerations and Comfortableness [42]*

Lat. Acceleration $[\frac{m}{s^2}]$	**Experienced Comfortableness**
$0 < \|a_y\| < 1.65$	Comfortable
$1.65 < \|a_y\| < 2.85$	Relative Comfortable
$2.85 < \|a_y\| < 4.05$	Uncomfortable
$\|a_y\| > 4.05$	Unbearable

3.3.6 Combined friction and comfort levels

To determine the maximum possible (due to friction) or allowable (due to comfort) acceleration during combined motions (lateral and longitudinal), the resulting accelerations are compared with the comfort levels. In Fig. 3.2 the resulting limit levels (ellipses) are shown, based on the results from section 3.3.3, 3.3.4 and 3.3.5.

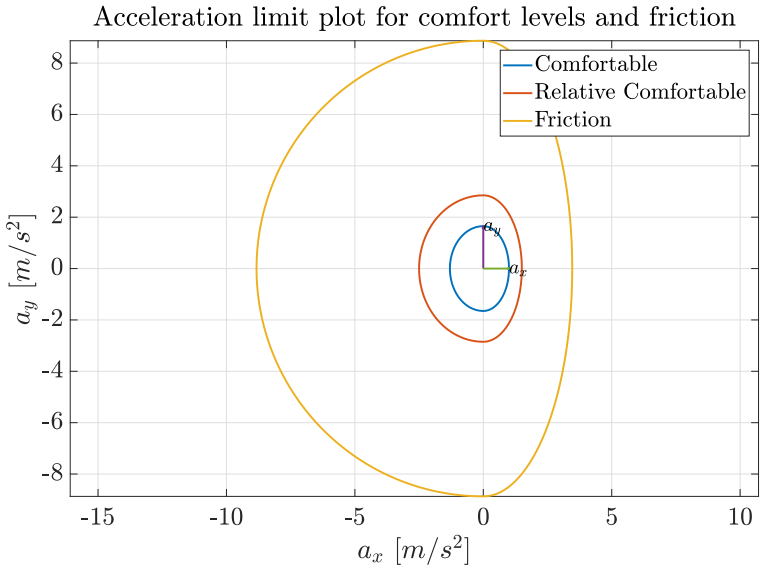

Figure 3.2: *Acceleration limit ellipses in (a_x, a_y) space*

The Friction limit for is the same ($-a_{x,max} = \mu g$, since braking is done via the four wheels). The Friction limit in Fig. 3.2 is asymmetric with respect to the vertical axis through zero, due to the fact that a FWD vehicle is investigated (an AWD vehicle results in a symmetric friction ellipse).

Resulting acceleration

The resulting acceleration a_r is defined as:

$$a_r = \sqrt{a_y^2 + a_x^2} \tag{3.20}$$

where a_x is the longitudinal- and a_y is the lateral acceleration. The resultant defines the combination of the two individual forces. To calculate the resulting acceleration, in Fig. 3.3 an overtaking manoeuvre is presented.

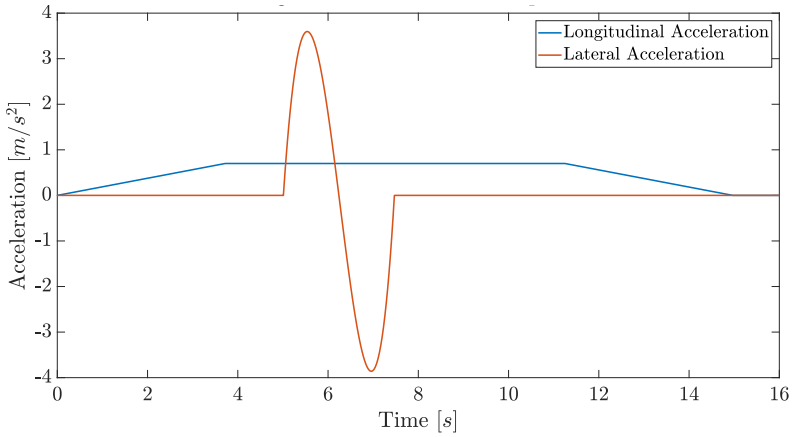

Figure 3.3: *A regular overtaking manoeuvre consists of a longitudinal- and lateral acceleration*

The inputs are: $T_y = 2.5$ seconds, $T_x = 15$ seconds, $T_{y,s} = 5$ seconds and $a_{x,max} = 0.8m/s^2$. The resulting accelerations are plotted in Fig. 3.4 (visualized with the vectors). The limit ellipses for comfortable- and relative comfortable accelerations are clearly violated (the resulting acceleration vectors are outside the circles defining the comfortable and relative comfortable levels), indicating that the performed overtaking manoeuvre is uncomfortable.

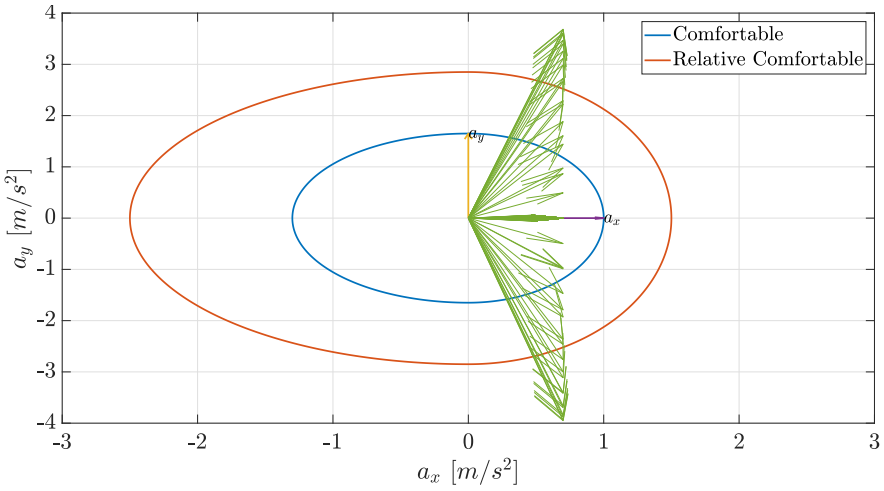

Figure 3.4: *Limit circles including resulting accelerations*

In Fig. 3.5 the resultants of the longitudinal and lateral accelerations are plotted as a function of time and lateral position. The black line indicates the lateral position, which is the origin of each vector. The colour of the vectors represent the Comfort level belonging to the specific resulting acceleration (green vectors represent comfortable accelerations, orange vectors represent relative comfortable accelerations and the red vectors represent uncomfortable accelerations).

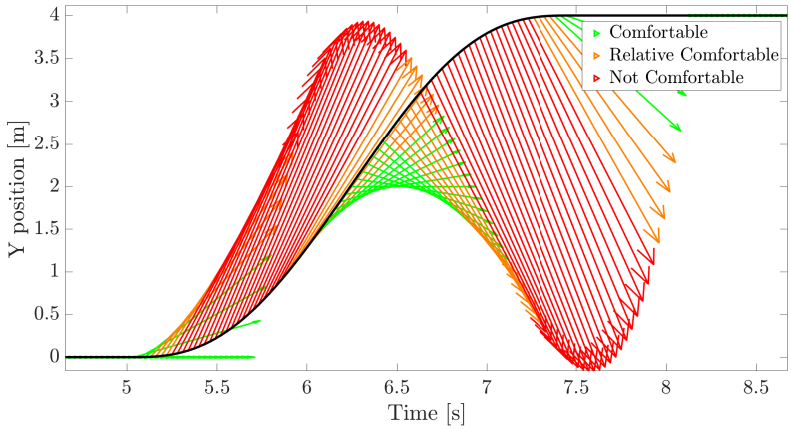

Figure 3.5: *Resulting acceleration including comfort levels*

Determining comfortableness of a manoeuvre

The comfortableness of an overtaking manoeuvre is based on the resultants of the combined longitudinal- and lateral acceleration, using the Root Mean Square (RMS). The RMS of a signal calculates the square root of the mean square of the values $\hat{y}_t$:

$$RMS = \sqrt{\frac{\sum_{n=1}^{N}(\hat{y}_t(n))}{N}} \tag{3.21}$$

where N is the number of samples (signal is in discrete time) and n represents a sample. In this context, finding the optimal path means reducing the value of RMS. Since the comfort lines are

ellipses in the (a_x, a_y) space, the longitudinal and lateral accelerations are scaled to the comfort limits, see Tables 3.2, 3.3 and 3.4. The RMS_c value (RMS value, scaled to comfort levels) is calculated via:

$$RMS_c = \sqrt{\frac{\sum_{n=1}^{N}(a_{r,s}(n))}{N}} \tag{3.22}$$

where $a_{r,s}$ is the scaled resulting acceleration and N is the duration of the manoeuvre (number of samples). The RMS_c calculates the obtained scaled resulting accelerations, which will be minimized in the controller.

Scaling
In the scaling process, the longitudinal acceleration a_x is divided by the longitudinal comfort levels, while the lateral acceleration a_y is divided by the lateral comfort levels from Tables 3.2, 3.3 and 3.4. Using scaling, the effect of inequality in experienced comfort during acceleration is taken into account (a certain acceleration a_x is less comfortable than a deceleration with $-a_x$).

The scaled resulting acceleration $a_{r,s}$ becomes:

$$a_{r,s} = \sqrt{\left(\frac{a_x}{C_{x,c}}\right)^2 + \left(\frac{a_y}{C_{y,c}}\right)^2} \tag{3.23}$$

where a_x and a_y are the longitudinal- and lateral acceleration vectors, respectively. $C_{x,c}$ and $C_{y,c}$ are the longitudinal- and lateral comfort levels, as defined in Table 3.2, 3.3 and 3.4.
This results in the following equation for the RMS_c:

$$RMS_c = \sqrt{\frac{\sum_{n=1}^{N}\left(\sqrt{\left(\frac{a_x(n)}{C_{x,c}}\right)^2 + \left(\frac{a_y(n)}{C_{y,c}}\right)^2}\right)^2}{N}} \tag{3.24}$$

The scaled resulting accelerations are normalized vectors, indicating that for each resultant the length L_r is determined (see Eq. 3.20). If $L_r > 1$, the resulting acceleration is outside the Comfort ellipse indicating that the motion is Relative Comfortable.
The scaling method is performed both for positive and negative accelerations (whose comfort criteria are different), and for the two Comfort levels: Comfortable and Relative Comfortable. The RMS_c value increases for increasing resulting accelerations, but does not take into account the length of an overtaking manoeuvre, since the sum of the square roots of the squared resultants is divided by the number of samples N.

Scaling process
In Figures 3.6 and 3.7 the scaling process is shown. Fig. 3.6, presents on the left, the applied combined motion (where the inputs are: maximum acceleration $a_{x,max} = 0.6m/s^2$, duration $T_x = 10$ s, duration of the lateral movement $T_y = 4$ s and the start time of the lateral movement $T_{y,s} = 8$ s). On the right, the resulting acceleration is plotted for the combined longitudinal- and lateral movement.

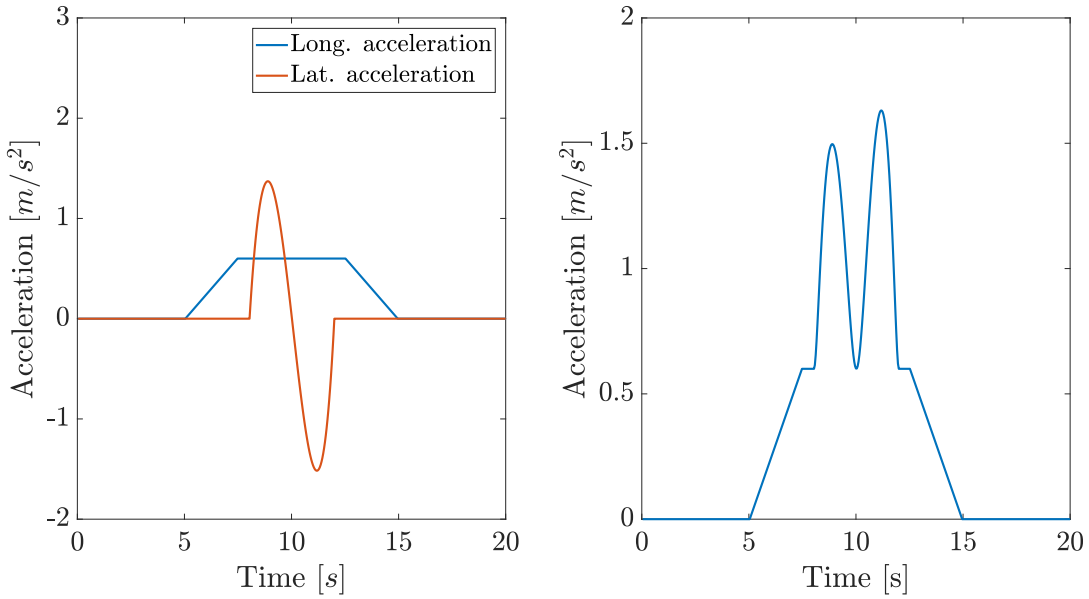

Figure 3.6: *Combined motion (left) and resulting accelerations (right)*

Fig. 3.7 shows the scaled resulting accelerations and the scaled comfort level circle, with radius 1. The height of the scaled resulting accelerations on the left indicate that the combined motion is not fully comfortable(crossing the comfort line). On the right, the resulting acceleration vectors are plotted, including the comfort limit circle. The blue arrows outside the circle indicate the uncomfortable accelerations.

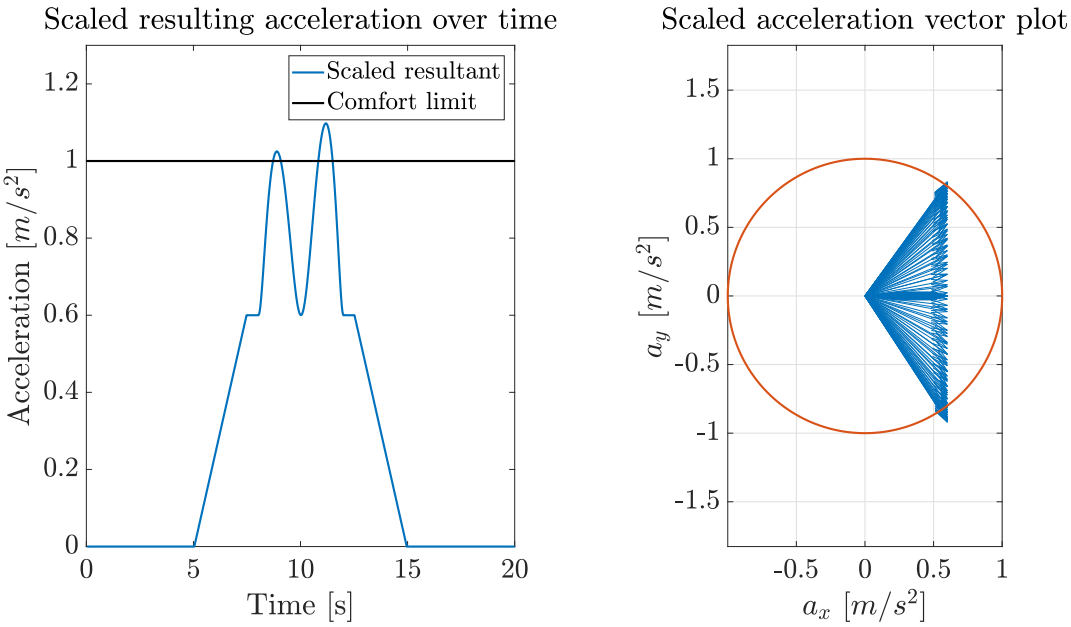

Figure 3.7: *Scaled resulting acceleration (left) and vector plot (right)*

Results

In Tab. 3.5 the results of two simulations are shown, including the values for RMS_c. The first row indicates the results from Fig. 3.6.

Table 3.5: *Value of RMS_c depends on the max. acceleration and duration of the lateral movement*

$a_{x,max}[m/s^2]$	$T_y[s]$	$RMS_c[-]$
0.6	4	0.6331
-0.6	4	0.5487

Comparing the RMS_c values in Tab. 3.5, it appears that decelerating with $a_x = -0.6m/s^2$ results in a lower RMS_c value compared to accelerating with $a_x = 0.6m/s^2$, indicating that the deceleration with $a_x = -0.6m/s^2$ is more comfortable than the acceleration with $a_x = 0.6m/s^2$.

Selection optimal path

Finally, the optimal path is selected by finding the combination of Lateral and Longitudinal motion giving the lowest RMS_c value. For the paths having the same RMS_c value, the duration of the longitudinal acceleration is minimized to obtain the most comfortable manoeuvre.

3.3.7 Reaction times

The reaction times of human drivers and the Host are investigated in this section.

Other drivers
In [44] a study is carried out on the reaction time of human drivers. It appears that the reaction time is influenced by many aspects, e.g. to what extend an object can be distinguished from its environment. In case the Predecessor suddenly starts braking, most drivers are capable of responding in less than $2.5s$. On the other hand, when drivers have a relatively high expectancy that a fast response will be required, the reaction time is about one second [44].
In this project, the reaction time of the other road users is taken at 1.5 seconds, as a compromise for drivers having certain expectation that a response is required. The choice of the reaction times will not influence the method of deriving the longitudinal strategies (in case the assumed reaction time is increased, the controller is required to increase the inter-vehicle distances, ensuring that safety is obtained).

Host
Considering the Host, the reaction time depends on the type and amount of systems that is used. In case there is an error or offset in the sensor signal, the error will propagate through the system (from the sensor to the A/D Converter to the Signal Processing and to the controller). Moreover, it takes time to perform all different steps. After controlling, the signal should be converted again for the actuators (steering and accelerating/braking).
In this project, the used Host response time is $0.5s$, to account for error propagation, uncertainties and processing times.

3.4 Modelling an overtaking manoeuvre

In this section, the modelling is described. Here, a typical overtaking manoeuvre is described, as well has the highway overview.

3.4.1 Overtaking manoeuvre

A typical overtaking manoeuvre consists of accelerations in two directions: longitudinal and lateral. The longitudinal acceleration is used to obtain the average speed on the adjacent lane (prevent hindering the other traffic) or to create a safe inter-vehicle distance so that the Host can merge. The lateral motion ensures that the Host moves from the initial- to the adjacent lane.

Table 3.1 shows the parameters of the longitudinal and lateral movement.

Table 3.1: *Overtaking manoeuvre parameters*

Parameter	Description
$T_{x,s}$	Start time longitudinal acceleration phase
$T_{x,e}$	End time longitudinal acceleration phase
$T_{x,0}$	Duration longitudinal acceleration phase
$T_{x,j}$	Duration non-zero jerk phase
$T_{y,s}$	Start lateral acceleration phase
$T_{y,e}$	End time lateral acceleration phase
$T_{y,0}$	Duration lateral acceleration phase
$a_{y,max}$	Max. lateral acceleration
$a_{x,max}$	Max. longitudinal acceleration

3.4.2 Longitudinal Movement

For the longitudinal movement, a trapezoid function is used, having a constant jerk (see Fig. 3.8). The acceleration $a_H(t)$ depends on time and has a maximum of $a_{x,max} = 0.3m/s^2$ in this case.

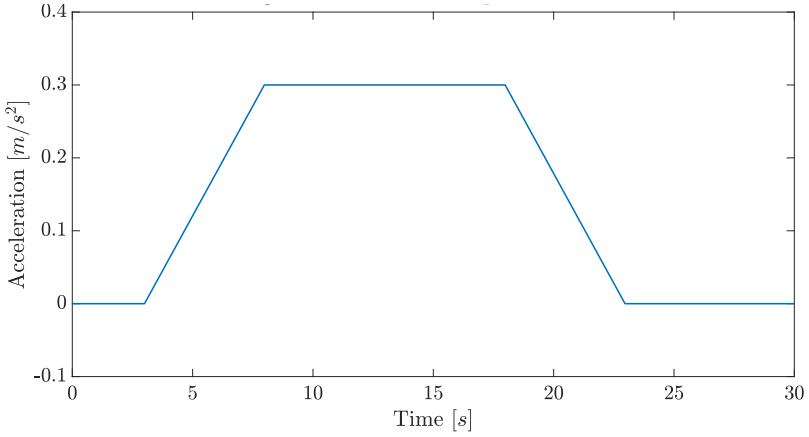

Figure 3.8: *Longitudinal acceleration profile over time*

The profile consists of three parts: positive jerk, constant acceleration and negative jerk. T_j is the time for which the jerk is positive (or negative). The value of the jerk (j, in m/s^3) is defined as:

$$j = a_{x,max}/T_j \tag{3.25}$$

The surface below an acceleration graph is the difference in velocity:

$$\Delta V_H = a_{x,max}(T_{x,0} - T_{x,j}) \tag{3.26}$$

where $a_{x,max}$ is the maximum longitudinal acceleration, $T_{x,0}$ is the total duration of the longitudinal acceleration and $T_{x,j}$ is the time after which the acceleration is at its maximum value (duration jerk-phase). The velocity V becomes:

$$V_H(t) = V_{H,0} + \int_0^t a_H(t)dt \tag{3.27}$$

where a_H is the longitudinal acceleration, dependent on time. The controller has to find the optimal duration and maximum acceleration that are required to drive smooth and safe. The maximum value of the acceleration can also be negative.

3.4.3 Lateral Movement

For the lateral movement, a fifth order polynomial is used as the reference path [45].
To specify initial and final values for the lateral acceleration, a fifth-order polynomial is used, with six boundary conditions (position, velocity and acceleration at $y = W_l/2$ and $y = W + W_l/2$ are defined). This also ensures that the position-, velocity- and acceleration profiles are continuous over time.
The lateral position and the derivatives, as function of the longitudinal position, are given as:

$$y(x) = d\Big[10(\frac{x}{L})^3 - 15(\frac{x}{L})^4 + 6(\frac{x}{L})^5\Big] \tag{3.28}$$

$$\frac{\partial y(x)}{\partial x} = \frac{30d}{L}\Big[(\frac{x}{L})^2 - 2(\frac{x}{L})^3 + (\frac{x}{L})^4\Big] \tag{3.29}$$

$$\frac{\partial^2 y(x)}{\partial x^2} = \frac{60d}{L^2}\Big[(\frac{x}{L}) - 3(\frac{x}{L})^2 + 2(\frac{x}{L})^3\Big] \tag{3.30}$$

Here, L is the length of the lateral movement, and d is the required lateral displacement.
The described polynomial (and its derivatives) depend on the longitudinal position x. However, the outputs of the controller are the start time and duration of the lateral motion, so that the polynomial will have to depend on time: $y(t)$. To transfer Eq. 3.28 and the derivatives to time, the partial derivative to time is taken:

$$\frac{\partial y}{\partial t} = \frac{\partial y}{\partial x} \cdot \frac{\partial x}{\partial t} = \frac{\partial y}{\partial x} \cdot V_H(t) \tag{3.31}$$

where $V_H(t)$ is the longitudinal velocity of the Host. To determine the acceleration, the curvature k is required, which is defined as [46]:

$$k = \frac{\frac{\partial^2 y}{\partial x^2}}{\Big[1 + (\frac{\partial y}{\partial x})^2\Big]^{\frac{3}{2}}} \tag{3.32}$$

Using this, the acceleration becomes [46]:

$$\frac{\partial^2 y}{\partial t^2} = k \cdot V_H(t)^2 \tag{3.33}$$

In Fig. 3.9 the resulting lateral position, velocity and acceleration are plotted (using $T_{y,s} = 0s$ and $T_y = 10s$).

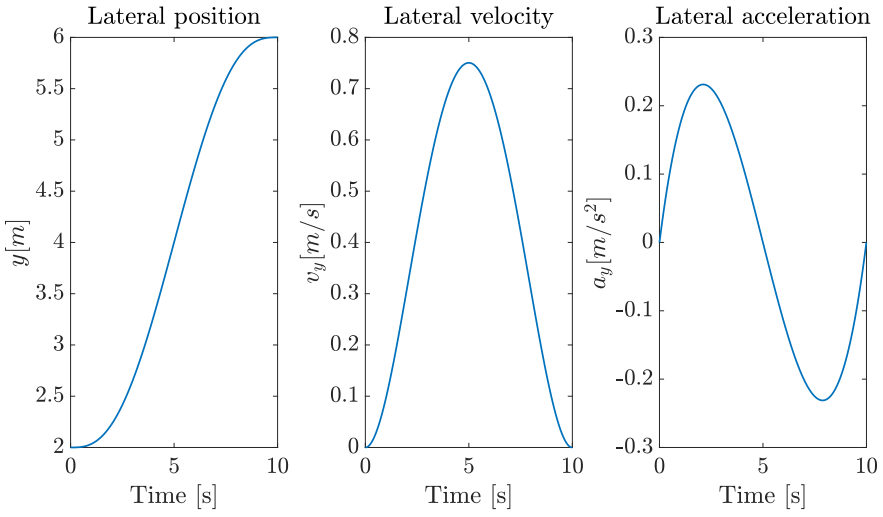

Figure 3.9: *Lateral position, velocity and acceleration over time*

The time-dependent lateral motion is given by (using $x = V_H(t) \cdot t$ and $L = V_H(t) \cdot T$, where T is the duration of the lateral movement):

$$y(t) = d\Big[10(\frac{V_H(t) \cdot t}{V_H(t) \cdot T})^3 - 15(\frac{V_H(t) \cdot t}{V_H(t) \cdot T})^4 + 6(\frac{V_H(t) \cdot t}{V_H(t) \cdot T})^5\Big] \tag{3.34}$$

which is written as:

$$y(t) = d\Big[10(\frac{t}{T})^3 - 15(\frac{t}{T})^4 + 6(\frac{t}{T})^5\Big] \tag{3.35}$$

indicating that the lateral position is independent of the longitudinal Host velocity $V_H(t)$.

Overtaking manoeuvre
Combined, in Figure 3.10 a typical overtaking manoeuvre is shown. Here, both the longitudinal and lateral motion are implemented, combined resulting in an overtaking manoeuvre.

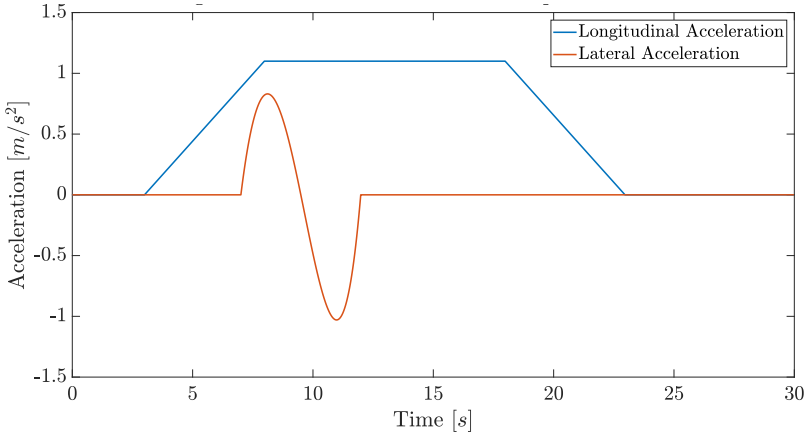

Figure 3.10: *Typical overtaking manoeuvre*

The input parameters for the controller are:

- T_x: Duration longitudinal acceleration
- $a_{x,max}$: Maximum acceleration (positive or negative)
- $T_{y,s}$: Start time lateral movement
- T_y: Duration lateral movement

Highway

In Fig. 3.11 a top view of (a part of) the highway that is used, is shown. The Host is modelled driving on the right-hand lane with velocity V_H. The Predecessor is driving on the same lane with V_P. Vehicles on the adjacent lane are named Vehicle 1 and 2, having velocity V_1 and V_2.

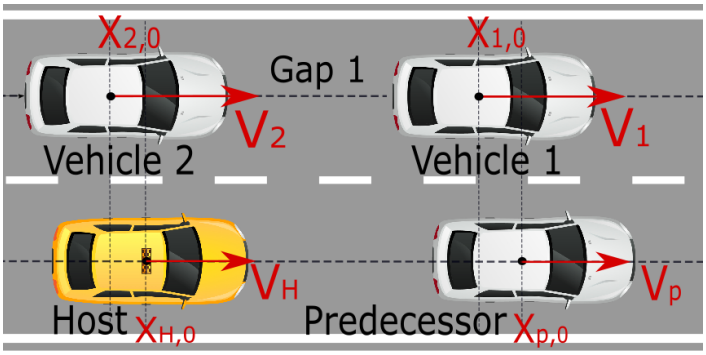

Figure 3.11: *Highway top view*

3.4.4 Conclusion

In this chapter, various assumptions, definitions and criteria are mentioned and elaborated. Using the specified motions for the longitudinal- and lateral movement, the controller that will be designed will optimise the overtaking manoeuvre in order to minimize the resulting accelerations and satisfy all constraints, which are explained in the next chapter.

Chapter 4

Scenarios

This chapter elaborates on the different investigated scenarios. The scenarios are based on the number of other road users, while each scenario elaborates on the applied methods considering the switching strategies. In each scenario, a straight and flat highway is considered, having two lanes in each direction (no oncoming traffic). In the first scenario, there is one other road user, driving in front of the Host. In the second scenario, there are two other road users, from which one is driving in front and one in the adjacent lane. In the third scenario, there is one vehicle driving in front, and four other vehicles are driving on the adjacent lane.
In each scenario the methods of determining the relevant parameters that describe the required overtaking manoeuvre, are explained. Especially, the first- and last moments to merge are determined, based on the available traffic data. The properties of the lateral motion are based on these first- and last moments to merge. For each scenario, simulations are performed to visualize the obtained results of the applied methods.

4.1 Scenario 1: free adjacent lane

In the first scenario, there is one other road user: a Predecessor (with velocity V_P), driving in front of the Host (with velocity V_H, see Fig. 4.1). The adjacent lane is empty. The inter-vehicle distance can exhibit three global profiles: the inter-vehicle distance might either: 1) decrease ($V_H > V_P$), 2) increase ($V_H < V_P$) or 3) remain equal ($V_H = V_P$). Options 2) and 3) indicate that merging is not required, which is not in the scope of this project.
In this initial situation, the Host will have to switch to the adjacent lane in order to prevent collision with the Predecessor (option 1), $V_H > V_P$). Since there is no other traffic, a longitudinal acceleration is not necessary.

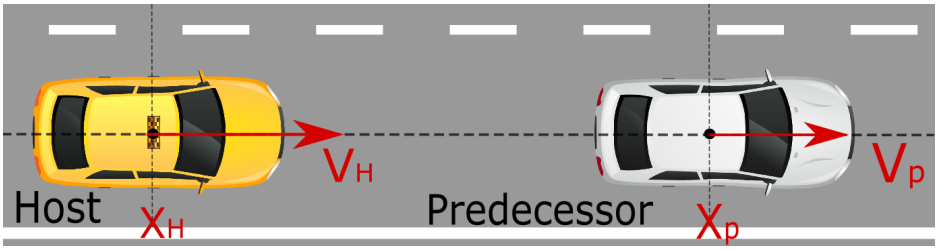

Figure 4.1: *Highway overview of Scenario 1*

X_P and X_H are the positions of the Predecessor and the Host, respectively.

4.1.1 Assumptions and goals

In this scenario, the two vehicles are driving with a constant velocity ($V_H > V_P$) in the x-direction. The lateral position y_P of the Predecessor is constant. The Host will have to merge in order to

prevent collision. There is no other traffic, indicating that the duration of the lateral motion is only limited by the maximum duration ($T_{y,max} = 20s$). The goal is to perform a comfortable lane change, while satisfying safety constraints (safe longitudinal- and lateral inter-vehicle distances).

4.1.2 Criteria

The two main criteria that are involved, are:

1. Inter-vehicle distance to the Predecessor, which is used to determine the TTC and the last moment to merge (for safety)

2 . Lateral offset of the Predecessor, which determines the properties of the lateral manoeuvre of the Host

Inter-vehicle distance to Predecessor

The actual inter-vehicle distance $DX_{P\rightarrow H} = DX$ between the Host and the Predecessor is defined as:

$$DX_{P\rightarrow H} = DX = X_P - X_H - L_v \tag{4.1}$$

where X_H and X_P define the X-position of the Predecessor and Host, respectively. L_v is the length of a vehicle (the actual inter-vehicle distance is the difference in X-positions minus two times half the length of a vehicle).
The inter-vehicle distance to the Predecessor is investigated for two purposes:

1. To determine the TTC, which determines the properties of the lateral motion (will be explained in Section 4.1.4)

2. To determine the last moment to merge, to ensure safety in case of an emergency stop from the Predecessor.

Fig. 4.2 presents the inter-vehicle distance to the Predecessor over time.

Determination TTC
The Time To Collision (TTC) is based on the prediction of the inter-vehicle distance (DX) over time, using the input parameters (positions of the Predecessor) of the sensors. The TTC is equal to the time untill the inter-vehicle distance is zero.
To visualize the determination of the TTC, a simulation is performed. In Fig. 4.2 a typical DX-profile is plotted over time. Table 4.1 presents the initial conditions for this simulation.

Table 4.1: *Initial conditions of scenario 1*

$X_{H,0}$ **[m]**	$X_{P,0}$ **[m]**	$V_{H,0}$ **[m/s]**	$V_{P,0}$ **[m/s]**
0	100	27.8	22.2

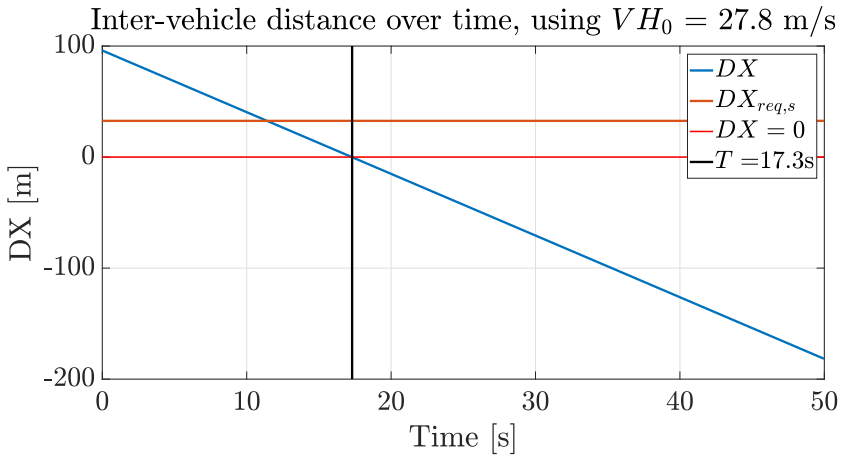

Figure 4.2: *DX over time, and $DX_{req,s}$ and $DX = 0$*

From Fig. 4.2 it appears that after $T = 17.3$ seconds, the inter-vehicle distance DX is zero, indicating that a collision with the Predecessor occurs. This means that the $TTC = 17.3$ seconds, indicating the need for a lateral motion to prevent collision. The horizontal line described by $DX_{req,s}$ is the required safety inter-vehicle distance, which is explained in the next section 4.1.3.

4.1.3 Safety

The inter-vehicle distance DX to the Predecessor determines the last moment to merge (last moment to merge in order to keep a safe inter-vehicle distance). The stopping distances of the Predecessor and Host define the required safe inter-vehicle distances. The Predecessor starts braking suddenly. The Host will start braking after the respond time $T_{r,H}$ (see section 3.3.2).

The stopping distance S_P of the Predecessor is:

$$S_P = \frac{V_P^2}{2\mu g} \tag{4.2}$$

and the stopping distance S_H of the Host is:

$$S_H = \frac{V_H^2}{2\mu g} + T_{r,H} V_H \tag{4.3}$$

where V_P and V_H are the initial velocity of the Predecessor and Host, respectively. μ is the friction coefficient (see section 3.3.3), g is the gravitational constant ($g = 9.81 m/s^2$) and $T_{r,H}$ is the reaction time or respond time of the Host.
When the Predecessor starts performing an emergency stop, the stopping distance of the Host should be equal to the stopping distance of the Predecessor minus a safety margin D_{min} (to account for uncertainties, like differences in friction, weight, and uncertainties in reaction times). This results in an expression for the required minimal inter-vehicle distance $DX_{req,s}$:

$$DX_{req,s} = S_H - S_P + D_{min} \tag{4.4}$$

In Fig. 4.2 the red line indicates the required safe inter-vehicle distance $DX_{req,s}$. The applied method results in a last moment to start merging (the moment when $DX = DX_{req,s}$).

4.1.4 Lateral motion

In section 4.1.3, it is indicated that a lateral motion is required in order to prevent collision with the Predecessor. In this section, the lateral motion is investigated. The two parameters describing the lateral movement, are:

1. The start time of the lateral movement: $T_{y,s}$
2. The duration of the lateral movement: T_y.

The final lateral position of the Host is the centre of the adjacent lane, the initial lateral position is the centre of the initial lane.

Minimal lateral distance
The minimal lateral distance Y_{min} the Host is required to move in order to prevent collision is determined first, based on the lateral offset of the Predecessor. At the moment the Host starts merging, there is a certain TTC to the Predecessor. During that time, the Host should have travelled Y_{min} in order to prevent collision. To incorporate the lateral offset of the Predecessor, three possible methods exist:

1. The first option assumes that there is no detailed information present of the lateral position of the Predecessor (which indicates that for safety the Host should move completely to the adjacent lane during TTC). In every situation, the minimal lateral distance of the Host is described by Y_{min}, which in this case is defined as: $Y_{min} = W_l + W_v/2 + Y_s$ after TTC seconds, where W_l is the width of a lane, W_v is the width of a vehicle (same for Host and Predecessor) and Y_s is a lateral safety distance.
2. The lateral position of the Predecessor is directly measured before merging, and used as a reference for the lateral minimal distance the Host has to travel during TTC. Again, a lateral safety distance Y_s is used, so that: $Y_{min} = Y_{P,0} + W_v + Y_s$.
3. The third option is a combination of both method 1) and 2): When the Predecessor (with width W_v) is driving on the centreline or to the right of it ($Y_{P,0} \leq W/2 - W_v/2$), the centre line of a lane plus the lateral safety distance Y_s is used as a reference: $Y_{min} = W_l/2 + Y_s$. Otherwise, the measured lateral position of the Predecessor is used as a reference: $Y_{min} = Y_{P,0} + W_v + Y_s$.

In this project, the third option is applied. In Fig. 4.3 and 4.4 the two limits are shown. In Fig. 4.3, the Predecessor is driving on the left of the centre lane, while in Fig. 4.4 the Predecessor is driving on the right of the centre lane (from the Host's perspective). In both cases, Y_{min} is the required lateral distance the Host will have to travel in order to prevent collision.

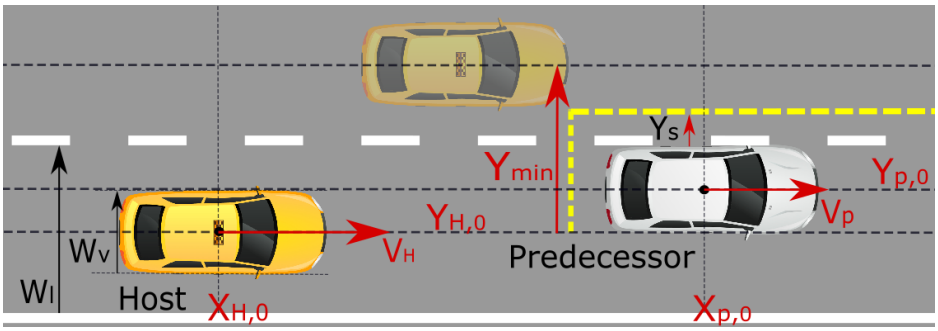

Figure 4.3: *Predecessor driving on the left of the lane centre line:* $Y_{min} = Y_{P,0} + W_v + Y_s$

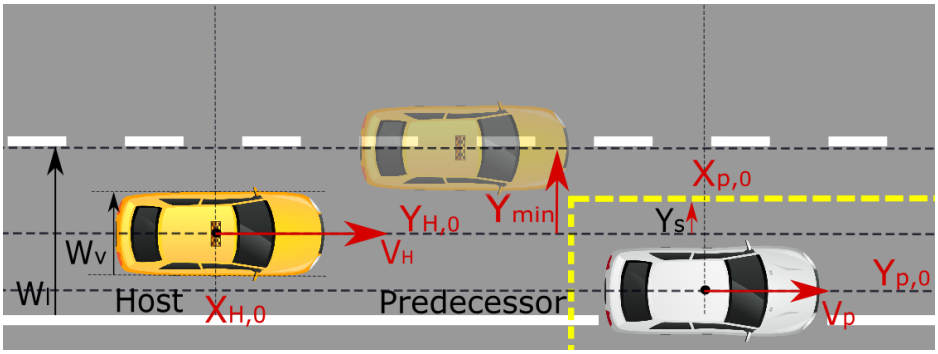

Figure 4.4: *Predecessor driving on the right of the lane centre line:* $Y_{min} = W_l/2 + Y_s$

After defining the required lateral distance that the Host has to travel, the duration of the lateral motion is calculated, based on the TTC.

Duration lateral motion

At the start time of the lateral motion, there is a certain TTC to the Predecessor. This TTC defines the remaining time for the Host to move a certain distance laterally (during the period of TTC-seconds, the Host should have moved a required minimal lateral distance so that the Host passes the Predecessor safely, laterally and longitudinally).

The duration of the lateral movement is determined using the following three steps:

1. In advance, for an arbitrary lateral motion, the time T_l for which the lateral position is equal to the required lateral position Y_{min} of the Host, is determined. The duration of the lateral motion is divided by the time to reach the lateral position. The obtained factor $TY_{min} = T_l/T_y$ is called the *time-multiplication factor* and is used to determine how long the lateral motion should take in order to move the distance Y_{min} laterally.

   This method uses the fact that a lateral motion is scalable, indicating that the ratio (duration of the lateral motion divided by the time to reach a certain lateral distance) is constant. The ratio is independent of the duration of the lateral motion, and independent of Host velocity, see section 3.4.3.

2. The start time $T_{y,s}$ of the lateral motion is determined (the maximum start time depends on the required inter-vehicle distance to Predecessor, in case there is no other traffic on the adjacent lane, the lateral manoeuvre is chosen such that $T = T_{y,max}$).

3. In case there is other traffic on the adjacent lane, the TTC at the moment when the Host starts merging is divided by TY_{min} to obtain the required duration of the lateral motion.

Fig. 4.5 shows the results of the applied methods. The positions of the Host and Predecessor are plotted for two specific moments: start of the lateral movement ($T = T_{y,s}$) and the moment when a collision would have occurred in case the Host would not have moved laterally ($T = T_{y,s} + TTC(T_{y,s})$). Due to the lateral motion, at $T = T_{y,s} + TTC(T_{y,s})$ the Host has moved Y_{min} meter laterally resulting in safe longitudinal- and lateral margins.

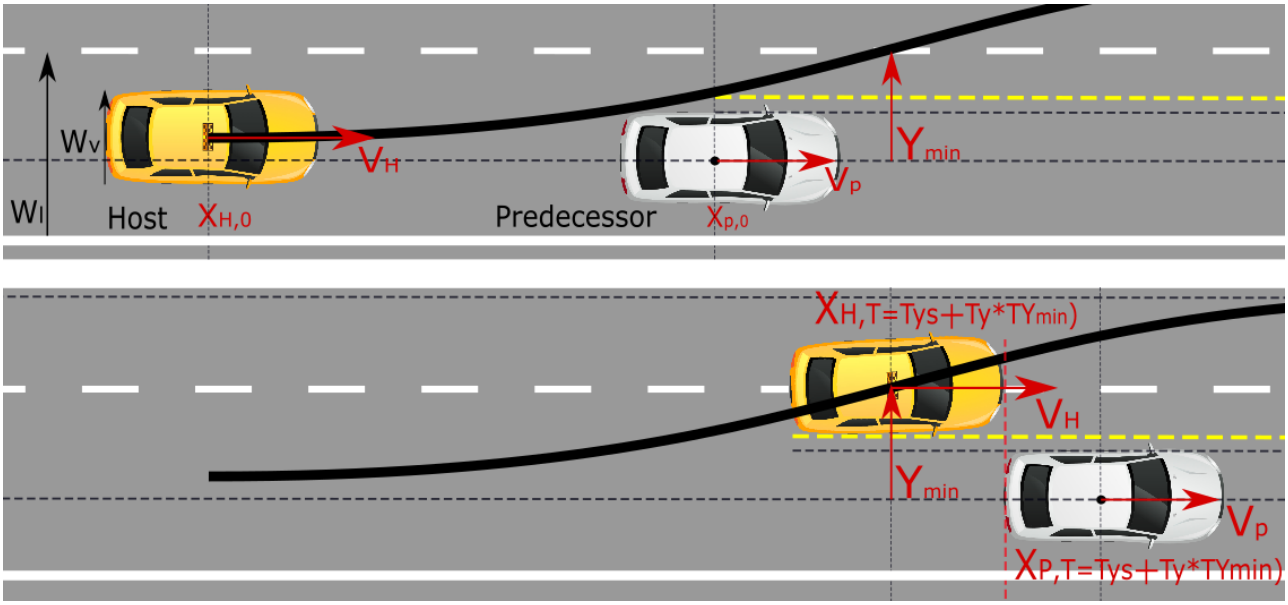

Figure 4.5: *Host (yellow) and Predecessor (white), plotted at $T = T_{y,s}$ (upper figure) and $T = T_{y,s} + TTC(T_{y,s}) = T_{y,s} + T_Y \cdot TY_{min}$ (lower figure)*

Fig. 4.6 shows the graphical representation of the applied method. Using the maximum start time and the lateral requirements, the wedge creates a combined longitudinal- and lateral safety margin. The Host is not allowed to drive in this wedge to obtain the required safety margins.

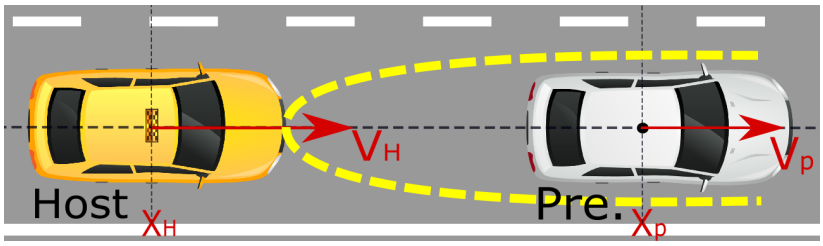

Figure 4.6: *Behind the Predecessor, a wedge is created in which the Host is not allowed to drive*

The Host will not collide with the Predecessor, as long as the duration of the lateral movement is equal or bigger than TTC at the start of the lateral movement divided by TY_{min}: $T_y \geq TTC_{T=T_{y,s}}/TY_{min}$s.

4.1.5 Visualizing the applied methods

In this section, the results are shown for the initial simulation. Tab. 4.2 presents the initial conditions for this simulation, including the lateral positions. The lateral offset of the Predecessor is $Y_{P,0} = W/2 = 2m$, (the Predecessor is driving in the middle of the lane).

Table 4.2: *Initial conditions of scenario 1, including lat. positions*

$X_{H,0}$ [m]	$X_{P,0}$ [m]	$V_{H,0}$ [m/s]	$V_{P,0}$ [m/s]	$Y_{H,0}$ [m]	$Y_{P,0}$ [m]
0	100	27.8	22.2	W/2	W/2

The required lateral distance the Host is required to travel is (using $Y_s = 0.5$m): $Y_{min} = Y_{P,0} + W_v + Y_s = 4.5m$. Using a regular lateral motion (see Fig. 4.7, where $T_y = 10$), the time T_l to reach $Y = Y_{min}$ is equal to 5.7s seconds, resulting in a *time-multiplication factor* $TY_{min} = T_l/T_y = 5.7/10 = 0.57$.

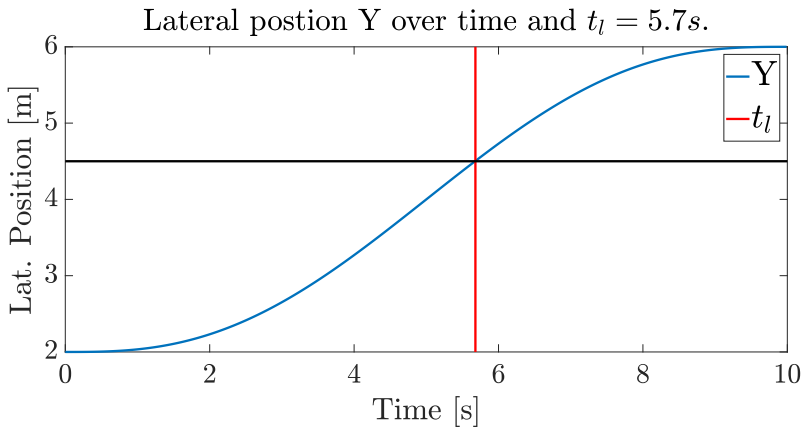

Figure 4.7: *Lateral position over time*

Since there is no other traffic on the adjacent lane, the maximum length of the lateral motion is used in order to minimize the accelerations. The length of a lateral motion is limited at $T_{y,max} = 20$. This indicates that the start time of the lateral motion is at the moment when $TTC = T_{y,max} \cdot TY_{min} = 11.4$ seconds ($11.4/0.57 = 20$ seconds).
Fig. 4.8 presents the TTC over time, on the left. At $T = T_{ys,max} = 5.9s$, the $TTC = 17.3 - 5.9 = 11.4$ seconds. Here, the black line indicates the maximum merging time $T_{ys,max}$. Starting at $T_{ys} = 5.9$ seconds ensures that the duration of the lateral movement is $20s$, while at the moment the longitudinal inter-vehicle distance DX, the lateral inter-vehicle distance is $0.5m$.

In Fig. 4.8, on the right, the inter-vehicle distances are plotted, including the required inter-vehicle distance for safety $DX_{req,s}$. According to this limit, the absolute maximum merging start time $Tys_{max,s} = 12.5$ seconds. The Host will start merging earlier, indicating that the performed overtaking manoeuvre is longitudinally safe.

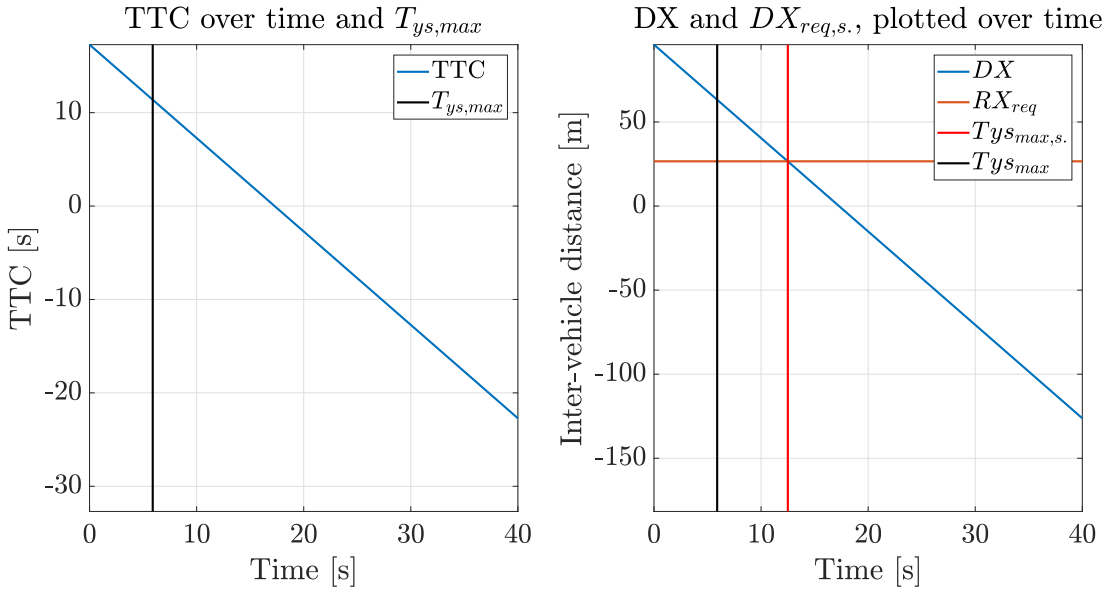

Figure 4.8: *Time To Collision (left) and inter-vehicle distance (right) plotted over time, including* $T_{ys,max}$

In Fig. 4.9, the positions of the Host and Vehicle 1 are plotted for five different moments in time:

1. Start lateral movement: $T = T_{y,s} = 5.9$s. The lateral position of the Host is equal to the initial position.

2. On a quarter of the lateral movement: $T = T_{y,s} + \frac{T_y}{4} = 10.9$s
3. Halfway lateral movement: $T = T_{y,s} + \frac{T_y}{2} = 15.9$s
4. On three-quarter of the lateral movement: $T = T_{y,s} + \frac{3T_y}{4} = 20.9$s
5. End lateral movement: $T = T_{y,s} + T_y = 25.9$s. The lateral position of the Host is equal to the final lateral position (middle of adjacent lane).

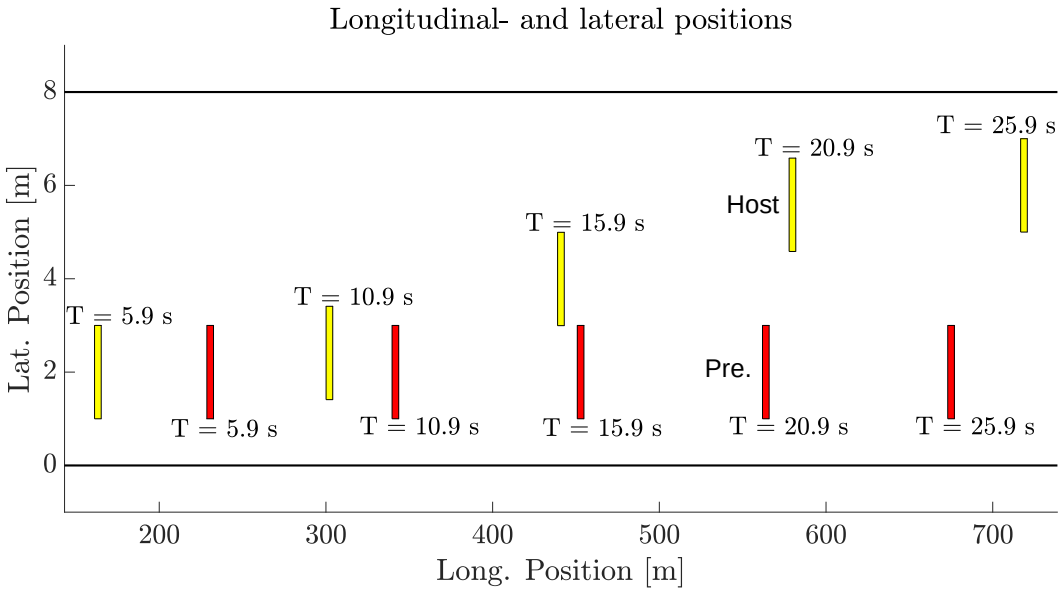

Figure 4.9: *Positions of the Host (yellow) and Predecessor (red)*

Fig. 4.9 shows that halfway the lateral motion (at $T = 15.9s$, where the lateral inter-vehicle distance is zero) the longitudinal positions are not equal. This ensures that at the moment when the longitudinal positions are equal the lateral motion is chosen in such a way that laterally the safety distance is fulfilled. This is shown in Fig. 4.10, where the positions of the Host and Predecessor are plotted at $T = T_{y,s} + T_{y,max} \cdot TY_{min} = 17.3$ seconds. The Host drives at $Y_H = 4.5m$, indicating the lateral safety distance of $Y_s = 0.5m$ is satisfied.

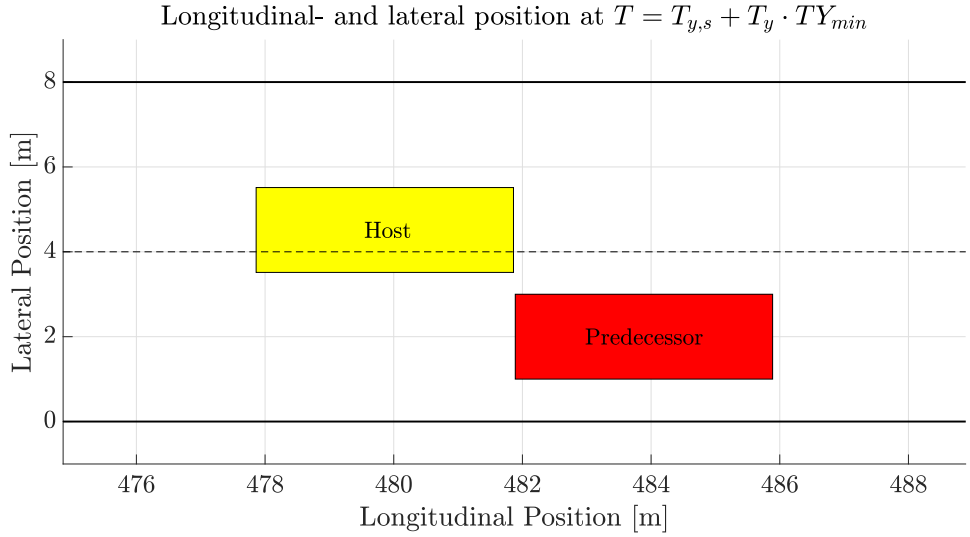

Figure 4.10: *Position of the Host and Predecessor at $T = 17.3$ s*

4.1.6 Conclusion Scenario 1

Scenario 1 indicates that the applied method of combining the TTC and the lateral position of the Predecessor ensures that longitudinally and laterally the safety margins are satisfied, resulting in a safe overtaking manoeuvre. The wedge behind the Predecessor (see Fig. 4.6) combines longitudinal- and lateral safety margins.

4.2 Scenario 2: one vehicle on the adjacent lane

In this scenario, there are two other road users: the Predecessor, and Veh. 1, on the adjacent lane, see Fig. 4.11. The velocity and position of the Host are given as: V_H and X_H, respectively, the velocity and position of the Predecessor are V_P and X_P, respectively and the velocity and position of Vehicle 1 are V_1 and X_1, respectively.

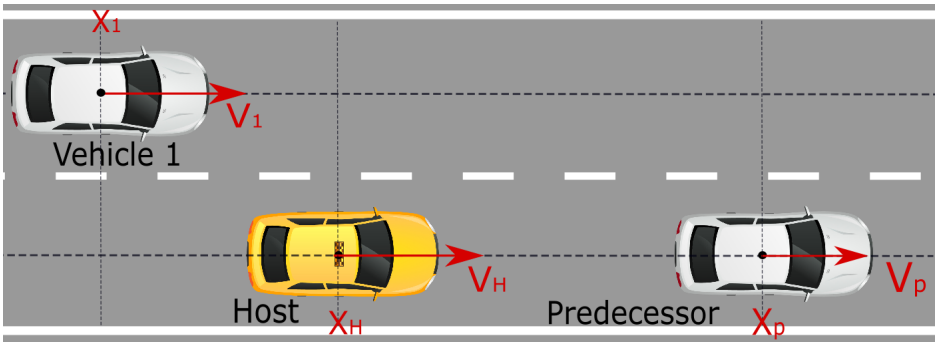

Figure 4.11: *Highway overview of Scenario 2*

4.2.1 Assumptions and goals

In addition to Section 4.1.1, the Host might have to decelerate or accelerate in order to obtain the requirements considering comfort and safety with respect to the other vehicles. Depending on the situation, the Host will merge in front or behind Veh. 1. When the Host merges in front, the expected deceleration of Veh. 1 is taken into account to determine the optimal switching moment. The expected deceleration of Vehicle 1 is simulated using Adaptive Cruise Control. When the Host merges behind, the Longitudinal Following Time (longitudinal following time to a vehicle on the adjacent lane, see section 4.2.3) determines the optimal moment to start merging laterally. The goal is to reduce the resulting accelerations of the Host while satisfying safety- and comfort requirements.

4.2.2 First- and last moments to merge

The path of the longitudinal- and lateral motions is based on the the first- and last moments to merge. Since there is another vehicle in the adjacent lane, a longitudinal acceleration might be required, in order to adapt speed and obtain required inter-vehicle distances. The controller (see Chapter 5) varies both the longitudinal acceleration and the belonging duration to obtain the smoothest acceleration profile, minimizing RMS_c.

Considering lane changing, the Host has two options:

- Merge in front of Vehicle 1
- Merge behind Vehicle 1

For both options, the first- and last moments to merge define the optimal merging start times. The last moment to merge depends on:

1. The Predecessor: the inter-vehicle distance to the Predecessor is defining the absolute last moment to merge to obtain safety (see Section 4.1.2)

2. Veh. 1 in the adjacent lane indicates the last moment to merge. In particular, the expected deceleration of Veh. 1 when the Host merges in front determines the optimal moments to merge in front. When the Host merges behind Veh. 1, the Longitudinal Following Time determines the optimal switching moment for the Host.

Last moment to merge - TTC

To determine the TTC to the Predecessor, the function $DX_{P\rightarrow H} = DX$ is investigated over time. For each combination of a_H and T_x the TTC is the time after which $DX_{P\rightarrow H} = DX$ becomes zero. Different combinations of a_H and $V_{H,0}$ result in three main phenomena, as shown in Fig. 4.12. Here, $DX(t)$ is defined as:

$$DX(t) = X_P(t) - X_H(t) = (X_{P,0} + \int_0^t V_P(t)dt) - (X_{H,0} + \int_0^t V_H(t)dt) \tag{4.5}$$

where the term $V_H(t)$ incorporates the acceleration a_H, see Eq. (3.27).

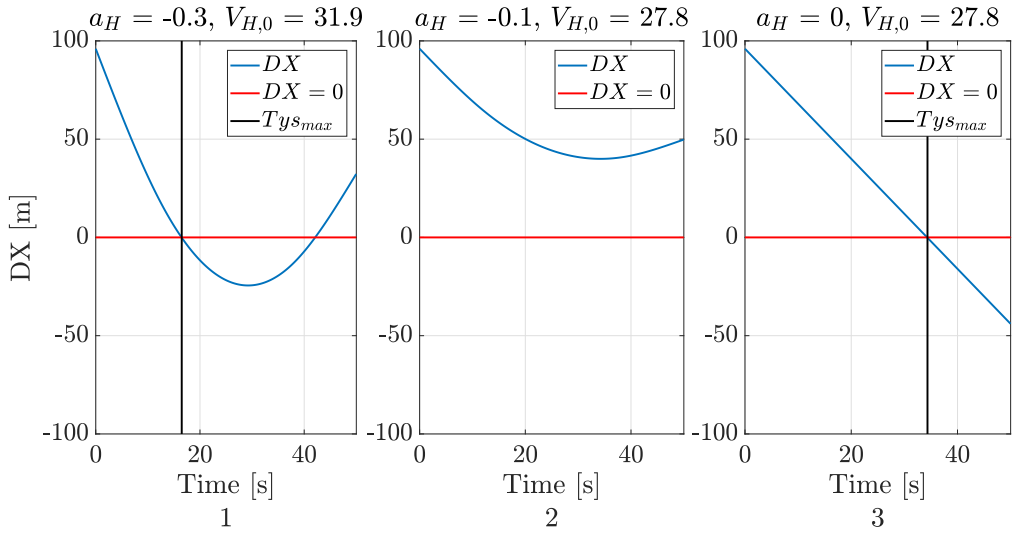

Figure 4.12: *Inter-vehicle distance to the Predecessor*

1. For $V_{H,0} > V_P$ and $a_H < 0$, the inter-vehicle distance reduces first, until $V_{H,0} < V_P$, so that $DX_{P\rightarrow H}$ increases again (Fig. 4.2, 1).

2. For specific combinations of $V_{H,0} \geq V_P$ and $a_{H,0} < 0$ the inter-vehicle distance is always positive (Fig. 4.2, 2). This indicates the Host does not have to merge (assuming that the minimal inter-vehicle distance is not violated).

3. For $V_{H,0} > V_P$ and $a_H \geq 0$, the inter-vehicle distance to the Predecessor will decrease and become negative(Fig. 4.2, 3).

Since the Host and the Predecessor are initially driving in the same lane, the first moment when the inter-vehicle distance becomes zero is the TTC.

Last moment to merge - Required inter-vehicle distances

In Fig. 4.13 the actual- and the required inter-vehicle distances are plotted over time (using the a_H and $V_{H,0}$ from Fig. 4.2). The inter-vehicle distances DX are based on Eq. (4.5), while section 4.1.3 indicates the derivation of the required inter-vehicle distance $DX_{req,s}$.

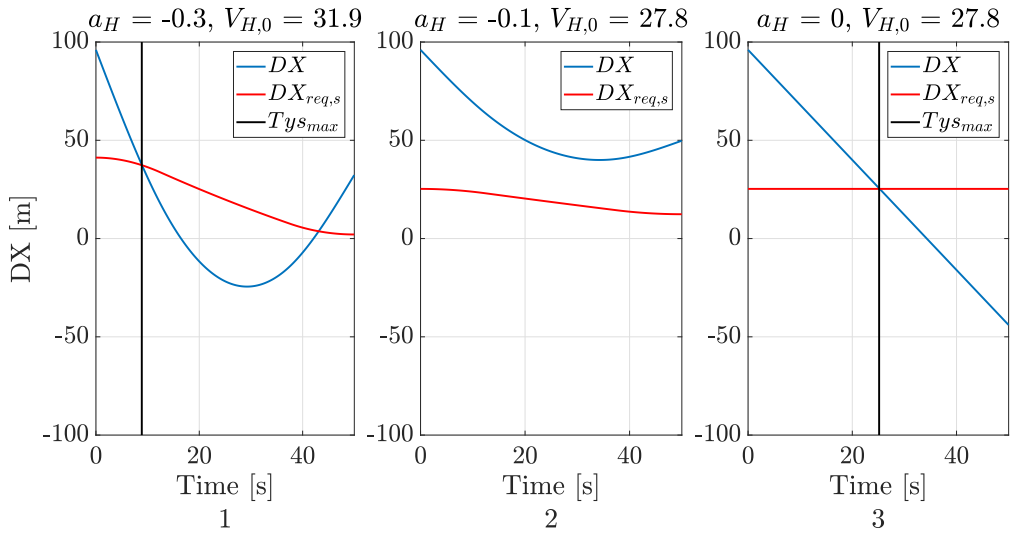

Figure 4.13: *Inter-vehicle distance to the Predecessor and $DX_{req,s}$*

In contrast to sub-plot 3, in sub-plots 1 and 2 the required inter-vehicle distance decreases since the Host is decelerating (a lower velocity allows a smaller inter-vehicle distance, see Eq. 4.4). The first intersection between DX and $DX_{req,s}$ in Fig. 4.13 1 and 3 define the last moments to merge for the Host, while in sub-figure 2 there is no need to move laterally, since the required inter-vehicle distance is always satisfied.

4.2.3 Merging behind the vehicle on adjacent lane

To merge behind a vehicle, the merging start time limits are determined using the Longitudinal Following Time (LFT). The LFT is equal to the TTP, except from the fact that the reference vehicle (Veh. 1) is not an initial Predecessor of the Host. The LFT over time to Veh. 1 is given as:

$$LFT(t) = \frac{X_1(t) - X_H(t)}{V_H(t)} \tag{4.6}$$

Required LFT

The first- and last moment to merge behind a vehicle are defined by the moment when the LFT crosses the LFT_{req}. Assuming a required Gap length of two seconds (see Section 4.3), it is stated that the Host can merge behind Veh. 1 if the LFT is more than one second ($LFT > LFT_{req}$).

LFT profiles

In Fig. 4.14 a LFT-graph is shown (using $a_H = -0.3m/s^2$ and $V_{H,0} = 31.9m/s$). In blue, the LFT is shown over time, which crosses the red LFT_{req} line at $T = 10.88$ and T = 46.4 s, which are the maximum- and minimum merging start times, respectively.

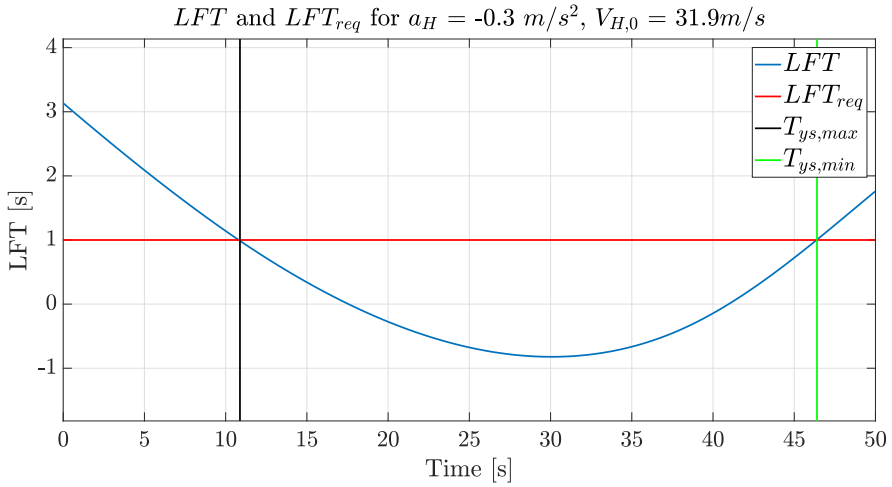

Figure 4.14: *Longitudinal Following Time (LFT) and required Longitudinal Following Time $LFT_{req,s}$*

In Tab. 4.1 the main initial conditions and simulation parameters are given.

Table 4.1: *Initial conditions and sim. parameters*

$V_{H,0}$	$X_{H,0}$	a_H	T_x	$X_{1,0}$	$V_{1,0}$ [m/s]
115 km/h	0 [m]	-0.3 $[m/s^2]$	50 [s]	100 [m]	90 m/s

Fig. 4.14 indicates there are two possibilities for the Host to merge behind Veh. 1:

- Between T = 0 and T = 10.88s
- After T = 46.4s.

Based on different combinations of initial inter-vehicle distances and velocities, in addition to the profile in Fig. 4.14 four different global LFT-profiles are obtained, see Fig. 4.15.

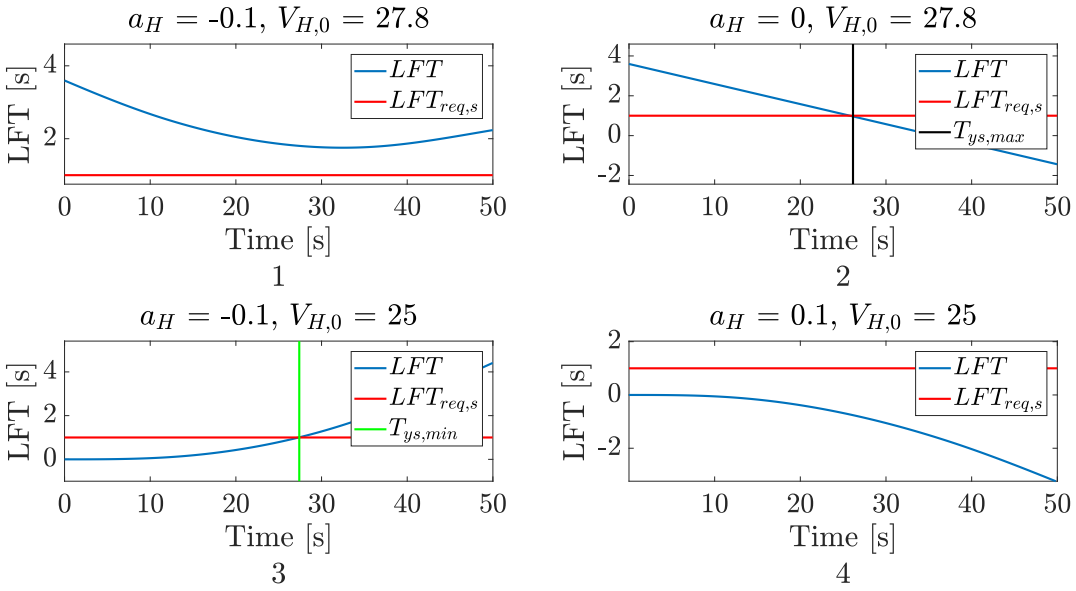

Figure 4.15: *Linear Following Time (LFT) and $LFT_{req,s}$ in four different situations*

- Sub-plot 1 in Fig. 4.15 indicates that the LFT to Veh. 1 decreases first, but is always above the limit $LFT_{req,s}$, indicating that merging behind is always possible
- In sub-plot 2, the LFT decreases and crosses the limit, indicating that there is a maximum merging start time $T_{ys,max}$
- In sub-plot 3, the opposite is shown: the LFT starts below the limit (merging behind is not possible, initially). However, the LFT increases and at $T_{ys,min}$ the Host can merge behind
- Sub-plot 4 indicates the situation where merging behind is never possible: LFT is always below the limit.

Tab. 4.1 presents for each scenario in Fig. 4.15 the initial conditions and the minimal- and maximal merging time for the Host.

Table 4.2: *Initial conditions and minimum- and maximum merging start times*

Scenario	$X_{2,0}$ [m]	$V_{2,0}$ [m/s]	$T_{ys,min}$ [s]	$T_{ys,max}$ [s]
1	100	30	0	50
2	200	30	0	26.15
3	200	30	27.4	50
4	200	30	NP*	NP*

*Not Possible: LFT is below the limit, indicating that the Host is driving in front of Veh. 1 and that merging behind is not possible. The LFT to the vehicle in the adjacent lane define the maximal- and minimal merging start times.

4.2.4 Merging in front of the vehicle on the adjacent lane

If the Host wants to merge in front of Veh. 1, there is a required minimum inter-vehicle distance for which the Host might start moving laterally.
The two criteria for merging are: **Safety** and **Comfort**. The safety criteria indicates the minimum inter-vehicle distance that should be satisfied in any case. The comfort criteria are more strict, indicating for the three different comfort levels the required inter-vehicle distance.

Safety

Considering safety, the minimum inter-vehicle distance is limited using the stopping distances of the vehicles, see Section 4.1.3. The stopping distance S_H of the Host is:

$$S_H = \frac{V_H^2}{2\mu g} \tag{4.7}$$

and the stopping distance of Vehicle 1 is:

$$S_1 = \frac{V_1^2}{2\mu g} + T_{r,1}V_1 \tag{4.8}$$

Since the Host can either drive slower or faster than Veh. 1, by setting Eq. (4.7) and (4.8), equal to each other, the critical Host velocity $V_{H,crit}$ (where the stopping distances are equal) becomes:

$$V_{H,crit} = \sqrt{V_1^2 + 2\mu g T_{r,1} V_1} \tag{4.9}$$

If the Host is driving faster than $V_{H,crit}$, the required inter-vehicle distance would theoretically become positive, which is physically not valid. This indicates why the following switching rule for the the required inter-vehicle distance between Veh. 1 and the Host is applied:

$$DX_{min} = S_H - S_1 - D_{min} = \frac{V_H^2 - V_1^2}{2\mu g} - T_{r,1}V_1 - D_{min} = X_{1,0} - X_{H,0} \quad for \quad V_H < V_{H,crit} \tag{4.10}$$

$$DX_{min} = -D_{min} \quad for \quad V_H >= V_{H,crit} \tag{4.11}$$

Comfort

When merging in front of Veh. 1 in combination with a small inter-vehicle distance, Veh. 1 will have to decelerate to prevent collision and obtain a safe inter-vehicle distance again. To obtain overall comfort driving behaviour, the estimated deceleration of Veh. 1 is required to be within the comfort criteria, as discussed in Section 3.3.4 (a manoeuvre might cause a maximum deceleration of $a_{x,1} = 1.3m/s^2$ to obtain comfortable deceleration of Vehicle 1).
In Appendix A the expected deceleration of Veh. 1 when the Host merges in front, is determined, under the assumption that the deceleration is constant. In Appendix A it is concluded that this method faces shortcomings in case the Host accelerates during the lateral movement or when a string of vehicles is driving on the adjacent lane.
The remarks listed above indicate that a more general solution has to be found, in order to simulate the deceleration profile of human drivers.

ACC

Section 2.5.1 shows that *ACC* can be used as a method to simulate realistic human driving behaviour. In this section, a PI-ACC controller is used (the human driving behaviour is simulated using a ACC controller where Proportional- and Integral gains are taken into account). Appendix B shows the minor influence of adding an differential action (PID-ACC). The Proportional gain k_p is multiplied with the velocity error e_v, while the Integral gain k_i is multiplied with the position error e_x (integral of velocity is the position). The output $U(t)$ of a PI-ACC Controller is:

$$U(t) = k_p e_v(t) + k_i \int_0^t e_v(\tau) d\tau \tag{4.12}$$

where the error $e_v(t)$ is the velocity error. k_p and k_i are the proportional and integral gains, respectively. For a certain vehicle k and predecessor $k-1$, the error in velocity is given as:

$$e_v(t,k) = V(t,k-1) - V(t,k) \tag{4.13}$$

where $V(t,k-1)$ represents the velocity of the vehicle $k-1$ in front. The position error is described as:

$$e_x(t) = X(t,k-1) - X(t,k) - T_r \cdot V(t,k) \tag{4.14}$$

Here, $X(t,k-1)$ represents the position of the vehicle $k-1$ in front and T_r is the reaction time of vehicle k (which is equal for all vehicles, except from the Host, see Section 3.3.7). The term $Tr \cdot V(t,k)$ represents the desired inter-vehicle distance. The output term of the ACC controller for each vehicle k is defined (for each time step t, indicating that time is discrete) as:

$$U_{acc}(t,k) = (k_p \cdot e_V(t,k) + k_i \cdot e_X(t,k))/t \tag{4.15}$$

The new velocity V of vehicle k is updated using:

$$V(t,k) = V(t-dt,k) + U_{acc}(t,k) \cdot t \tag{4.16}$$

indicating that the output $U_{acc}(t,k)$ is the acceleration of vehicle k.

Implementation and Analysis
To validate the ACC controllers, simulations are performed. Tab. 4.3 presents the initial conditions. The Host merges in front of the string of Vehicles at $T_{y,s} = 5$ seconds.

Table 4.3: *Initial conditions of the vehicles*

Vehicle	X_0**-position [m]**	V_0 **[km/h]**
Host	270	90
2	200	100
3	150	100
4	100	100
5	50	100

Section 3.3.7 indicates that the reaction time of a human driver is 1.5 seconds. The controller calculates the merging start time $T_{y,s}$ in advance. Using the reaction time of human drivers, the turning signals are put on 1.5 seconds before merging, indicating that the start time of the lateral movement is equal to the moment when the vehicles behind the Host start decelerating. The ACC system itself directly responds on velocity differences.
The determination of the values of $k_p = 0.010$ [-] and $k_i = 0.0010$ $[\frac{1}{s}]$ (see Appendix B) results in the velocity-, acceleration- and inter-vehicle distance profiles as shown in Fig. 4.16.
Due to the fact that the inter-vehicle distances at $T_{y,s}$ are larger than the required inter-vehicle distance, Vehicles 3, 4 and 5 start accelerating in order to close the gaps and obtain the desired inter-vehicle distance.

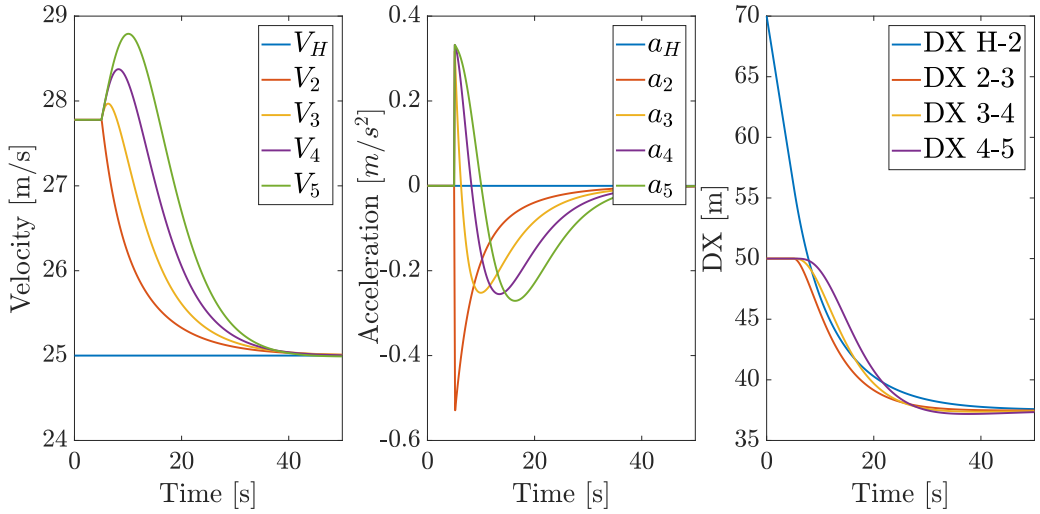

Figure 4.16: *Velocities (left), accelerations (middle) and inter-vehicle distances (right) over time*

Set speed Control
To prevent gap closing, the controller is extended by adding a Proportional multiplier on the error between the actual speed and the set speed V_{set} (like it is used in Cruise Control). A proportional term $K_{P,ss}$ is applied, so that the output of this Set Speed Controller (SSC) is given as:

$$U_{ss}(t,k) = K_{p,ss}(V_{set}(k) - V(k,t)) = K_{p,ss}E_{v,set} \tag{4.17}$$

In the control loop, the output is the minimum from both outputs $U_{ss}(t,k)$ and $U_{acc}(t,k)$, so that applied control output $U_{app}(k,t)$ is given as:

$$U_{app}(k,t) = min(K_{p,ss}E_{v,set}(t,k) \;\; , \;\; k_pE_V(t,k) + k_iE_X(t,k)) \tag{4.18}$$

Fig. 4.17 shows the addition of Set Speed control on the acceleration graph of Vehicle 5. The applied input $U_{app}(k,t)$ prevents gap closing between $T = 5$ and $T = 16$ seconds. After $T = 16$, the Set Speed Controller (4.17) suggests a positive acceleration, while the PI-ACC controller requires the vehicle to decelerate in order to obtain a safe inter-vehicle distance.

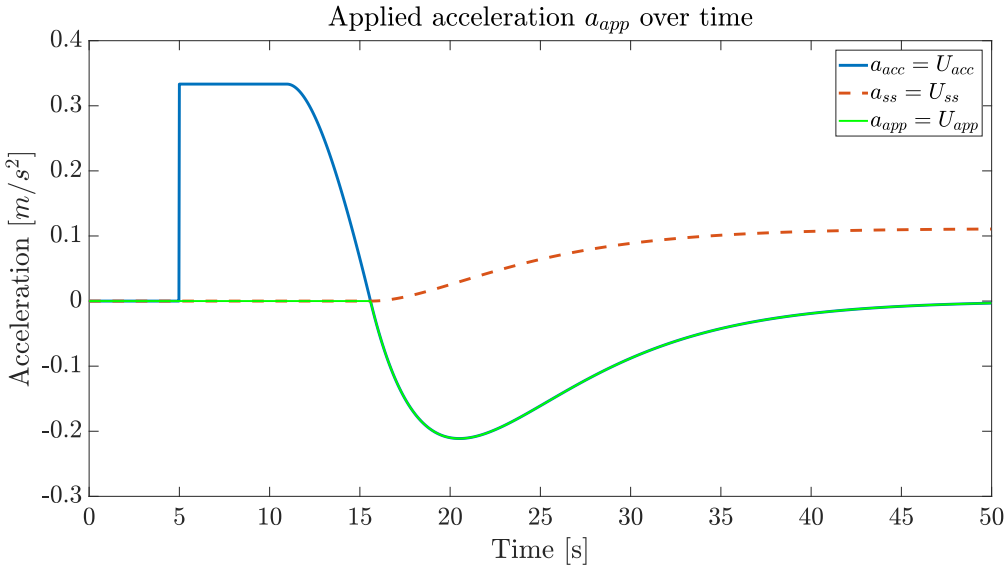

Figure 4.17: *a_{acc}, a_{ss} and applied acceleration a_{app} over time*

Results

In Appendix B, the determination of the Set speed Control gain $K_{p,ss}$ is described. Using $K_{p,ss} = 0.001$, in Fig. 4.18 the accelerations of the vehicles are plotted over time. Fig. 4.19 presents the velocities and inter-vehicle distances. Instead of accelerating to close a gap, the vehicles will keep the set speed until the control output U_{acc} forces them to decelerate.

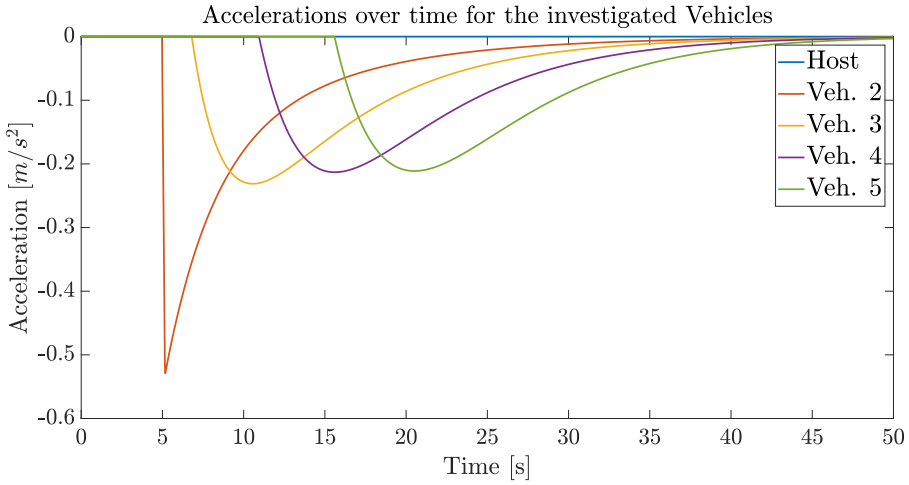

Figure 4.18: *Accelerations of the Vehicles, using ACC and Set speed Control*

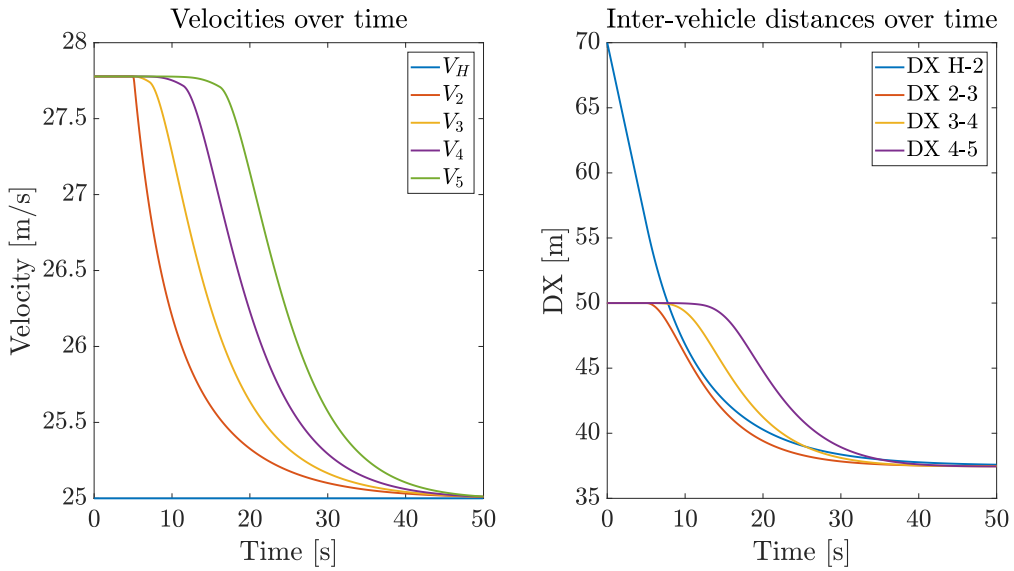

Figure 4.19: *Velocities and inter-vehicle distances over time, using ACC and Set speed Control*

4.2.5 First- and last moment to merge using ACC

Using the results from the PI-ACC model, the accelerating behaviour of the vehicle on the adjacent lane is predicted, in order to determine the first and last moment to merge. The expected peak accelerations are plotted over time. The limit deceleration of Veh. 1 is limited at $A_{lim} = -1.3m/s^2$ (Table 3.2, using the comfort level).
Fig. 4.20 shows the expected peak accelerations of the vehicle, in case the Host is merging in front (the expected acceleration is only defined in case the Host is longitudinally driving in front of the vehicle). $T_{ys,min}$ indicates the minimum merging start time, which is the moment when the expected deceleration of the vehicle on the adjacent lane is above the limit $A_{lim} = -1.3m/s^2$. In Fig. 4.20, $T_{ys,min} = 39.84$s (the expected deceleration of Veh. 1 is only defined in case the inter-vehicle distance $DX = X_H - X_1 > 0$).

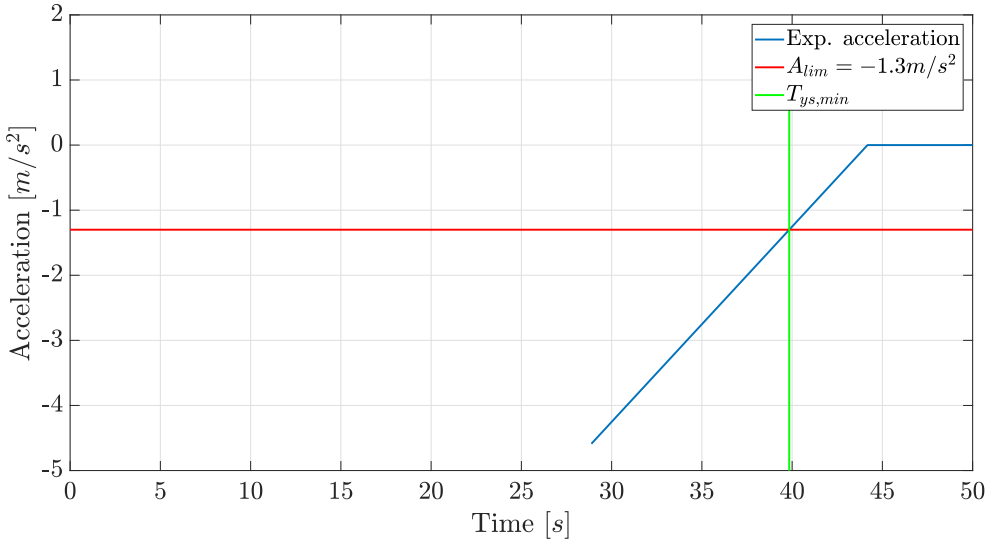

Figure 4.20: *Expected- and required acceleration A_{lim} over time, including first moment to start merging*

Fig. 4.21 $T_{ys,max}$ indicates the maximum merging start time, since after that moment the expected

deceleration of the vehicle on the adjacent lane is below the limit A_{lim}. In Fig. 4.21, $T_{ys,max} = 30.23$s.

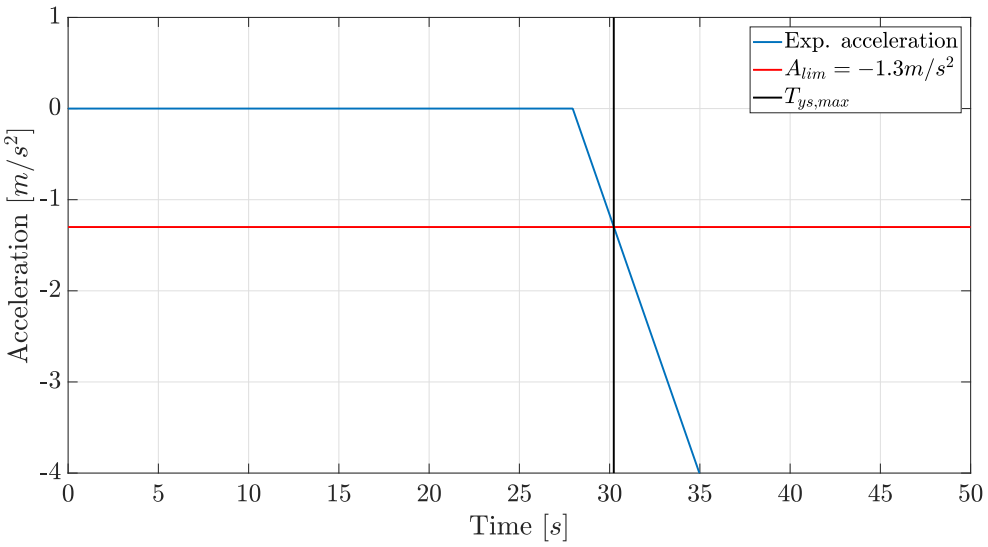

Figure 4.21: *Expected- and required acceleration A_{lim} over time, including last moment to start merging*

Using the PI-ACC method, the expected deceleration of the vehicle on the adjacent lane is plotted over time. The minimum- or maximum merging starts time are defined by the deceleration limit A_{lim}.

4.2.6 Visualizing the applied methods

In this section, simulations are performed to visualize the applied methods. Two special scenarios are performed: 1) Merging in front and 2) merging behind the vehicle on the adjacent lane. In the first scenario, the initial conditions are such that the Host has to accelerate. In the second scenario, the Host decelerates to merge behind.

Accelerate to merge in front

In this situation, the Host initially starts behind Veh. 1 and will accelerate to merge in front, see Fig. 4.22. In practice, overtaking from the right is not allowed, but by allowing overtaking from the right in the simulations, the amount of longitudinal strategies is extended.

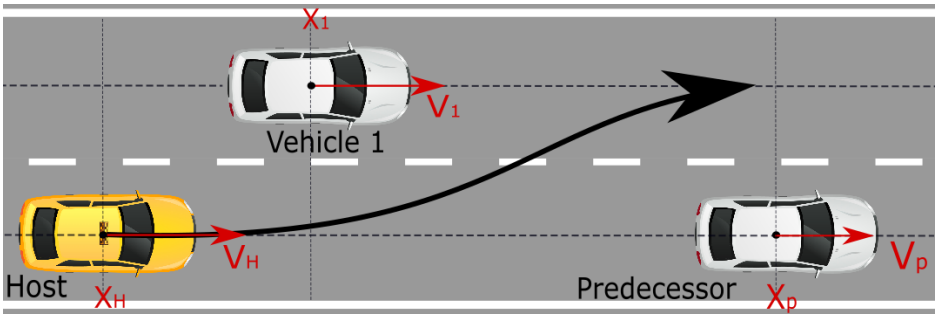

Figure 4.22: *Highway overview of Scenario 2*

Inputs
Tab. 4.4 presents the initial conditions for this simulation. These are the input variables for the controller.

Table 4.4: *Initial conditions*

Vehicle	X_0 [m]	V_0 [m/s]	Y_0 [m]
Host	-50	27.8	2
Pre.	300	22.2	2
1	100	27.8	6

Based on the input variables, the controller predicts the future states of all road users and searches for an overtaking resulting in the lowest accelerations while satisfying all constraints:

- The inter-vehicle distance DX to the Predecessor is required to be above the safety limit $DX_{req,s}$, see section 4.2.2.
- Maximum deceleration of Vehicle 1 is required to be above the limit A_{lim}, see section 4.2.5.

Outputs
Table 4.5 presents the parameters describing the longitudinal- and lateral movements of the Host, calculated by the controller. The longitudinal acceleration takes 16 seconds. The longitudinal Host acceleration $a_H = 0.2m/s^2$.

Table 4.5: *Resulting path parameters*

a_H $[m/s^2]$	T_x [s]	a_y $[m/s^2]$	$T_{y,s}$ [s]	T_y [s]
0.2	16	0.1776	39.9	11.40

Fig. 4.23 presents the belonging velocities on the left, and the accelerations on the right. The Host accelerates to $V_H = 30.18$ m/s. The green line indicates the merging start time $T_{y,s}$.

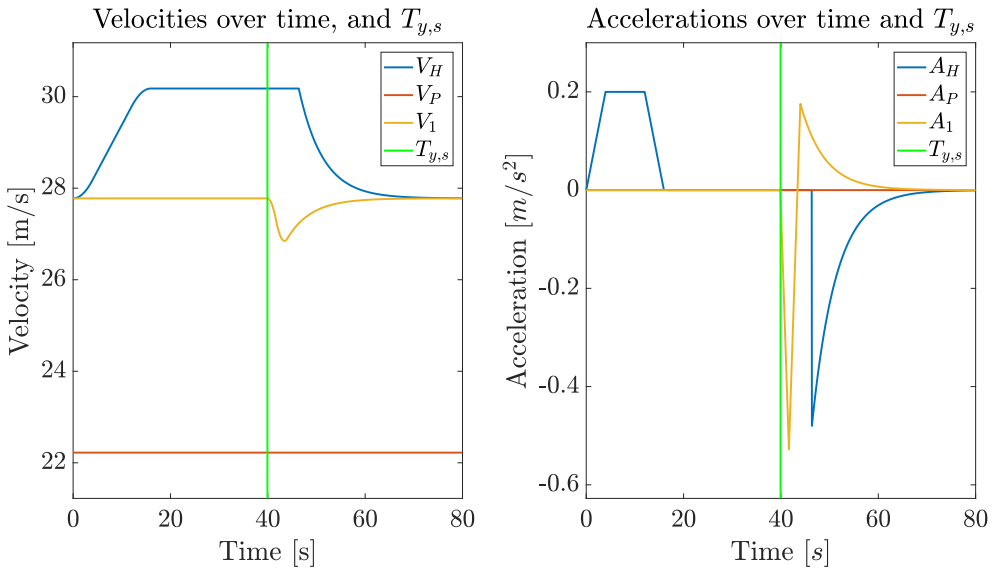

Figure 4.23: *Velocities (left) and Accelerations (right) over time, and $T_{y,s}$*

Fig. 4.24 shows on the left the inter-vehicle distance DX to the Predecessor, and the required inter-vehicle distance DX_{req} for keeping the longitudinal safety distance. $T_{ys,max,s}$ indicates the maximum merging start time (from that point $DX \leq DX_{req}$). On the right, the minimum merging time $T_{y,s}$ is indicated, based on the expected deceleration of Vehicle 1.

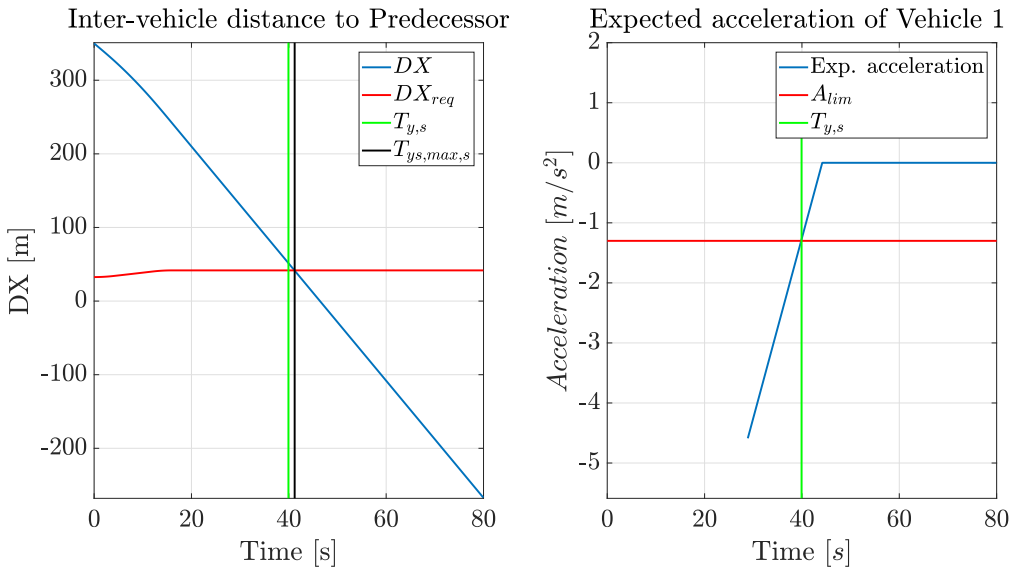

Figure 4.24: *Inter-vehicle distance (left) and expected acceleration (right) over time, including required inter-vehicle distance $DX_{req,s}$ and maximum deceleration A_{lim}*

Fig. 4.24 shows that the minimum merging start time $T_{y,s}$, resulting from the expected acceleration of Veh. 1 is lower than the maximum merging start time based on the inter-vehicle distance DX ($T_{ys,max,s} = 41.20s$ while $T_{y,s} = 39.9$s) This indicates that the overtaking manoeuvre is safe.

Decelerate to merge behind

In case the Host initially starts longitudinally in front of Veh. 1 and merges behind Veh. 1 (in contradiction to Fig. 4.22), the Host has two options: decelerate or keep the initial set speed . The optimal strategy depends on the inter-vehicle distance to the Predecessor, which defines the maximum merging start time.

Inputs

Tab. 4.6 presents the initial conditions for this simulation. Again, the controller predicts the future states of the other road users and searches for an overtaking resulting in the lowest accelerations while satisfying all constraints. In this case, since the Host merges behind, the LFT to Veh. 1 is used as the criteria to find the minimum merging start time (see section 4.2.3). The inter-vehicle distance DX to the Predecessor defines the maximum merging start time.

Table 4.6: *Initial conditions*

Vehicle	X_0 [m]	V_0 [m/s]	Y_0 [m]
Host	150	27.8	2
Pre.	300	22.2	2
1	100	27.8	6

Outputs

Table 4.7 presents the obtained resulting path parameters considering the longitudinal and lateral motion. The Host decelerates with $a_H = -0.2m/s^2$ in order to prevent collision and create a sufficient LFT to Veh. 1.

Table 4.7: *Resulting parameters describing the merging manoeuvre*

a_H $[m/s^2]$	T_x [s]	$T_{y,s}$ [s]	T_y [s]
-0.2	19	35.8	16.64

Fig. 4.25 shows the velocities of the Host, Predecessor and Veh. 1. At $T_{y,s} = 35.8$ s, the lateral motion is started. The velocity of Veh. 1 remains constant since the Host merges behind.

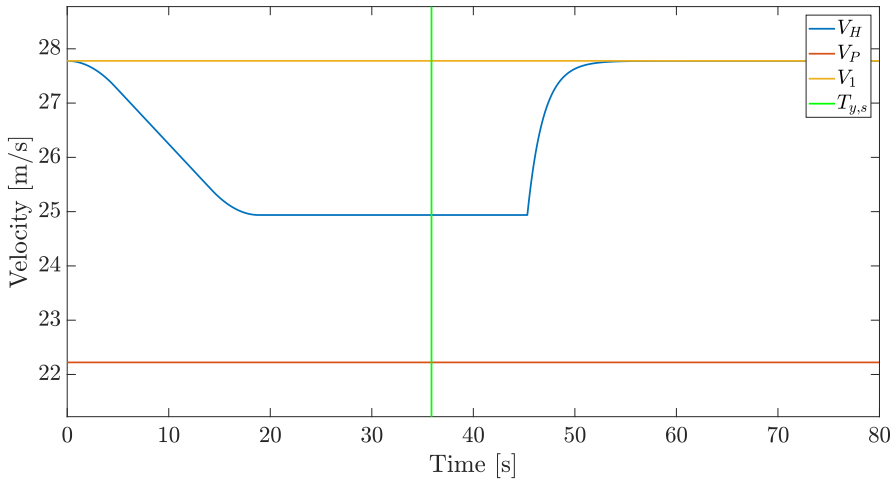

Figure 4.25: *Velocities over time, and $T_{y,s}$*

After merging, using the Cruise Control, the Host accelerates to the initial set speed. The acceleration starts when the Host has laterally reached the required safety distance with the Predecessor:

$$Y_H = Y_l + Wv/2 \tag{4.19}$$

where Y_l is the lateral safety distance. In this case, the acceleration start time $T_{s,acc}$ is determined as $T_{s,acc} = 45.3$ seconds.
In Fig. 4.26, the left figure shows the inter-vehicle distance DX to the Predecessor, including the safety limit $DX_{req,s}$. The black line at $T_{ys,max,s} = 37$ seconds indicates the maximum merging start time. The right figure presents the LFT and LFT_{req}. The minimum merging start time is at $T_{y,s} = 35.8$. Since $T_{y,s} < T_{ys,max,s}$, the calculated path satisfies all constraints.

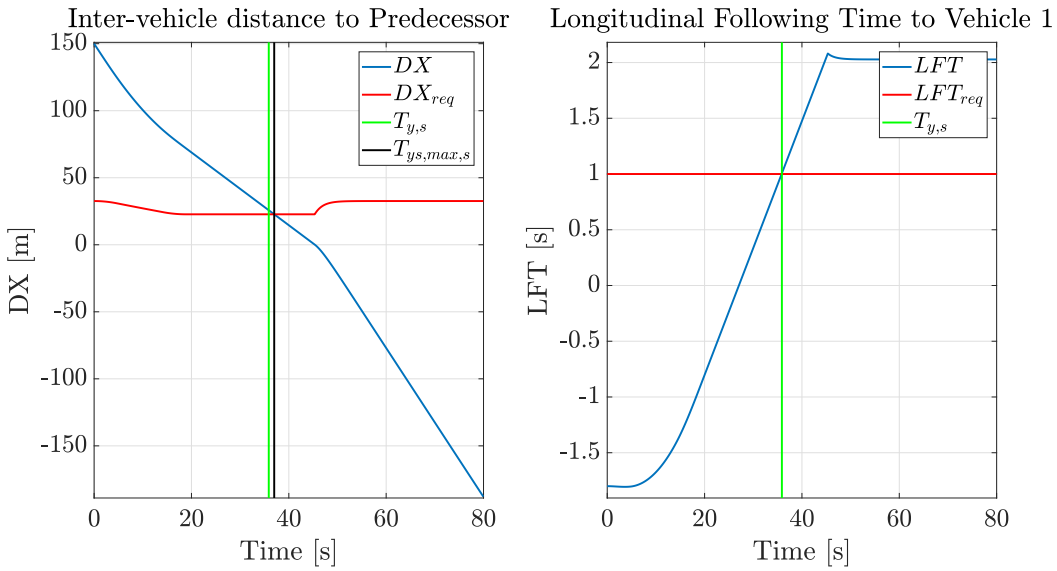

Figure 4.26: *Inter-vehicle distance to Predecessor DX, Longitudinal Following Time to Vehicle 1 LFT and the start of the lateral acceleration phase $T_{y,s}$ as function of time.*

4.2.7 Conclusion Scenario 2

Scenario 2 describes the longitudinal strategy of the Host in case there is one vehicle on the adjacent lane and one vehicle in front. The Host might either decelerate to merge behind or accelerating to merge in front. The optimal merging start times are based on three criteria: Inter-vehicle distance DX to Predecessor, LFT to Veh. 1 (in case of merging behind Veh. 1) and expected acceleration of Veh. 1 (in case of merging in front Veh. 1).

4.3 Scenario 3: multiple vehicles on the adjacent lane

This scenario investigates the situation where five other road users are involved. In addition to the Predecessor, on the adjacent lane there are four other vehicles (Veh. 1, 2, 3 and 4), resulting in three possible gaps (1, 2, 3) for the Host to merge into, see Fig. 4.27. The velocity of Veh. 2, 3 and 4 is initially higher than the Host velocity.

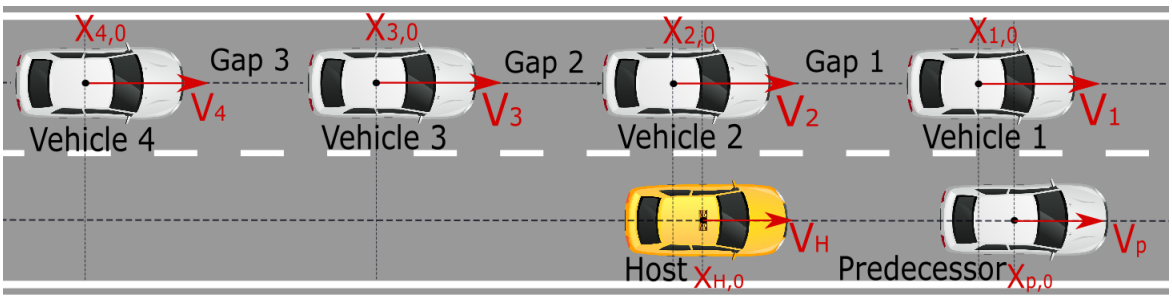

Figure 4.27: *Schematic highway overview of Scenario 3*

4.3.1 Assumptions and goals

In this scenario, the next assumptions are taken into account: a flat and straight highway, with five other road users, initially driving at a constant velocity and with a constant lateral position. In addition to section 4.2.1, the goal is to merge safely in a gap, while optimizing the Host comfortableness. To obtain a safe overtaking manoeuvre, the inter-vehicle distances are determined, as well as the expected deceleration of a gap's rear vehicle and the LFT to a gap's front vehicle.

Gap length requirement
In section 3.3.2 it was stated that the average time gap between vehicles on the highway A13 is 1.9 seconds. In this scenario, for convenience, a minimal time gap $TTP_{min,gap}$ of *two* seconds is assumed: the Host can merge in a gap if the rear vehicle is driving at least two seconds behind its Predecessor. This indicates that after merging the TTP for the Host to the new Predecessor (gap's front vehicle) is one second. After merging, the controller ensures that the inter-vehicle distance becomes equal to $T_{r,H}V_H$.

4.3.2 Merging Limits

The longitudinal strategies are strongly influenced by the Predecessor and the two vehicles defining a gap:

1. **Predecessor:** Considering the Predecessor, the absolute merging start time is limited by the safe inter-vehicle distance requirement (see section 4.1.3)
2. **Front Vehicle of a gap:** The limit for merging behind the Gap's front vehicle is based on the LFT (see section 4.2.3). The gap's front vehicle defines:
   - **2.1)** A maximum merging start time (in case the gradient of the LFT-graph is negative, while initially starting above the limit LFT_{req}, see Fig. 4.15 sub-plot 2), or

- **2.2)** A minimum merging start time (in case the gradient of the LFT-graph is positive, while initially starting below the limit LFT_{req}, see Fig. 4.15 sub-plot 3).

3. **Rear vehicle of a gap:** The limit for merging in front of the gap's rear vehicle is based on the expected deceleration of the vehicle (see section 4.2.5) The gap's rear vehicle defines:
   - **3.1)** A minimum merging start time (in case the gradient of the ACC-graph is positive, while initially starting below the deceleration limit A_{lim}, see Fig. 4.20) or
   - **3.2)** A maximum merging start time (in case the gradient of the ACC-graph is negative, while initially starting above the deceleration limit A_{lim}, see Fig. 4.21).

Merging conditions
The conditions for merging in a gap are:

- The minimum merging start time defined by gap's front vehicle is equal to or smaller than than the maximum merging start time due to the Predecessor, and
- The minimum merging start time defined by gap's rear vehicle is equal to or smaller than the maximum merging start time due to the Predecessor, and
- The minimum merging start time according to the gap's front vehicle is equal to or smaller than the maximum merging start time defined by the gap's rear vehicle, and
- The minimum merging start time defined by the gap's rear vehicle is equal to or smaller than the maximum merging start time according to the gap's front vehicle, and
- the Host velocity at the moment of merging is bigger or equal to the minimum highway velocity ($V_H(T_{y,s}) \geq V_{min}$). and,
- the Host velocity at the moment of merging is smaller or equal to the maximum highway velocity ($V_H(T_{y,s}) \leq V_{max}$).

Controller longitudinal strategies

In preparing a lane change, the Host has three options : accelerate, decelerate or holding the set speed.

Accelerate
If the target gap is in initially in front of the Host or when the average velocity on the adjacent lane is higher than $V_{H,0}$, longitudinal acceleration is required. The duration of the longitudinal acceleration phase and the maximum acceleration depend on the gap's rear vehicle (preventing the gap's rear vehicle to decelerate beyond the limit A_{lim}, see section 4.2.5). The Predecessor and the gap's front vehicle limit the duration and maximum value.

Decelerate
The Host will have to decelerate if the target gap is initially behind the Host, and the Predecessor limits the maximum merging time below the minimum merging of the gap.

Holding the set speed
In case acceleration or deceleration is not required for merging into a specific gap, the Host holds the set speed.

4.3.3 Visualizing the applied methods

This section deals with the results of the applied methods in this scenario. Table 4.1 presents the initial conditions.

Table 4.1: *Initial conditions of scenario 3*

Vehicle	X_0 [m]	V_0 [m/s]	Y_0 [m]
Host	40	27.8	W/2
Pre.	100	25	W/2
1	100	27.8	W+W/2
2	40	27.8	W+W/2
3	-20	27.8	W+W/2
4	-80	27.8	W+W/2

All vehicles are driving with equal initial velocity, except from the Predecessor ($V_{P,0} = 25$ m/s). The gap lengths are equal ($DX_{1\to2} = DX_{2\to3} = DX_{3\to4} = 60m$) and satisfy the requirement for minimal gap length, see section 4.3.1. The initial position of the Host is next to Veh. 2.
The Host can either merge in gap 1, 2 or 3. Each scenario is elaborated in the next sections. In the controller, the decesions for optimal merging times are based on the three criteria: inter-vehicle distance to Predecessor ($DX_{H\to P}$), LFT to gap's front vehicle ($LFT_{H\to1}$) and the expected acceleration from the gap's rear vehicle.

Merging in gap 1
In case the Host merges in gap 1, the Host will accelerate to ensure that Veh. 2 will not have to decelerate below the limit A_{lim}. In Table 4.2 presents the parameters calculated by the controller.

Table 4.2: *Resulting parameters describing the merging manoeuvre*

a_H $[m/s^2]$	T_x [s]	$T_{y,s}$ [s]	T_y [s]
0.10	9.00	8.28	15.48

Fig. 4.28 presents the criteria from the vehicles on the adjacent lane. In the upper figure, the expected acceleration is plotted over time. $T_{ys,min}$ defines the minimum merging start time based on the expected deceleration of Veh. 2. The lower figure indicates the LFT to Veh. 1, including the limit $T_{ys,max}$.

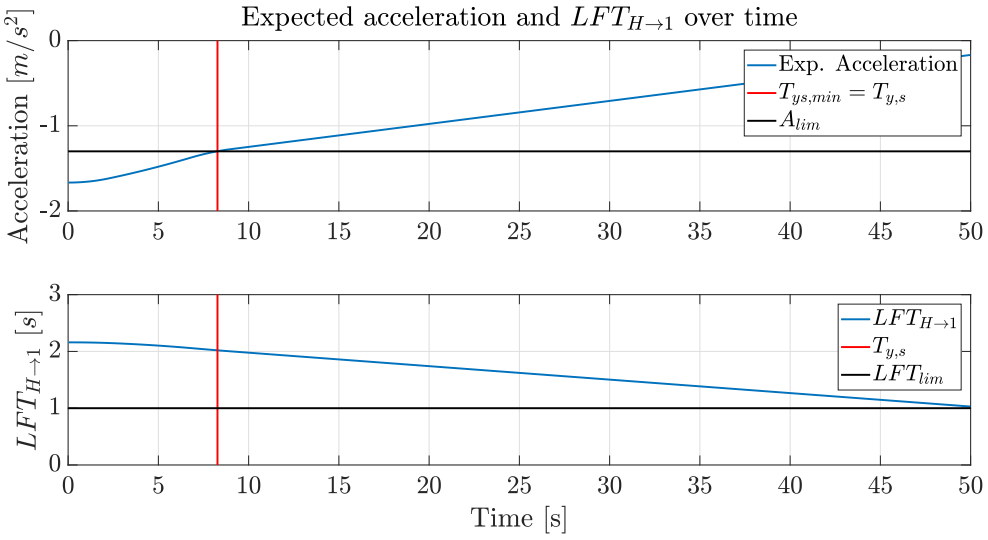

Figure 4.28: *Expected- and required acceleration (upper figure) and LFT (lower figure) over time,*

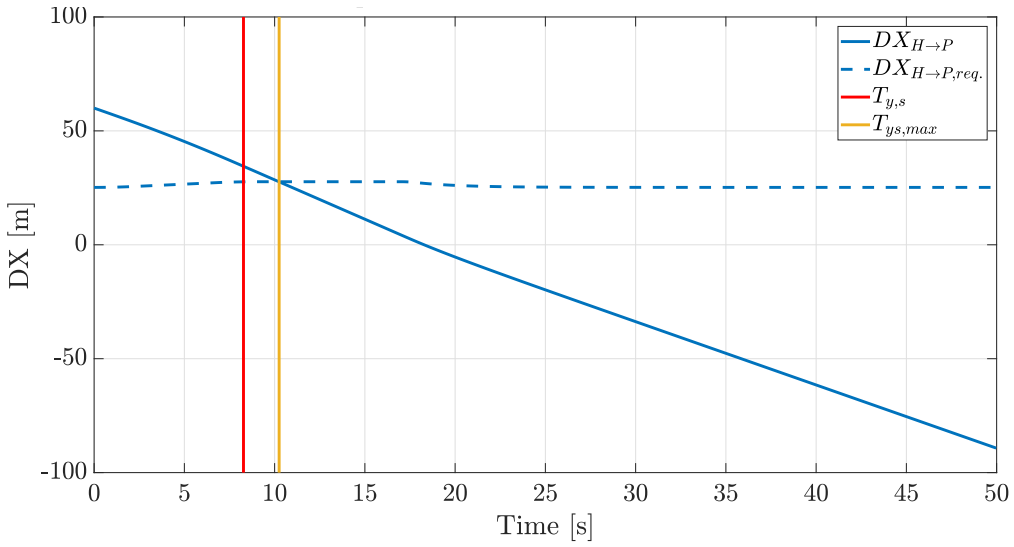

Figure 4.29: *Inter-vehicle distance to Predecessor $DX_{H\rightarrow P}$, required inter-vehicle distance $DX_{H\rightarrow Preq}$, maximum merging start time $T_{ys,max}$ and start time $T_{y,s}$*

In Fig. 4.29 it is shown that the maximum merging start time due to a safe inter-vehicle distance to the Predecessor is 10.1 s. This is higher than the minimum merging start time based on the expected acceleration of Veh. 2 (see Fig. 4.28, upper figure), indicating that the obtained overtaking manoeuvre is safe (the maximum merging start time due to the LFT to Veh. 1 is 49.5s).

Fig. 4.30 shows the resulting acceleration- and velocity profiles. Veh. 2 decelerates with $a_{x,2} = -1.177m/s^2$.

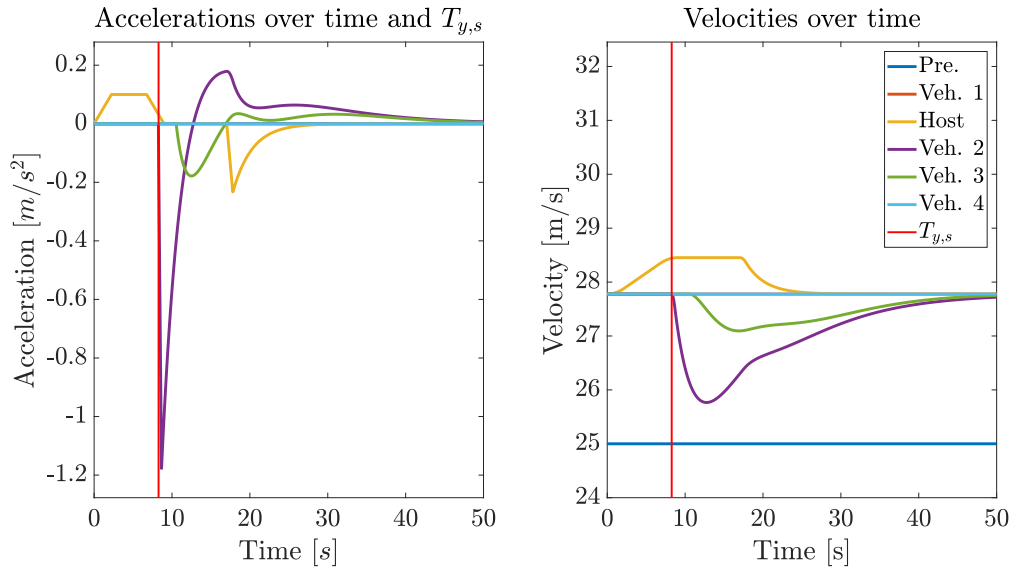

Figure 4.30: *Accelerations (left) and velocities over time*

Merging in Gap 2

When the Host tends to merge in the second gap, the longitudinal strategy is to decelerate in order to merge. Table 4.3 presents the resulting parameters for the determined overtaking manoeuvre, while Fig. 4.31 shows the accelerations and velocities of the road users.

Table 4.3: *Resulting parameters describing the merging manoeuvre*

a_H $[m/s^2]$	T_x [s]	$T_{y,s}$ [s]	T_y [s]
-0.20	11.00	21.35	20

Fig. 4.31 shows the resulting accelerations and velocities of the road users. The Host accelerates to $V_{H,0}$ after moving Y_{min} laterally.

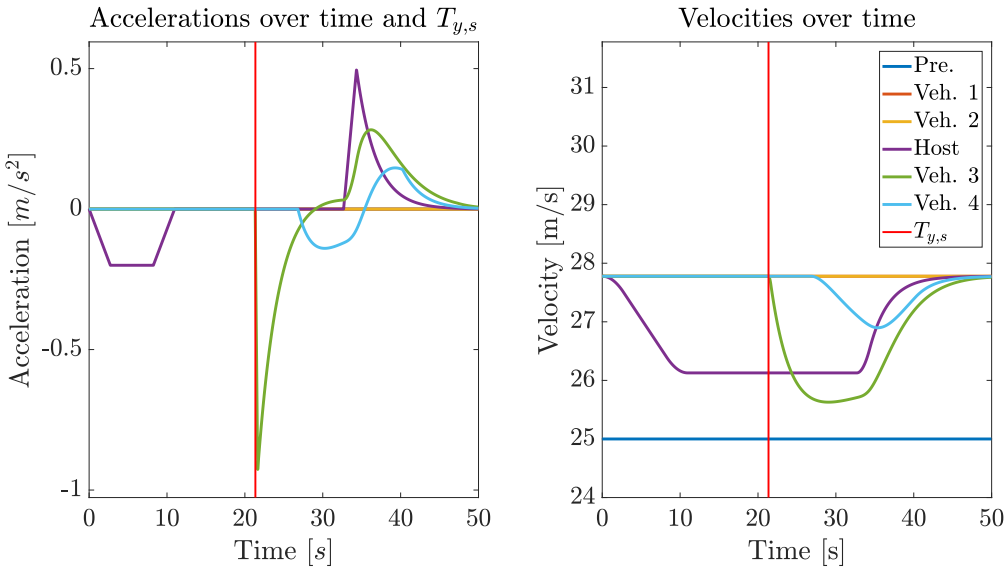

Figure 4.31: *Accelerations (left) and Velocities over time*

Appendix D presents the plots showing the different criteria and the maximum- and minimum merging start time. The maximum merging start time due to the inter-vehicle distance is $T_{ys,max,s} = 24.5$ s. The minimum merging start time $T_{ys,min} = 21.35$ s (based on the LFT to the gap's front vehicle).

Merging in Gap 3

Considering merging in Gap 3, Table 4.4 presents the resulting parameters for the determined overtaking manoeuvre, while Fig. 4.32 shows the accelerations and velocities of all road users.

Table 4.4: *Resulting parameters describing the merging manoeuvre*

a_H $[m/s^2]$	T_x [s]	$T_{y,s}$ [s]	T_y [s]
-0.40	12.00	29.40	20

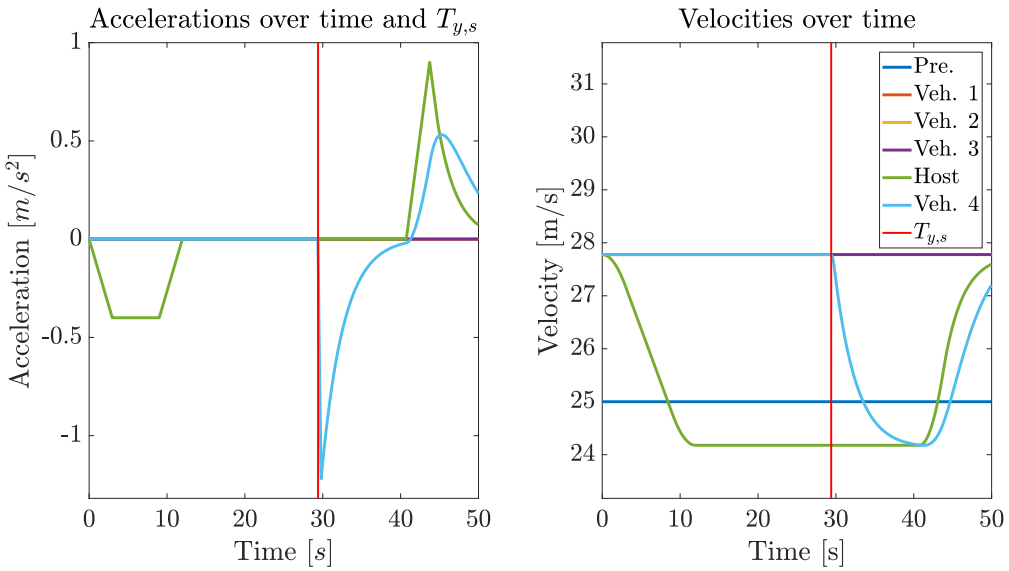

Figure 4.32: *Accelerations (left) and Velocities over time, and start time lateral movement* $T_{y,s}$

Appendix D presents the criteria plots on which decision-making is based.

From Fig. 4.32 it appears that merging is not the optimal strategy. The path that is determined results in a Host velocity which is lower than the Predecessor. This indicates that there is no need for a lateral movement in this case.

4.3.4 Conclusion Scenario 3

Scenario 3 implements the criteria and methods from Scenario 2 for determining the optimal switching moments. In addition, requirements are applicable to ensure that merging is safe. In the next section, the influence of uncertainties in the measurement signals is investigated.

4.4 Influence of uncertainties on the Host

In each measurement signal, uncertainties are present influencing the output variables of the Host controller. In this project, there are two uncertainties that influence the controller input signals: uncertainties in position and in velocities. In the following, by implementing uncertainties the 'measured' positions and velocities changes.

4.4.1 Uncertainties in measured positions

In case there are uncertainties in the measured positions of all road users, the resulting Host velocity- and acceleration profile will face different behaviour. The uncertainty in X-positions of the other vehicles is called U_x (in meter).
In Table 4.1 shows the influence of U_x on the longitudinal- and lateral Host accelerations, and on the duration of the longitudinal acceleration phase T_x and the RMS_c value. Here, the Host merges in Gap 1.

Table 4.1: *Influence of uncertainties in X-positions on resulting Host accelerations*

U_x [m]	$a_{x,max}$ $[m/s^2]$	$a_{y,max}$ $[m/s^2]$	T_x [s]	RMS_c [-]
0	0.100	0.096	9	1.866
1	0.100	0.1079	10	1.988
-1	0.100	0.0861	8	1.7467
2	0.100	0.1217	11	2.1145
-2	0.100	0.0787	7	1.6338
5	0.200	0.1026	6	2.7572
-5	0.100	0.0636	4	1.2849

From Table 4.1 it appears that if there is a positive uncertainty $U_x > 0$ in the longitudinal positions of the other road users, the resulting RMS_c value increases. This indicates that the experienced comfort is decreased.

4.4.2 Uncertainties in velocity

The second option includes uncertainties in velocity. In fact, velocities are determined via processing of the position measurements over time. This section indicates the influence of uncertainties in velocities.
In Table 4.2 the influence of uncertainties in velocities U_v is presented. The first row indicates the results when no uncertainties are present, which could be seen as the real velocities.

Table 4.2: *Influence of uncertainties in longitudinal velocity on resulting Host accelerations*

U_v $[m/s]$	$a_{x,max}$ $[m/s^2]$	$a_{y,max}$ $[m/s^2]$	T_x [s]	RMS_c [-]
0	0.100	0.096	9	1.866
1	0.300	0.1262	10	5.0647
-1	0	0.0577	0	0.7091
2	0.700	0.1239	7	9.6545
-2	0	0.0577	0	0.7091
5	NP*	NP*	NP*	NP*
-5	0	0.0577	0	0.7091

*Not Possible: controller indicates that merging in Gap 1 is not possible.

Table 4.2 indicates that uncertainties in velocities highly influence the Host overtaking manoeuvre. For negative U_v the comfortableness of the overtaking manoeuvre improves: the RMS_c value decreases. In this simulation, for $U_v < -1$ m/s, the maximum Host acceleration becomes zero. This indicates that controller decides that a longitudinal Host acceleration is not required in order to find the optimal path for merging. This strongly influences safety, since the real measurements (where $U_v = 0$ in Table 4.2 show that a longitudinal acceleration is required). For increasing measured velocity, the RMS_c values increases. For $U_v > 5$ m/s merging in Gap 1 is no longer possible.
In Fig. 4.33 the obtained velocity profiles of the Host and other vehicles are plotted for four values of U_v. It shows that a decreasing 'measured velocity' ($U_v = -1$ and $U_v = -2$) prevents the Host from accelerating to merging in Gap 1, while an increasing 'measured velocity' ($U_v = 1$ and $U_v = 2$) results in increasing velocity variations, both from the Host and the other traffic.

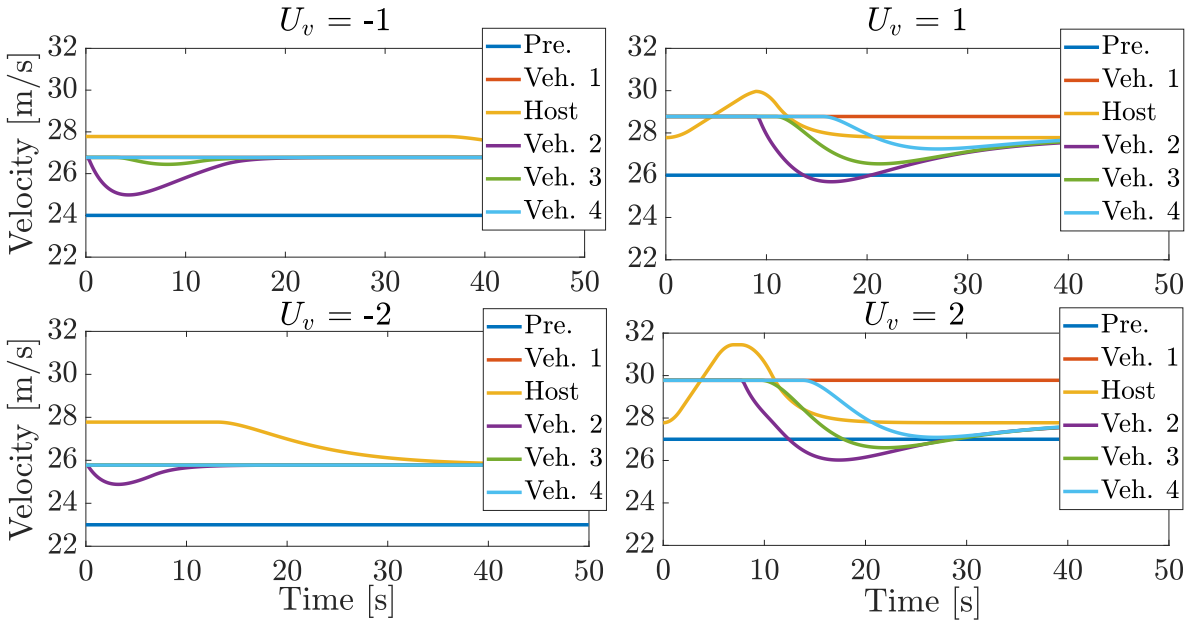

Figure 4.33: *Velocities over time, for different values of uncertainties in velocity U_v*

Conclusion

In this section it is indicated that uncertainties in both controller input signals (positions and velocities) strongly influences the obtained Host overtaking strategies. Differences in measured- and real velocities might ensure that the controller decides merging is not possible. For smaller uncertainties in velocity, the controller increases the assigned longitudinal accelerations to the Host (see Table 4.2, where $U_v = 2$m/s).

Uncertainties play an important role in the path planning method and are required to be minimized in order to prevent the controller from assigning unnecessary high accelerations. For smooth automated driving, the reduction of uncertainties is an important aspect and strongly determines the safety of highway driving.

Chapter 5

Decision-making algorithms

This chapter elaborates on the decision-making algorithms that are implemented in the simulations. Decision-making is based on optimization problems. Two optimization problems are distinguished: path optimization and comfort optimization.
In the path optimization, an object function is generated. A controller algorithm is applied to predict the states of the other road users and to determine and execute an optimal path, satisfying safety- and comfort constraints.
In the comfort optimization problem, the limit values for the accelerations are varied, using the different comfort levels (see Tables 3.2, 3.3 and 3.4). Different comfort levels are distinguished, each with certain acceleration limits. Considering the comfort optimization problem, the goal is to minimize the accelerations of the Host.

5.1 Path optimization problem

The path optimization problem includes a path calculator, which assigns and describes the paths of the Host vehicle. The path optimization problem consist of a preparation part, a calculation (or main) part and an execution part.

Preparation
In the preparation part, a path prediction of the states (positions and velocities) of all road users is generated, based on sensor measurements (RADAR, LIDAR, or Camera). The system determines the gap length in case there are multiple vehicles driving in the adjacent lane. If the length of a Gap does not face the requirements for minimal gap length, in the calculation part this Gap is ignored.

Calculation
The calculation part determines the optimal path (longitudinal and lateral accelerations) for the Host, while satisfying the safety- and comfort constraints. In case just a Predecessor is present, the maximum merging start time is calculated.
When there are multiple vehicles on the adjacent lane, in the calculation part the controller is analysing multiple suggested paths. Here, the longitudinal acceleration a_H of the Host is varied, as well as the duration of the longitudinal acceleration T_x.
The two individual vehicles belonging to a specific gap define the minimal- and maximal merging times. The Predecessor defines the absolute maximal merging time, considering safety and comfort. If merging in a gap for the specific longitudinal movement (maximum value and belonging duration) is possible, the RMS_c value is determined. After analysing all suggested paths, the optimal path is chosen, by finding the minimum RMS_c value and minimizing the duration of the longitudinal acceleration.

Execution
In the execution part, the optimal path that was determined in the calculation part, is executed. The resulting accelerations and velocities are determined. ACC is applied to ensure other road users are

reacting on a merging Host in front. If possible, ACC is applied to the Host in order to reach the set speed again.

Optimization problem

The optimization problem for the controller is separated in control laws before- and after the merging manoeuvre.

Before merging

In case the Host merges into a gap on the adjacent lane, the optimization strategy is given as (using path Object function O_p equal to the RMS_c value, see Eq. (3.24)

minimize $(O_p(a_H, a_y), T_x)$
where:

$$O_p = \sqrt{\frac{\sqrt{\left(\frac{a_H}{C_x}\right)^2 + \left(\frac{a_y}{C_y}\right)^2}^2}{N}} \tag{5.1}$$

such that (see section 4.3.2):

$$max(V_H) \leq V_{max} \tag{5.2}$$
$$min(V_H) \geq V_{min} \tag{5.3}$$
$$T_{ys,min,f}(a_H, T_x) \leq T_{ys,max,p}(a_H, T_x) \tag{5.4}$$
$$T_{ys,min,r}(a_H, T_x) \leq T_{ys,max,p}(a_H, T_x) \tag{5.5}$$
$$T_{ys,max,r}(a_H, T_x) \leq T_{ys,min,f}(a_H, T_x) \tag{5.6}$$
$$T_{ys,min,r}(a_H, T_x) \geq T_{ys,max,f}(a_H, T_x) \tag{5.7}$$
$$a_y \leq C_y \tag{5.8}$$
$$a_H \leq C_{x,p} \quad if \quad a_H \geq 0 \tag{5.9}$$
$$a_H \geq C_{x,n} \quad if \quad a_H \leq 0 \tag{5.10}$$

where:

$$V_H(t) = V_{H,0} + \int_0^t a_H(t)dt \tag{5.11}$$

and $T_{ys,max,p}(a_H, T_x)$ is defined as the maximum merging start time, based on the required safe inter-vehicle distance to the Predecessor. $T_{ys,min,f}(a_H, T_x)$ and $T_{ys,max,f}(a_H, T_x)$ indicate the minimum- and maximum merging start time, respectively, based on the LFT to the gap's front vehicle.
$T_{ys,min,r}(a_H, T_x)$ and $T_{ys,max,r}(a_H, T_x)$ indicate the minimum- and maximum merging start time, respectively, based on the expected deceleration of the gap's rear vehicle. C_x in Eq. (5.1) indicates the relevant comfort criteria in longitudinal direction ($C_x = C_{x,p}$ if $a_H \geq 0$ or $C_x = C_{x,n}$ if $a_H \leq 0$), while C_x defines the lateral acceleration comfort criteria.

Eq. (5.2) till (5.7) refer to the constraints considering highway limits and safety. Eq. (5.8) till (5.10) refer to the comfort constraints, these values are varied in the Comfort optimization problem, see section 5.2.

After merging

Considering merging, there are two options: after merging the Host notices a new Predecessor or the Host does not notice a new Predecessor. Both situations result in different approaches considering

the Host accelerations.

Host notices no Predecessor after merging
In this case, the Host will decelerate in case $V_H(T_{y,s}) > V_{H,0}$ or accelerate if $V_H(T_{y,s}) < V_{H,0}$. The error in velocity e_v is defined as:

$$e_v(t) = V_{H,0} - V_H(t) \tag{5.12}$$

where V_H is the velocity of the Host and $V_{H,0}$ is the initial Host velocity. The Host velocity is updated via:

$$U_H(t) = k_p \cdot e_v(t) \tag{5.13}$$
$$V_H(t) = V_H(t-1) + U_H(t) \tag{5.14}$$

Host notices a new Predecessor after merging
In this case, the Host will decelerate in case $V_H(T_{y,s}) > V_{H,0}$ or try to accelerate if $V_H(T_{y,s}) < V_{H,0}$. The new Predecessor defines if the desired acceleration is possible. The following rule is applied for the target Host velocity $V_{H,T}$ after merging:

$$V_{H,T} = min(V_{H,0}, V_P) \tag{5.15}$$

where V_P is the velocity of the new Predecessor. The Host velocity $V_H(t)$ is updated via:

$$e_v(t) = V_{H,T} - V_H(t) \tag{5.16}$$
$$e_x(t) = X_H(t) - X_P(t) + T_{r,H}V_H(t) \tag{5.17}$$
$$U_H(t) = k_p \cdot e_v(t) + k_i \cdot e_x(t) \tag{5.18}$$
$$V_H(t) = V_H(t-1) + U_H(t) \tag{5.19}$$

where X_P is the location of the new Predecessor.

5.2 Comfort optimization problem

In the comfort optimization problem the acceleration limits are varied in order to optimize the comfortableness, while obtaining safety requirements. Table 5.1 presents the acceleration-based comfort levels. Here, $a_{x,max}$ is the maximum longitudinal acceleration, $a_{x,n,max}$ is the maximum longitudinal deceleration and $a_{y,max}$ is the maximum lateral acceleration.

Table 5.1: *Comfort levels, see section 3.3.3, 3.3.4 and 3.3.5*

Level	$a_{x,max}$ $[m/s^2]$ (accelerating)	$a_{x,n,max}$ $[m/s^2]$ (decelerating)	$a_{y,max}$ $[m/s^2]$ (steering)
Comfortable	1	-1.3	1.65
Relative Comfortable	1.5	-2.5	2.85
Uncomfortable	2.5	-4.24	4.05

The object function for this optimization problem is given as:

minimize $(C_{x,p}|C_{x,n}, C_y)$

such that:

$$RMS_c(C_{x,p}|C_{x,n}, C_y) \geq 0 \tag{5.20}$$

and all safety constraints (Eq. (5.2) till (5.10)) are still required to be satisfied. In Eq. 5.20, $C_{x,p}$, $C_{x,n}$ and C_y are given as:

$$C_{x,p} = \begin{bmatrix} 1 \\ 1.5 \\ 2.5 \end{bmatrix}, C_{x,n} = \begin{bmatrix} -1.3 \\ -2.5 \\ -4.24 \end{bmatrix}, C_y = \begin{bmatrix} 1.65 \\ 2.85 \\ 4.05 \end{bmatrix} \tag{5.21}$$

For each comfort level, the RMS_c value is determined (using section 5.1), as well as the requirements for the path controller (Eq. (5.2) till (5.10)). The comfort algorithm varies the comfort criteria $C_{x,p}$, $C_{x,n}$ and C_y, starting with the first level. In case this comfort level does not result in a valid lane-change, the level of comfort is decreased (lower comfort level indicates higher allowable accelerations), until a solution is found or the Host is required to decelerate in order to prevent collision with the Predecessor. The resulting accelerations- and velocities of the road users are influenced in two ways:

- The deceleration of other road users increases in case the comfort level is decreased and the Host merges in front
- The longitudinal- and lateral accelerations of the Host are influenced (either positive or negative).

Deceleration other road users

In case the Host merges in front of an other road user, this vehicle will have to decelerate in order to obtain a safe inter-vehicle distance TrV (assuming initially $DX_{H \to Veh.} < TrV$, where $DX_{H \to Veh.}$ is the initial inter-vehicle distance and TrV is the reaction time multiplied with the actual Velocity, see Section. 4.2.4). For decreasing Comfort levels, higher decelerations of the other road user are accepted. This requires a lower Host acceleration, since the required inter-vehicle distance at $T_{y,s}$ is decreased. Fig. 5.1 shows the resulting accelerations for the three comfort levels, indicating that the longitudinal accelerations of the Host are decreased, see Table 5.2.

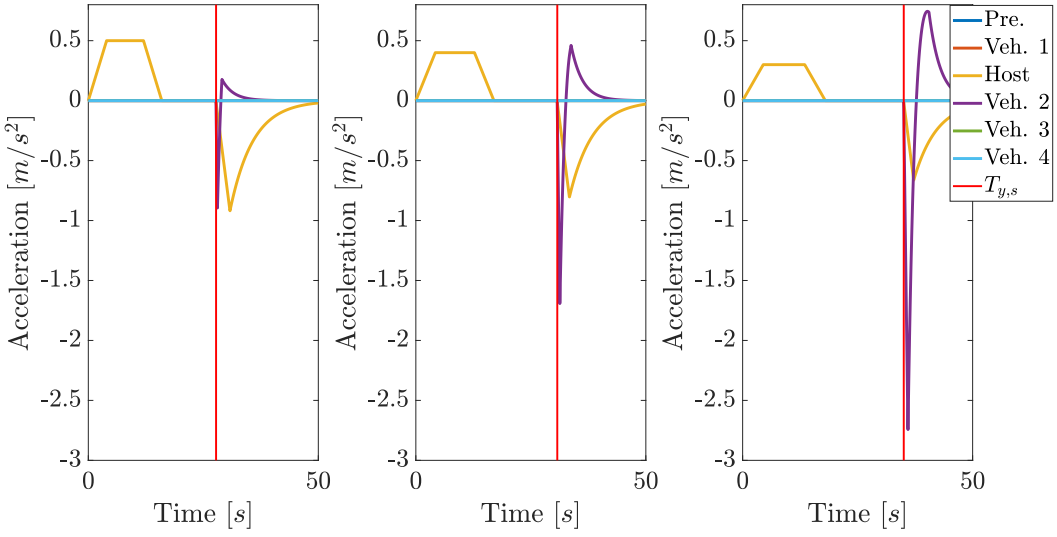

Figure 5.1: *Accelerations using the three Comfort levels*: comfortable (left), relative comfortable (middle) and uncomfortable (right)*

*Notice that the deceleration of the other road user is not facing the absolute limits due to jerk limitations.

Table 5.2: *Decreasing Host acceleration for different comfort levels of the approaching traffic*

Level	$a_{x,max}$	T_x
Comfortable	0.5	16
Relative comfortable	0.4	17
Uncomfortable	0.3	18

Table 5.2 shows that for decreased comfort levels of the other road users the maximum acceleration of the Host decreases.

Accelerating/decelerating to merge in front
For decreasing Comfort levels, the Host maximum acceleration increases. The maximum velocity of the Host is limited to $V_H <= V_{Max}$, indicating that a high acceleration can only last a few seconds, to prevent violating the maximum allowable highway speed.
Fig. 5.2 shows the resulting accelerations and velocities. The maximum Host acceleration is $a_H = 0.5m/s^2$, lasting for four seconds. The maximum Host velocity is $V_{H,max} = 35.28m/s$.

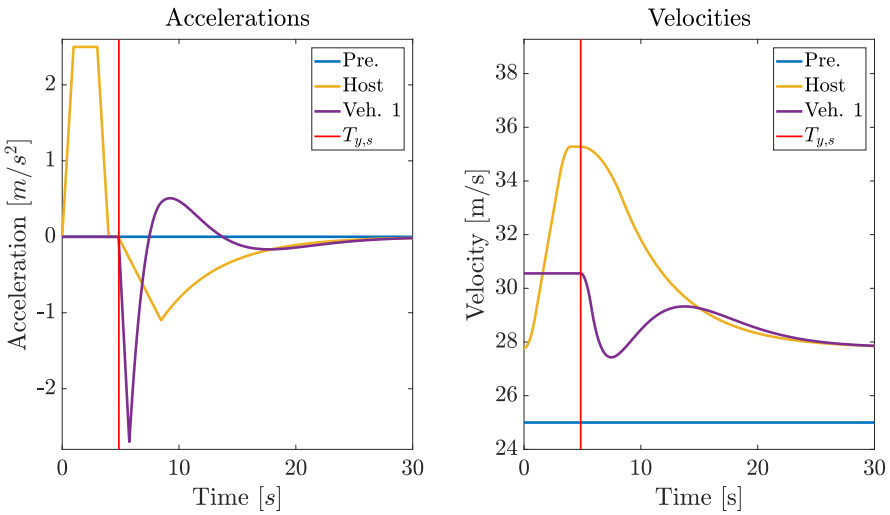

Figure 5.2: *Accelerations (left) and velocities (right) for the Uncomfortable level*

Table 5.3 presents the initial conditions for this simulation. A high longitudinal Host acceleration is required in order to merge in front of a vehicle on the adjacent lane.

Table 5.3: *Initial conditions*

Vehicle	X_0 [m]	V_0 [m/s]
Pre.	145	25
Host	50	27.78
Veh. 1	50	30.55

In Fig. 5.3 an example is given where the Host decelerates with $a_H = -1.7m/s^2$, indicating that this manoeuvre is Relative Comfortable.

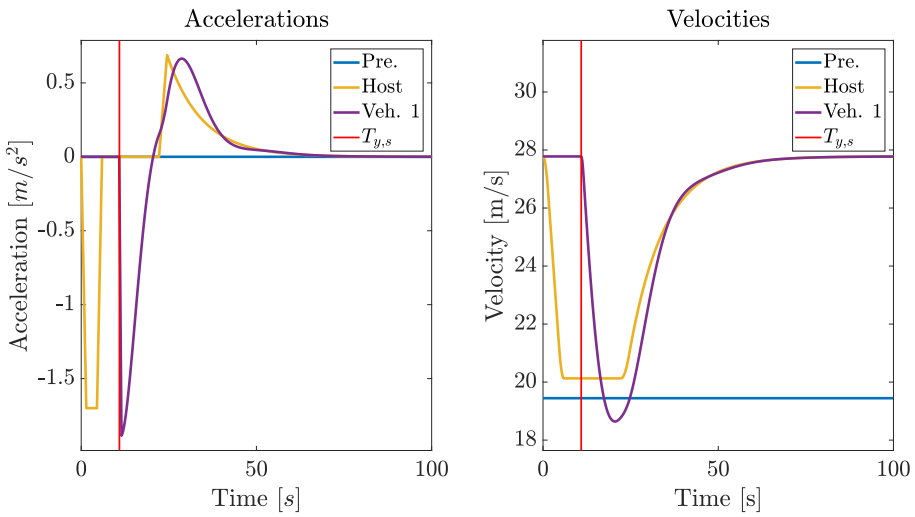

Figure 5.3: *Acceleration (left) and velocities (right) for the Relative comfortable level*

Arrival time
The arrival time of the Host depends on the different Comfort levels. In case of one vehicle on the adjacent lane, the optimal strategy for reducing the arrival time is to merge in front, while satisfying safety constraints.
In case of merging behind another vehicle, the arrival time is not influenced, since the target velocity of the Host is the minimum of the new Predecessor's velocity and the set speed of the Host.
The arrival time is decreased in case the Host merges into gaps ahead (using decreased comfort levels) that would not have been possible using the Comfort criteria. In the controller, for each gap the minimum value of the RMS_c is determined. This results in a vector where the length is equal to the number of gaps and the values are the minimum RMS_c values of each gap. Afterwards, in case the goal is to minimize comfort, the minimum of these gap-related RMS_c values is chosen (the gap that results in the minimum resulting accelerations). If the goal is minimizing the arrival time, the lowest gap number is chosen. This ensures that the Host always merges into the first (or leading) gap in a string of vehicles.

5.3 Conclusion

Considering the applied optimization problems, the ultimate goal is to reduce the resulting acceleration. Minimizing the RMS_c value results into the lowest resulting acceleration. The comfort optimization problem will decrease the comfort levels if required in order to make safe lateral movements possible.
Considering minimizing the arrival time, the gap with the lowest identity number (see Fig. 4.27) is chosen as the optimal gap to merge into. This indicates that the Host merges in the most forward, valid gap.

Chapter 6

Conclusions and Recommendations

Conclusions

The goal of this Master's Thesis is to investigate and develop control strategies for smooth highway driving. The focus is on preparing a lane change. In particular, the longitudinal motion is investigated in order to obtain safe and smooth lane changes.

Considering defining the optimal strategies, first the modelling is described. For the longitudinal motion a trapezoid acceleration profile is used, while the lateral motion is described by a fifth-order polynomial. Considering the longitudinal acceleration, especially the maximum acceleration and the duration of the longitudinal acceleration are parameters that have to be controlled. The start time of the lateral and the duration of the lateral movement describe the lateral motion. This values indicate the need for calculating the first- and last moments to merge.
The last moment to merge is determined by the Predecessor of the Host. A safe inter-vehicle distance is required, resulting in a last moment to start merging. In addition, the Time To Collision to the Predecessor is used to determine the duration of the lateral movement. Here, the lateral offset of the Predecessor determines the minimal required lateral distance that the Host should move within the time it takes before the collision would theoretically occur.
The last moment to merge can also depend on one (or more) vehicle(s) in the adjacent lane. Considering each vehicle on the adjacent lane, the Host can either merge in front or behind it.
In case of merging in front, the expected deceleration of the vehicle is used as a reference to determine the firs- or last moment to merge. For each comfort level, the maximum deceleration is used to limit the maximum expected deceleration.
In case the Host merges behind, the longitudinal following time the the new Predecessor is used to determine the first- or last moment to merge. For all options, the first and last moment determine the optimal switching moment. Using the switching moment, the duration of the lateral movement is determined, after which the resulting accelerations and the comfortableness of the particular overtaking manoeuvre are determined.
A comfort decision-making algorithm is used to vary the comfort levels if merging using the highest comfort level is not possible. Two main goals can be distinguished: maximize comfort (minimize resulting acceleration) or minimize arrival time. Considering minimizing arrival time, the leading valid gap is selected to merge into.

The influence of uncertainties in the measurement signals is investigated as well. Uncertainties appear to play an important role in the path planning method and are required to be minimized in order to prevent the controller from assigning unnecessary high accelerations. For smooth automated driving, the reduction of uncertainties is an important aspect and strongly determines the safety of highway driving.

Concluding, this thesis provides methods to prepare a lane change, by finding the optimal path while satisfying all constraints and criteria (e.g. first- and last moments to merge, and the duration of the

lateral movement based on TTC at the start of the lateral movement). This work is providing a sound base for future work on path planning for automated highway driving.

Recommendations

Regarding future work, several aspects still have to be investigated. In particular, unexpected events that happen should be taken into consideration. The algorithm uses measurement data to predict future states of other road users, resulting in the calculation of an optimal path. The model assumes stead-state surroundings (traffic will not accelerate and not merge).
To implement a fully working model in a real car, the main challenge is to react on unpredicted events (e.g. accelerating road users, road users switching lanes, emergency stops, traffic jams). In case these events occur, the calculated and optimized paths are still not valid. The Host will have to react on the actual situation rapidly. In Chap. 2 the potential field method is investigated. Each object that is sensed by RADAR, LIDAR or camera gets its own Potential function. This method is strongly recommended to use in case unexpected events happen near the Host. In contradiction to the method that is applied in this thesis, there is no path calculation controller, the Host will just follow the path with the lowest gradient (requiring controllers for translating the desired direction and velocities into actuator inputs). The Potential Fields method is described to be robust. A major recommendation is to combine the path planning method (described in this project) in combination with the Potential field method, resulting in an Host that is able to rapidly react on unexpected events.
In addition, the suggestion is to investigate how the optimal path calculation can be updated in case velocity of the other road users is not constant. Other suggestions for future work are to investigate methods for optimal lane switching to the initial lane. In this thesis, only one lateral movement was investigated. In fact a comparable method can be used to find the optimal moment (or Gap) to merge into on the initial lane. Furthermore, the path planning methods can be implemented in highway models having more than two lanes. Here, the Host should have a clear overview about all road users in the surroundings. Finally, the path planning problem should also work in extreme situations, e.g. in case of a traffic jam where the Host needs to merge to overtake or to switch.

Bibliography

[1] CBS (2017). *Doden en gewonden in het wegverkeer.* Aantal verkeersdoden in 2016 opnieuw toegenomen. Retrieved from www.cbs.nl/nl-nl/maatschappij/verkeer-en-vervoer/transport-en-mobiliteit/ at April 13th, 2018.

[2] Destatis (2018), *Causes of accident.* Accident statistics in Germany. Retrieved from https://www.destatis.de at November 15th, 2018.

[3] Nick Heath (2018), *Tesla's Autopilot: Cheat sheet* Tech Republic. Retrieved from https://www.techrepublic.com/article/teslas-autopilot-cheat-sheet/ at December 18th, 2018.

[4] Wikipedia contributors (2018). *Autonomous cruise control system.* Wikipedia, the free Encyclopedia. Retrieved from https://en.wikipedia.org/wiki/ at April 11th, 2018.

[5] Wikipedia contributors (2018). *Lane Centering* Wikipedia, the free Encyclopedia. Retrieved from https://en.wikipedia.org/wiki/ at December 18th, 2018.

[6] Wikipedia contributors (2018). *Lane_departure_warning_system#Lane Keeping* Wikipedia, the free Encyclopedia. Retrieved from https://en.wikipedia.org/wiki/ at January 28th, 2019.

[7] Melanie May (2017).*The 6 levels of self-driving car - and what they mean for motorists.* SAE has defined six levels of autonomy for self-driving, heres what they mean. Retrieved from www.thejournal.ie, at May 14th, 2018.

[8] Fortuna, C. (2017). Autonomous Driving Levels 05 + Implications. Retrieved from https://cleantechnica.com/2017/12/02/autonomous-driving-levels-0-5-implications/ at May, 22th, 2018.

[9] NATSH (2018).*Automated Vehicles for Safety.* United States Department of Transportation. Retrieved from https://www.nhtsa.gov/technology-innovation/automated-vehicles-safety, at December 18th, 2018.

[10] Michale Taylor (2017). *The Level 3 Audi A8 Will Almost Be The Most Important Car In The World.* Retrieved from: https://www.forbes.com/sites/michaeltaylor/2017/09/10/tthe-level-3-audi-a8-will-almost-be-the-most-important-car-in-the-world/ at January, 2th, 2019.

[11] Dom Galeon (2018). *Who Is Responsible When a Self-Driving Car Has an Accident?* BBC News, California DMV - GM Incident Report. Published: January 29, 2018.

[12] Rohan Kumar, Rajan Pathak (2012). *Adaptive Cruise Control - Towards a Safer Driving Experience.* International Journal of Scientific and Engineering Research Volume 3, Issue 8, August-2012.

[13] C. Kreuzen (2012). *Cooperative Adaptive Cruise Control.* Using information from multiple predecessors in combination with MPC. Master of Science Thesis, Faculty of Mechanical, Maritime and Materials Engineering, Delft University of Technology

[14] Jeroen Ploeg, Elham Semsar-Kazerooni, Guido Lijster, Nathan van de Wouw, and Henk Nijmeijer (2013). *Graceful Degradation of CACC Performance Subject to Unreliable Wireless Communication.* Proceedings of the 16th International IEEE Annual Conference on Intelligent Transportation Systems (ITSC 2013), The Hague, The Netherlands, October 6-9, 2013.

[15] Plamen Petrov, Fawzi Nashashibi (2013). *Adaptive Steering Control for Autonomous Lane Change Maneuver* IV 2013 - IEEE Intelligent Vehicles Symposium, Jun 2013, Australia. IEEE, pp.835- 840.

[16] Cao, W. et al (2014). Gap selection and Path Generation during Merging maneuver of Automobile Using Real-Time Optimization. SICE Journal of Control, Measurement and System Integration. Vol. 7, No. 4, p. 227-236. July 2014.

[17] Liu, K. et al (2017). A Model Predictive-based Approach for Longitudinal Control in Autonomous Driving with Lateral Interruptions. IEEE Intelligent Vehicles Symposium, Redondo Beach, CA, USA. June 11-14 2017.

[18] J. Wei, J. Dolan, B. Litkouhi (2010). A Prediction- and Cost Function-Based Algorithm for Robust Autonomous Freeway Driving. IEEE Intelligent Vehicles Symposium, University of California, CA, USA. June 21-24, 2010.

[19] Attia, R. Orjuela, R. and Basset, M. (2012) Longitudinal Control for Automated Vehicle Guidance. Workshop on Engine and Powertrain Control, The international Federation of Automatic Control. Ruell-Malmaison, France, October 23-25, 2012.

[20] Y. Yi and Z. Wang (2015). *Robot Localization and Path Planning based on Potential field for map building in static environments.* Engineering Review, Vol. 35, Issue 2, 171-178, 2015. Xian University of Technology, Xian, China.

[21] Wolf, Michael T. and Burdick, Joel W. (2008). Artificial Potential Functions for Highway Driving with Collision Avoidance. 2008 IEEE International Conference on Robotics and Automation. Pasadena, CA, USA, May 19-23, 2008.

[22] Brandt, Thorsten (2007). Predictive Potential Field Concept for Shared Vehicle Guidance. Dissertation at the University of Paderborn, Germany.

[23] Tang et al. (2010). *A Novel Potential Field Method for Obstacle Avoidance and Path Planning of Mobile Robot.* School of Electrical Engineering and Information Technology, Sichuan University, Chengdu, China. Computer Science and Information Technology (ICCSIT), 2010 3rd IEEE International Conference.

[24] Rasekhipour,Y. Khajepour, A. Chen, S Litkouhi, B. (2017) *A Potential Field-Based Model Predictive Path-Planning Controller for Autonomous Road Vehicles.* IEEE Transactions on Intelligent Transportation Systems, Vol. 18, No. 5, May 2017.

[25] M.Treiber and A.Kesting (2012). *Traffic flow Dynamics.* Chapter 11: Car-Following Models based on Driving Strategies. New York : Springer, 2012.

[26] Understanding Radar for automotive (ADAS) solutions (2018) Retrieved from: www.pathpartnertech.com/understanding-radar-for-automotive-adas-solutions at 14-12-2018.

[27] Advantages and Disadvantages of LiDAR (2018). Retrieved from: http://lidarradar.com/info/advantages-and-disadvantages-of-lidar at 14-12-2018.

[28] Timothy B. Lee (2018) Why experts believe cheaper, better lidar is right around the corner. Retrieved from: www.arstechnica.com/cars/2018 at 18-2-2019.

[29] Rao R. Tummala (2017). *Autonomous Cars: Radar, Lidar, Stereo Cameras.* Georgia Intsitute of Technology, United States of America. Georgia Tech PRC Presentations - IEEE CPMT Workshop - April 2017-2.pdf, consulted at: January, 12th, 2019.

[30] Fry, D. (2009). Adjusting and Calibrating Out Offset and Gain Error in a Precision DAC. Maxim Integrated Products, Inc. TUTORIAL 4602. Retrieved from: https://www.maximintegrated.com/en/app-notes/index.mvp/id/4602 at January, 12th, 2019.

[31] Dubbelman, G. (2017) Lecture: Sensors and Sensor modelling. Eindhoven University of Technology. Course: Vehicle Control (4AT050), Lecture 4A.

[32] Wikipedia contributors (2018) *Gaussian noise* Wikipedia, the free Encyclopedia. Retreived from: www.wikipedia.org/wiki/Gaussian_noise at January, 12th, 2019.

[33] Wikipedia contributors (2018) *Propagation of uncertainty* Wikipedia, the free Encyclopedia. Retreived from: www.wikipedia.org/wiki/Propagation_of_uncertainty at January, 12th, 2019.

[34] Wolff, Christian (2018). *Radars Accuracy*. Retrieved from: http://www.radartutorial.eu at January, 12th, 2019.

[35] Wilfried Elmenreich (2002). *An Introduction to Sensor Fusion*. Research Report 47/2001. Institut fur Technische Informatik Vienna University of Technology, Austria

[36] Wikipedia contributors (2018). *Left- and right-hand traffic* Wikipedia, the free Encyclopedia. Retrieved from https://en.wikipedia.org/wiki/ at April 11th, 2018.

[37] Hoberock, L.L. A Survey of Longitudinal Acceleration Comfort Studies in Ground Transportation Vehicles. ASME. J. Dyn. Sys., Meas., Control. 1977; 99(2):76-84. doi:10.1115/1.3427093.

[38] Autosnelwegen - Rijden en regels op de autosnelweg. https://auto-en-vervoer.infonu.nl/verkeer/92130-autosnelwegen-rijden-en-regels-op-de-autosnelweg.html (2012 - 2018). Consulted at: 19/06/2018.

[39] Wikipedia contributors (2018). *Bumperkleven* Wikipedia, the free Encyclopedia. Retreived from: https://nl.wikipedia.org/wiki/Bumperkleven at January, 2th, 2019.

[40] CBS (2017). *A13 blijft drukste rijksweg*. Retrieved from: https://www.cbs.nl/nl-nl/nieuws/2017/15/a13-blijft-drukste-rijksweg at January, 2th, 2019.

[41] J. Y. Wong (2008). Theory of Ground Vehicles. Fourth edition, Carleton University, Ottawa, Canada. http://hpwizard.com/tire-friction-coefficient.html

[42] Jin Xu, Kui Yang, Ti-Ming Shao (2017). *Ride Comfort of Passenger Cars on Two-Lane Mountain Highways Based on Tri-axial Acceleration from Field Driving Tests.* International Journal of Civil Engineering, March 2018, Volume 16, Issue 3, p. 335351

[43] Nile van Leeuwen (2018). TOP-10 Bestverkochte Modellen van 2017. January, 3th, 2018. Retrieved from https://autorai.nl/top-10-bestverkochte-modellen-van-2017/ at 28/06/2018.

[44] Thomas J. Triggs and Walter G. Harris (1982). *REACTION TIME OF DRIVERS TO ROAD STIMULI*. Human Factors Report No. HFR-12. Monash University, Australia.

[45] Shah, J., Best, M., Benmimoun, A., and Ayat, M. L. (2015). Autonomous rear-end collision avoidance using an electric power steering system. Proceedings of the Institution of Mechanical Engineers, Part D: Journal of Automobile Engineering, 229(12), 1638-1655.

[46] *Curvature at a Point on a Single Variable Real Valued Function.* (2018) Retrieved from: http://mathonline.wikidot.com/curvature-at-a-point-on-a-single-variable-real-valued-functi at 09/07/2018.

Appendix A

Deceleration rear vehicle

In this Appendix, the deceleration of a vehicle is investigated, in case the Host merges in front. Here, the expected deceleration is assumed to be constant. The reaction time of Vehicle 1 is $T_{r,1} = T_r$ in this case. Two vehicles are involved (Veh. 1 and Host), with $V_{1,0} > V_{H,0}$ and $X_{H,0} > X_{1,0}$) having inter-vehicle distance DX. The rear vehicle will have to decelerate in order to adapt its speed to the predecessor and keep a safe inter-vehicle distance. The Velocity of Veh. 1 is given as:

$$V_1 = V_{1,0} + a_{x,1} t_b \tag{A.1}$$

where a is the constant deceleration and t_b is the braking time, which is given as:

$$t_b = \frac{DV}{a_{x,1}} = \frac{V_{H,0} - V_{1,0}}{a_{x,1}} \tag{A.2}$$

Now, the braking distance of Veh. 1 is given as:

$$s_1 = \frac{1}{2} a_{x,1} t_b^2 = \frac{1}{2} \frac{DV^2}{a_{x,1}} \tag{A.3}$$

and the x-position of the Host and Veh. 1 after the decelerating manoeuvre:

$$X_H = X_{H,0} + V_{H,0} t_b \tag{A.4}$$

$$X_1 = X_{1,0} + V_{1,0} t_b + s_1 \tag{A.5}$$

Due to the fact that the final velocities are equal, the inter-vehicle distance only depends on the velocity of the vehicle(s) and the reaction time of the road user T_r, so that:

$$X_H(t_b) - X_1(t_b) = T_r V_{1,t_b} \tag{A.6}$$

which gives:

$$T_r V_{1,t_b} = X_{H,0} + V_{H,0} t_b - (X_{1,0} + \frac{1}{2} \frac{DV^2}{a_{x,1}} + V_{1,0} t_b) \tag{A.7}$$

The minimal inter-vehicle distance becomes (incorporating the minimum inter-vehicle distance D_{min}):

$$DX_{min} = \frac{(V_H - V_1)^2}{2a_{x,1}} + (V_1 - V_H) \frac{(V_H - V_1)}{a_{x,1}} + T_r V_1 + D_{min} \tag{A.8}$$

Rewriting Eq. A.8 leads to an expression for the expected value of $a_{x,1}$ for each combination of $(X_{H,0}, X_{1,0})$ and $(V_{H,0}, V_{1,0})$, which results in a inter-vehicle distance $T_r V_H$ and ensures that the velocities are equal. This is shown in the Fig. A.1.

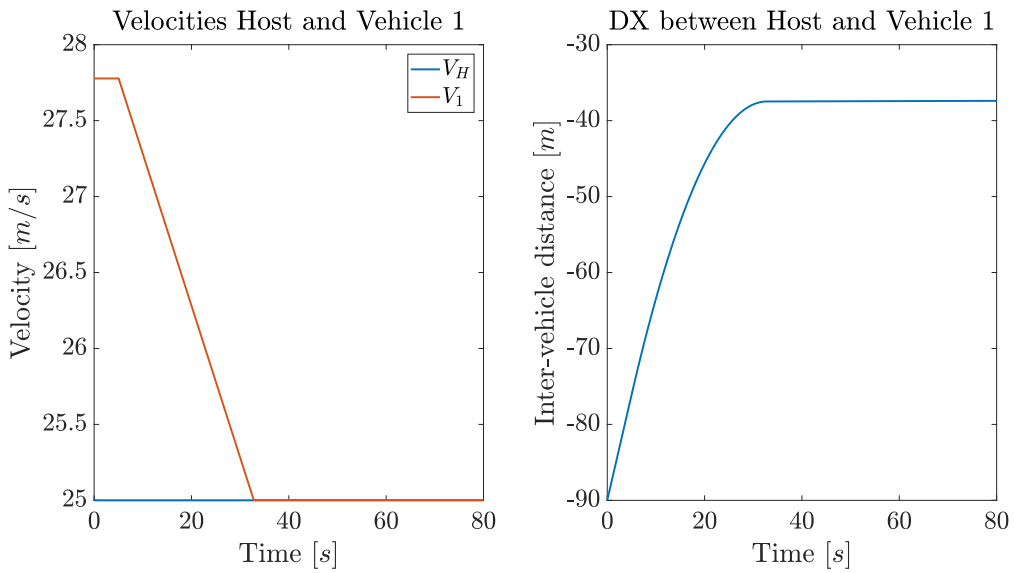

Figure A.1: *Velocities and inter-vehicle distance over time using a constant deceleration of Vehicle 1*

In Fig. A.1, initially the Velocity of Veh. 1 is constant, due to the reaction time. The initial velocity $V_1 = 100km/h = 27.78m/s$, the Host drives at $V_H = 90km/h = 25m/s$. The initial inter-vehicle distance DX is $90m$, the final inter-vehicle distance is $T_r V_H = 1.5 \cdot 25 = 37.5m$, see Fig. A.1.

Remarks
The method of constant deceleration appears to have some restrictions:

- **Increasing the number of vehicles:** The applied method works in case there is only one vehicle that has to decelerate in order to adapt speed and obtain safe inter-vehicle distance. If there is another vehicle (Veh. 2) driving on the same lane behind Veh. 1, the constant deceleration method is not valid any more. Assuming Veh. 2, with $V_{2,0} > V_{1,0} > V_{H,0}$, which will have to decelerate in order to prevent collision with Veh 1. However, since Veh. 1 is decelerating, the reference speed of Veh. 2 changes over time, indicating that $a_{x,2}$ is no longer constant.
- **Accelerating Host:** Section 2.5.1 indicates that the typical deceleration value from human drivers is not constant, but varies over time (decreasing to a limit and going back to zero again). Moreover, in case the Host is longitudinally accelerating or decelerating during the lateral motion, the reference velocity of Veh. 1 changes over time, again indicating that the deceleration can not be constant.

Regarding these shortcomings, in Section 4.2.4 an Adaptive Cruise Controller is implemented and validated in order to obtain realistic human decelerating behaviour.

Appendix B

Adaptive Cruise Control

In this Appendix, Adaptive Cruise Control (ACC) is elaborated further. First, the values of the gains k_p and k_i are determined, based on several tuning criteria. Secondly, the influence of a differential action to the controller is shown. Finally, the set speed control gain $K_{p,ss}$ is determined.

B.1 Determining the Proportional- and Integral gains

This section describes the determination of the Proportional- and Integral gains in the ACC. To validate the results, for the combinations of gains the velocities, accelerations and inter-vehicle distances are plotted over time. In all simulations, the same initial conditions are used, as given in Tab. 4.3. The output $U(t)$ of the PI controller is given as:

$$U(t) = k_p e_v(t) + k_i \int_0^t e(\tau) d\tau \tag{B.1}$$

where $e_v(t)$ is the velocity error and the integral term represents the error in longitudinal position. The output of the controller is used to update the velocity of a vehicle.

Criteria
The determination of the Proportional- and Integral gains is based on the following criteria:

- **1. String Stability:** The string of vehicles is required to be stable. The effect of decreasing the velocity of the leading vehicle (due to the Host merging in front) should not be amplified through the string of vehicles.
- **2. Peak value in acceleration:** The peak value of the Acceleration is limited to $-1.3 m/s^2$ for the Comfort criteria (see Sec. 3.3.4).
- **3. Minimum inter-vehicle distance DX:** The inter-vehicle distance $DX = X(k) - X(k-1)$ is required to be positive to prevent collisions. In addition, the inter-vehicle distance is required to be always greater than or equal to the reaction time multiplied with the actual speed: $DX(t,k) >= T_r V(t,k)$ for all (t,k), to obtain safety. This indicates that an overshoot in the DX-plot is not allowed.

String Stability
Fig. B.1 presents the resulting velocities (left), accelerations (middle) and inter-vehicle distance (right) using $k_p = 0.001$ [-] and $k_i = 0.01$ $[\frac{1}{s}]$. Figure B.1 clearly indicates that the string of vehicles is not string stable, since the peak value of the acceleration of each vehicle is lower than the predecessor's and the inter-vehicle distances and velocities are not converging to a constant value.

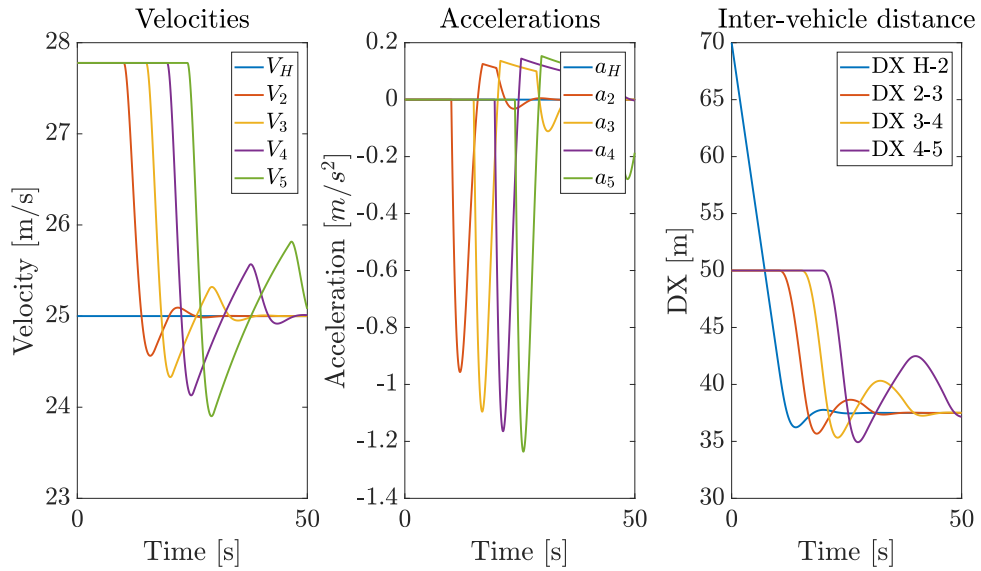

Figure B.1: *Velocities, accelerations and inter-vehicle distances using* $k_p = 0.001$ *and* $k_i = 0.01$

Peak in acceleration

Fig. B.2 presents the results when using $k_p = 0.001$ and $k_i = 0.1$. Here, the acceleration peak values are below the limit of $-1.3m/s^2$, indicating that this combination of multipliers is not valid.

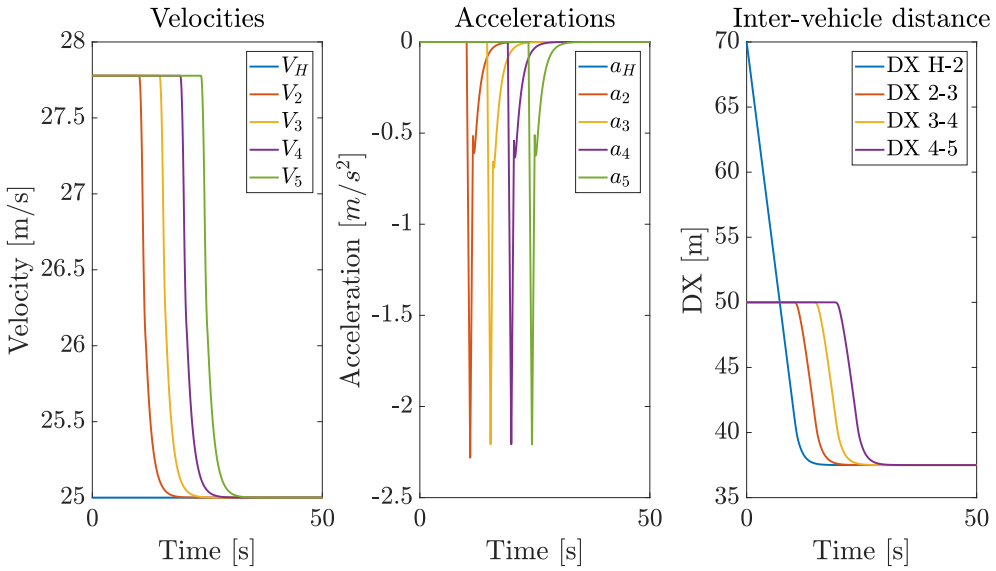

Figure B.2: *Velocities, accelerations and inter-vehicle distances using* $k_p = 0.001$ *and* $k_i = 0.1$

Inter-vehicle distance

Fig. B.3 shows the resulting inter-vehicle distances for $k_p = 0.001$ [-] and $k_i = 0.001$ $[\frac{1}{s}]$. The inter-vehicle distance plot shows that the Vehicles tend to drive closer to each other than the required inter-vehicle distance $T_r V(k)$, indicating that safety is not guaranteed.

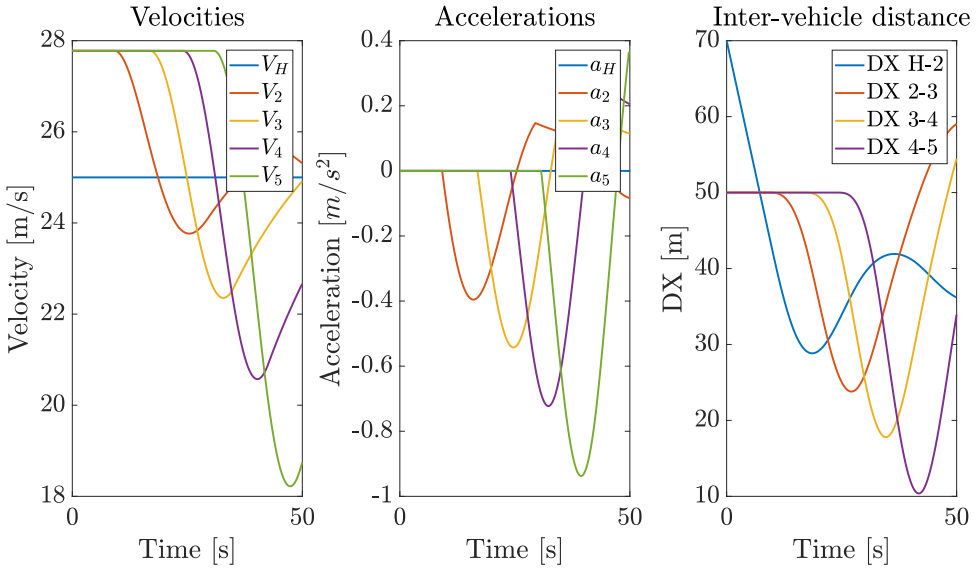

Figure B.3: *Velocities, accelerations and inter-vehicle distances using* $k_p = 0.001$ *and* $k_d = 0.001$

Results and Conclusion

The goal was to obtain String stability, minimize the peak in the accelerations and to ensure that safety is guaranteed (never exceeding the required for minimal inter-vehicle distance). Fig. B.5 presents the velocities and accelerations using $k_p = 0.01$ [-] and $k_i = 0.001$ $[\frac{1}{s}]$. These gains satisfy all requirements.

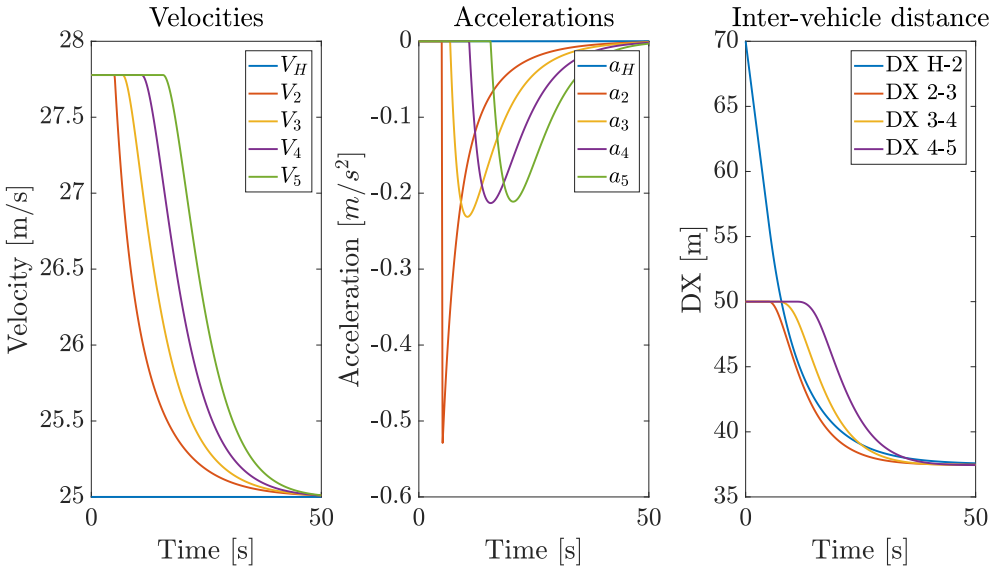

Figure B.4: *Velocities, accelerations and inter-vehicle distances using* $k_p = 0.01$ *and* $k_i = 0.001$

Time Constant

The *time constant* τ determines how quickly the system reaches a steady state value. It is defined as the time it takes before the Velocity reaches 63.2% of the total difference in velocity (DV). In this case, $DV = 27.78 - 25 = 2.78$ m/s. From Fig. B.5 it appears that it takes 6.1 seconds before $V_2 = V_0 - 0.632 \cdot V_{H,0}$. This indicates that the time constant for the Vehicle 2, $\tau = 6.1$ seconds.

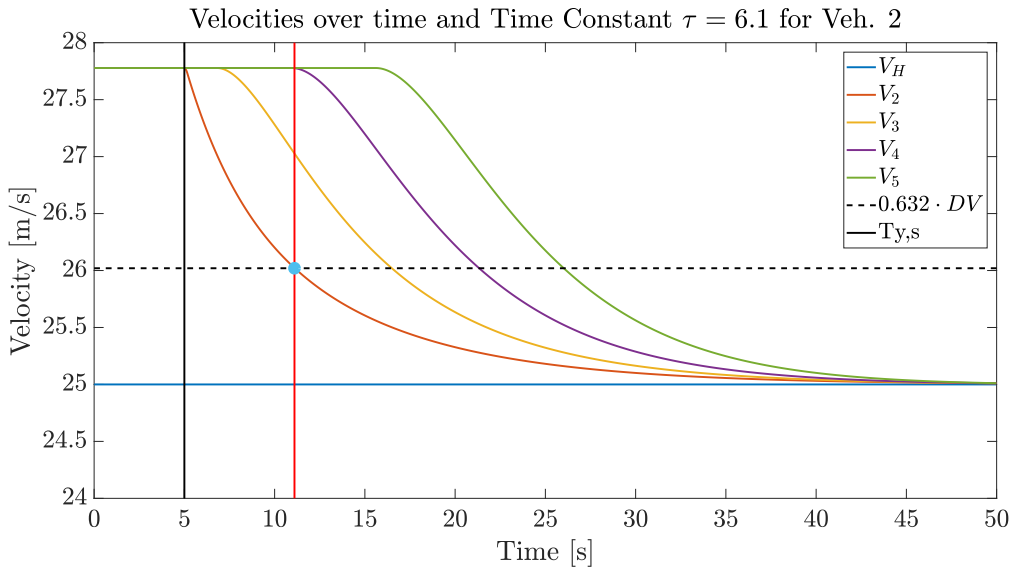

Figure B.5: *Velocities over time and time constant τ for Veh. 2*

The time constant τ is based on a constant input signal (Host merging in front). For the vehicles behind Veh. 2, the input signal (velocity of the predecessor) is not constant, indicating that τ is not determined for these vehicles.

B.2 Influence of the differential action

The controller in Section 4.2.4 is using e_V and e_X. By adding an differential error, the acceleration error is taken into account. The controller output using a PID controller is given as:

$$U(t) = k_p e(t) + k_i \int_0^t e(\tau)d\tau + k_d \frac{de(t)}{dt} \tag{B.2}$$

Here, the term k_p is the multiplier on the proportional error (velocity), the term k_i is the multiplier on the integral of the error (position) and the term k_d is the multiplier on the differential error (the term $k_d \frac{de(t)}{dt}$ represents the error in acceleration over time: $\frac{de(t)}{dt} = a(k,t) - a(k-1,t)$ for each vehicle k).

Fig.B.6 shows the influence of adding the differentiation term to the controller.
At $T = 5s$, the Host merges in front of the string of vehicles ($V_{H,0} = 22.2m/s$, see Table B.1). The bold lines indicate the velocities over time using a PI controller, while the striped lines indicate the velocities using a PID controller.
Adding the differential term decreases the initial accelerations (see Fig.), but from Fig. B.7 it appears that the minimum inter-vehicle distance is lowered (Table B.1 represents the initial conditions).
The decelerations are decreased since the Host is merging in front, without accelerating. To equalize the accelerations in the differential term, the controller suggests a lower deceleration first. This results in a larger velocity overshoot and thus a lower peak for the inter-vehicle distance.

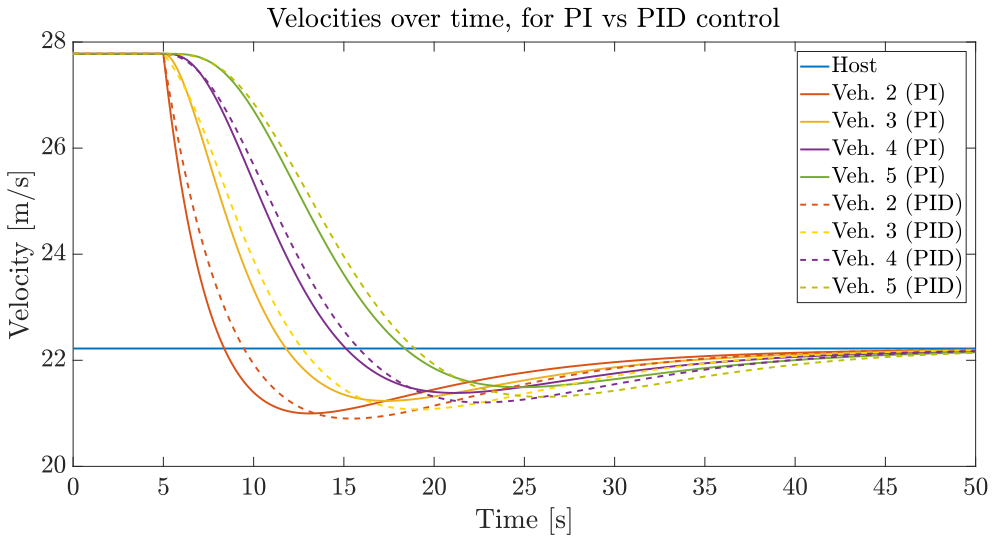

Figure B.6: *Velocities over time, using PI (green) and PID (red)*

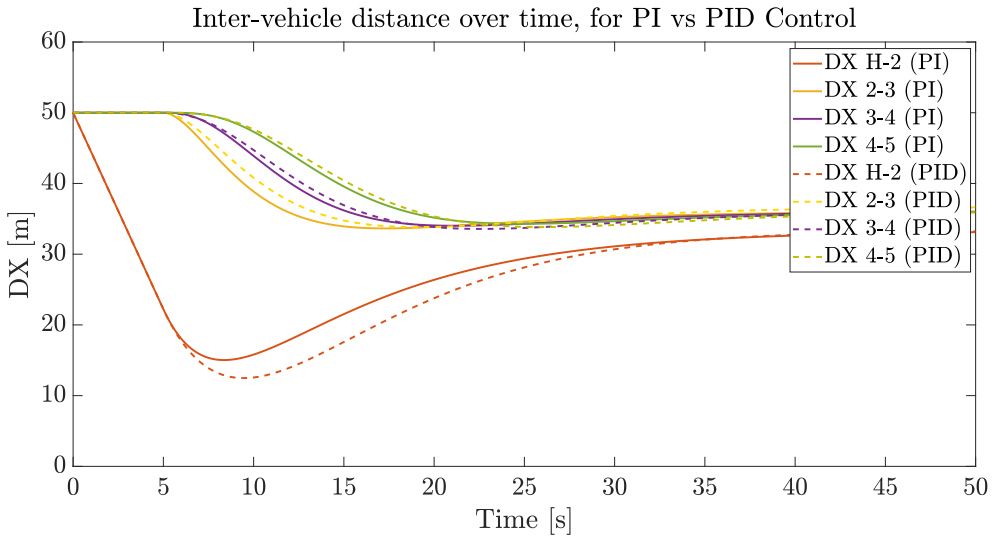

Figure B.7: *Velocities over time, using PD (green) and PID (red)*

Table B.1: *ACC: initial pos. of the five vehicles*

Vehicle	X_0**-position [m]**	V_0 **[km/h]**
1	250	90
2	200	100
3	150	100
4	100	100
5	50	100

From Fig. B.7 it appears that adding a differential action to the controller will decrease the inter-vehicle distance, which decreases safety (vehicles will drive too close to the predecessors). This indicates why a PI Controller is used in the project.

B.3 Determining the set speed control gain

In this section, the determination of the set speed controller gain $K_{p,ss}$ is elaborated. The set speed controller is implemented to prevent the vehicles from accelerating to close a gap. The criteria for the set speed controller are the same compared to the criteria for the Proportional- and Integral gains (see section B.1): the string of vehicles is required to be stable (change in velocity should not be amplified through the string), the inter-vehicle distance is required to be positive and be always greater or equal to $T_r V$ and the peak in acceleration is limited. Several simulations are performed in order to obtain the correct SSC gain. The initial conditions are given in Tab. 4.3.
In Fig. B.8 the velocities, accelerations and inter-vehicle distances are plotted over time, using $K_{p,ss} = 0.001$. In this simulation, the string of vehicles performs a stable driving behaviour (a change in velocity is not amplified through the string of vehicles).

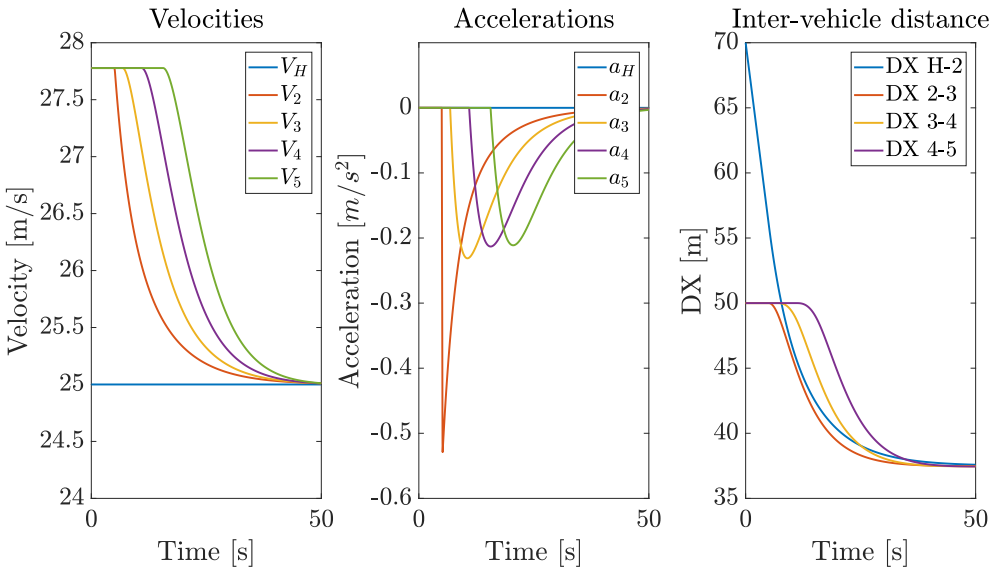

Figure B.8: *Velocities over time, using* $K_{p,ss} = 0.001$

In fact, any $K_{p,ss} > 0$ satisfies since adding the SSC only prevents the vehicle k from accelerating in case $DX_{k,k-1}(t) > T_r V(k,t)$ or when $V(k,t) < V(k-1,t)$ (velocity of a predecessor, vehicle $k-1$, is larger than velocity of vehicle k).

Appendix C

Speed adjustment Host after merging

After merging to the adjacent lane, the Host could accelerate or decelerate to adjust his speed either to the new predecessor or to the initial Host velocity.

Accelerating after merging

In case the Host decelerates in order to merge, The acceleration phase after merging starts when the Host has reached the required lateral distance to the Predecessor:

$$Y_H = Y_{min} \tag{C.1}$$

After obtained the required lateral distance for acceleration, there are three options:

- No acceleration
- Accelerating to $V_{2,0} = V_{3,0} = V_{4,0} = V_{5,0}$
- Accelerating to $V_{H,0}$

C.1 No acceleration

The Host can decide not to accelerate after moving Y_{min}. This will result in the lowest RMS_c, but the other road users (especially the one behind the Host) will have to decelerate significantly. This is shown in Fig. C.1.

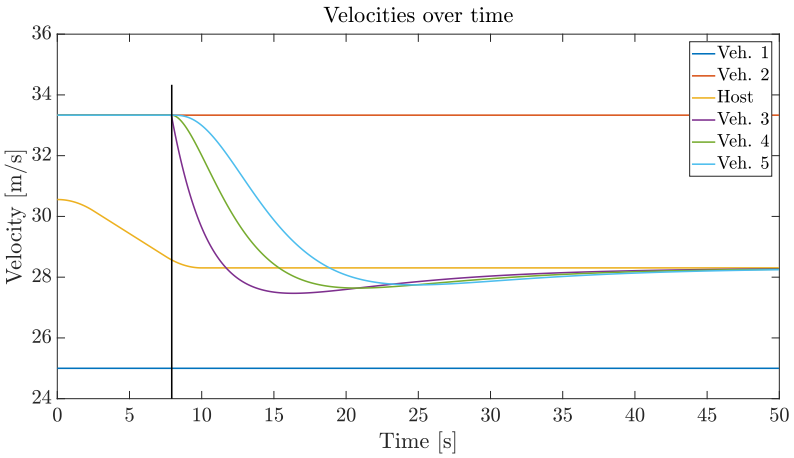

Figure C.1: *Velocity of the Host and the other road users over time*

C.2 Accelerating to average lane velocity

The second option for the Host is to accelerate to the average velocity on the adjacent lane. This is show in Fig. C.2. Dependent on the inter-vehicle distance from the vehicles behind and the Host, lower decelerations for the other road users are obtained.

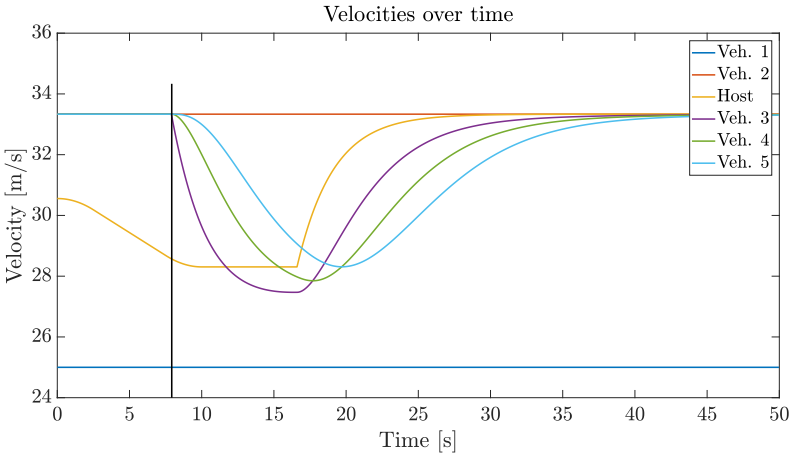

Figure C.2: *Velocity of the Host and the other road users over time*

C.3 Accelerating to $V_{H,0}$

The Host might also decide to accelerate again until the initial velocity $V_{H,0}$ is reached again. This situation uses the set speed of the Host as the target speed, which is the method that is applied throughout the project. In Fig. C.3 the resulting velocity profiles are shown.

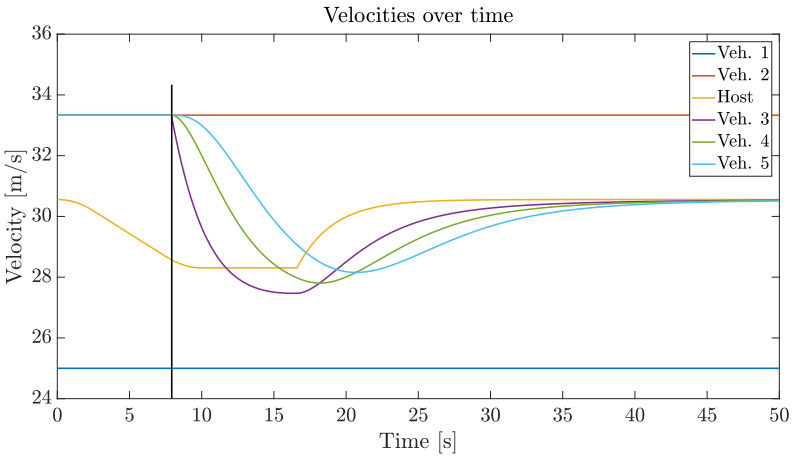

Figure C.3: *Velocity of the Host and the other road users over time*

Appendix D

Criteria for merging in a gap

This Appendix presents information about the criteria and decision-making of the controller. For gap 2 and 3, the expected acceleration from gap's rear vehicle and the LFT to the gap's front Vehicle are plotted, indicating the optimal switching moments.

D.1 Host merging in gap 2

Considering merging in gap 2, Fig. D.1 presents the expected acceleration of Veh. 3 in the upper figure and the LFT to Veh. 2 in the lower figure. From the upper figure, it appears that the maximum merging start time due to the expected deceleration of Veh. 3 is $Tys, max = 26.3$ s. The LFT plot indicates that the minimum merging start time $T_{ys,min} = 21.35$ s, which is the merging start time.

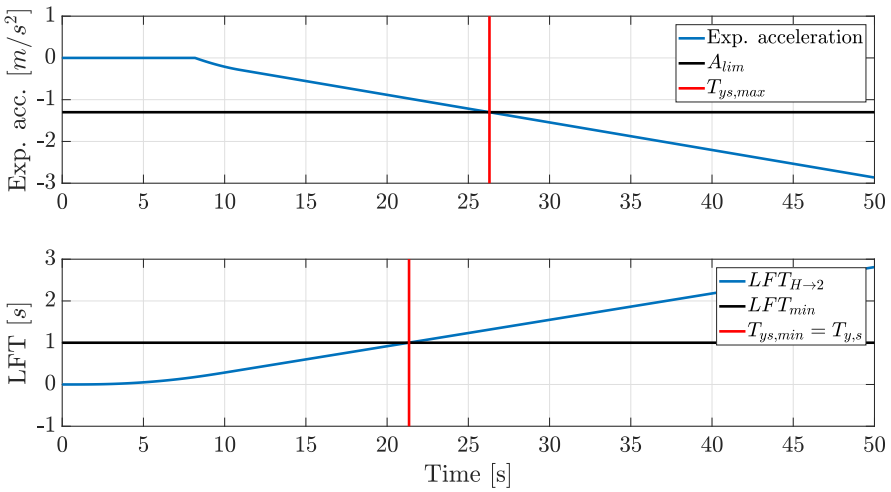

Figure D.1: *Expected acceleration (upper figure) and LFT (lower figure) over time*

Fig. D.2 presents the inter-vehicle distance to the Predecessor. The maximum merging start time $T_{ys,max,s} = 24.50$ s. Since $T_{ys,max,s} > T_{ys,min}$, the overtaking manoeuvre is longitudinally safe.

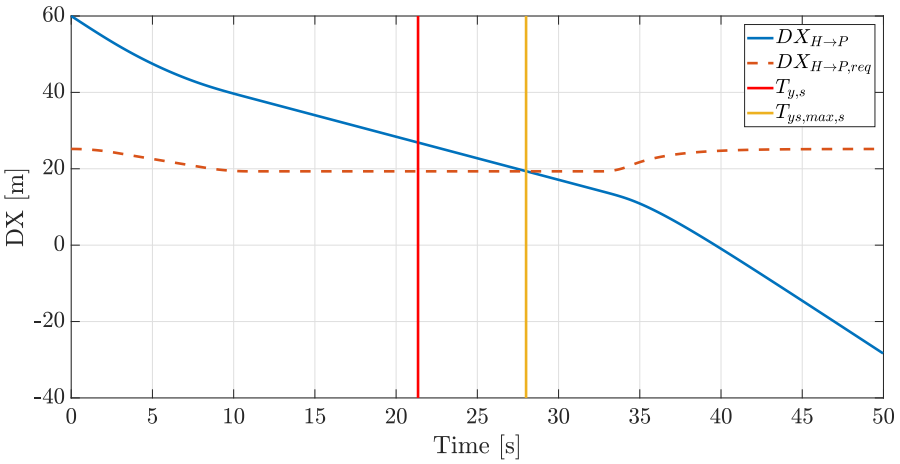

Figure D.2: *Actual- and required inter-vehicle distance to Predecessor over time*

D.2 Host merging in gap 3

Considering merging in gap 3, Fig. D.3 presents the expected acceleration of Veh. 4, LFT to Veh. 3 and Fig. D.4 presents the inter-vehicle distance to the Predecessor. The minimum merging start time $T_{ys,min} = 29.21$ s (lower sub-plot), while the maximum merging start time $T_{ys,max} = 29.50$ s (upper sub-plot).

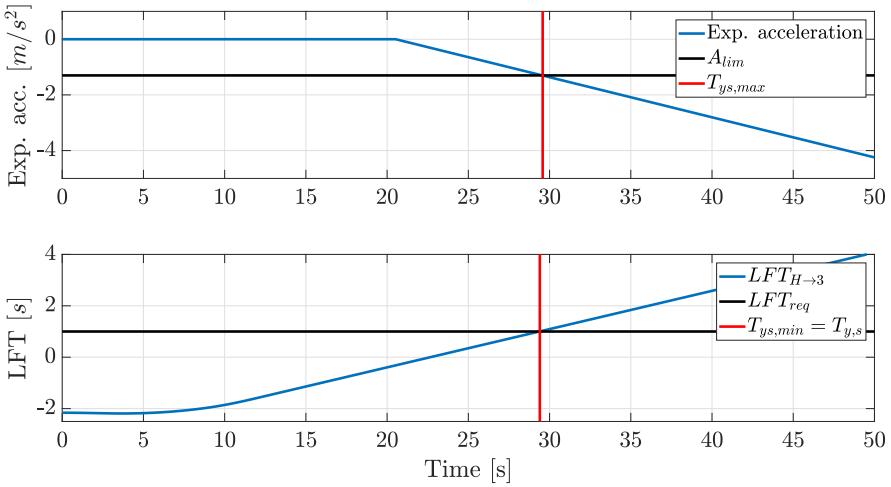

Figure D.3: *Expected acceleration (upper figure) and Longitudinal Following Time (lower figure) over time, including the limits*

Fig. D.4 shows that the maximum merging start time $T_{ys,max,s}$ is not defined (the Predecessor does not limit the merging start time). This indicates that the obtained overtaking manoeuvre satisfies all constraints. However, merging is not required from the perspective of the Predecessor.

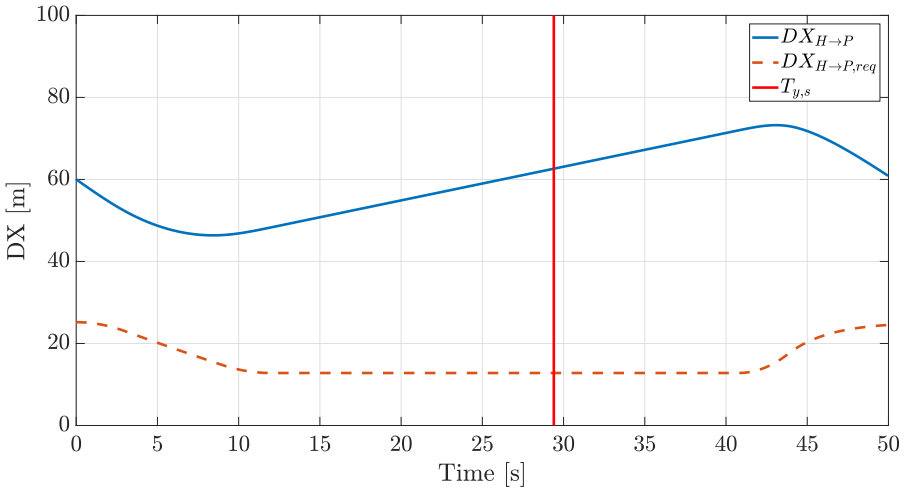

Figure D.4: *Inter-vehicle distance to Predecessor $DX_{H\to P}$ and required inter-vehicle distance $DX_{H\to P,req}$ over time, including start time lateral movement $T_{y,s}$*